Biocompatibility Studies on a Glucose Biosensor: Investigation of the In-Vivo Sensitivity Loss Phenomenon

By

Sandra L. Barnes

B.S. Alcorn State University, 1993

Submitted to the Department of Chemistry and the Faculty of the Graduate School of the University of Kansas in partial fulfillment of the requirements for the degree of Doctor of Philosophy

Date Submitted: 11/24/98

I wish to dedicate this book to all the people who, in some form or fashion, had a big impact on my obtaining this degree: Firstly, I thank God for giving me the strength to endure. I thank my loving husband Clinton for always being patient and supportive. I thank my parents Albert and Vergie for their love and for teaching me to be a strong person. I thank my twin sister Sheila for helping me through her faith and support as we traveled together through it all. I thank my sisters Lisa, Brenda and Alecia for supporting me in all the ways that they could. I thank Fredrick and Sarah for their kind hearts and generosity. I thank Rev. Johnny B. for taking a special interest in supporting me as a fellow Alcornite. I thank Prof. Thomas Bolden for being my mentor, believing in me, encouraging me, and supporting me in every way he could. Thanks to New Hopewell Missionary Baptist Church, Pastor O.D. Evans, and Victory Bible Church, Pastor Leo Barbee, Jr., for the many prayers.

THANK YOU, WITH ALL MY LOVE!

ACKNOWLEDGEMENTS

I wish to thank my advisor and mentor Prof. George S. Wilson for encouraging and challenging me throughout my graduate career. I thank Prof. James M. Anderson of Case Western Reserve University for assistance with the cell-culture experiment. I am grateful to the National ESCA and Surface Analysis Center for Biomedical Problems (NESAC/BIO) at the University of Washington for ESCA analysis of samples (Grant# RR-01296). I thank the National Institues of Health (NIH) for financial support. Finally, I would like to thank members of the Wilson and Anderson research groups, especially Yibai Hu (Wilson group) and Terry Collier (Anderson group), for support and discussions.

TABLE OF CONTENTS

List of Figures and Tables

1. General Introduction

Since the inception of the *in-vivo* electrochemical glucose biosensor, great expectations seemed to await insulin-dependent diabetics. However, even after decades of intense research, the sensor still suffers a major disadvantage: loss of sensitivity upon implantation *in-vivo*. If an implantable glucose biosensor is to be developed and used for reliable, long-term measurements of glucose, it will be important to address interactions between the sensor and tissue that may affect the sensor's performance as well as the tissue state. The sensor which has been developed in the Wilson group has been shown to be nontoxic, nonmutagenic, and noncarcinogenic to the tissue (1). However, the performance of the sensor in the tissue needs to be addressed. In this work, sensor performance is evaluated in relation to interactions of the sensor with endogenous biological molecules and cells.

Chapter 1 provides background information about diabetes, the glucose biosensor, and the biocompatibility issue. Proteins are known to adsorb on the surface of foreign objects implanted *in-vivo* (2) and are thought to affect the sensor's response (3,4). In chapter 2, a biocompatible polymer designed to prevent adsorption of protein was coated as an outer membrane on the sensor. The *in-vivo* response of the biocompatible membrane-coated sensor was compared to the *in-vivo* response of sensors that were not coated with the biocompatible membrane. In chapter 3, biomolecules extracted from previously implanted glucose biosensors were characterized and

identified. The purpose of the work was to determine the kinds of molecules taken up by the glucose biosensor that may potentially effect the sensor's *in-vivo* response. In chapter 4, cellular interaction with the sensor was studied. We wanted to examine whether or not macrophages grow on the surface of the sensor or in the vicinity of the sensing area. In either case, the sensor's response may be affected by the presence of macrophages. Finally, in chapter 5, possible causes of the *in-vivo* sensitivity loss are discussed based upon the results obtained.

2. Chapter 1: Diabetes Mellitus and the Glucose Biosensor

2.1. Background

Diabetes is a disease in which the body does not produce or properly use insulin, a hormone required to convert sugar, starches, and other food into energy. According to the American Diabetes Association, ADA, (5), each year at least 180,000 people die as a result of complications due to diabetes: blindness (diabetic retinopathy), kidney disease (diabetic nephropathy), heart disease and stroke, and nerve disease and amputations. Genetics and environmental factors such as obesity and lack of exercise are possible causes of the disease. There are two major types of diabetes: Type 1 (insulin-dependent) diabetes and Type 2 (non-insulin-dependent) diabetes. Type 1 is an autoimmune disease in which the body does not produce any insulin. It accounts for 5-10% of diabetes. Type 2 diabetes is a metabolic disorder due to the body's inability to make enough or properly use insulin. Type 2 accounts for 90-95% of diabetes; type 2 diabetes has almost become an epidemic due to an increased number of older americans, and a greater prevalence of obesity and a sedentary lifestyle. According to the ADA, there are 15.7 million people (5.9% of the population) in the United States who have diabetes, diabetes is the seventh-leading cause of death (sixth-leading cause of death by disease) in the United States, and diabetes is one of the most costly health problems in America; health care and other costs of lost productivity run $92 billion annually. Per capita health care

costs for diabetics amounted to $10,071 in 1997, while the costs for non-diabetics was $2,699 in 1997.

A cure for diabetes may be realized through islet beta cell transplantation, pancreas transplantation, or even through pharmacological approaches. However, transplantation does not meet the risk/benefit requirement because it is necessary for recipients to use dangerous immunosuppressive drugs and, pharmacological agents have been generally considered unsafe (6). Therefore, other approaches focus on treatment of diabetes rather than finding a cure. Conventional therapy for insulin-dependent diabetes involves pricking the finger to obtain a drop of blood, placing the drop of blood on a test strip, measuring the blood glucose with a meter, and injecting insulin intramuscularly to bring the glucose level under control. Unfortunately, problems with this method include boredom of repeated measurements, pain associated with prickings and injection, and fear of diabetic coma (hypoglycemia) caused by injection of too much insulin. Therefore, diabetic patients do not test their glucose levels nearly as often as they should (7,8).

In 1993, the Diabetes Control and Complications Trial, a multicenter, randomized clinical trial designed to compare intensive with conventional diabetes therapy, showed that intensive therapy, unlike conventional therapy, effectively delays the onset and slows the progression of vascular disease of the eye (retinopathy), kidney (nephropathy), and nerves (neuropathy) in patients with Insulin-Dependent Diabetes Mellitus (IDDM) (9). However, intensive insulin

therapy (3-4 insulin injections per day) greatly increases the risk of hypoglycemia.

In order for the diabetic patient to accept and benefit from intensive insulin therapy, detection of hypoglycemia by continuous glucose monitoring is imperative. One such device includes a hypoglycemic alarm coupled to a glucose biosensor (10). For long-term glycemic control, an ideal device would consist of a closed-loop wearable device that can continuously monitor glucose levels, determine real time glucose values, and deliver precise volumes of insulin when required; the artificial endocrine pancreas is being developed for this purpose (3). Unfortunately, a long-term reliable glucose biosensor is not yet available. However, there are a number of research groups working hard to produce such a device. Currently, the glucose biosensor is the only device available that would allow the diabetic patient to continuously monitor his or her glucose. The Biostator™ (11) can monitor glucose continuously. However, it is not a practical device because it is large and requires an extracorporal shunt to heparinize the blood. Noninvasive devices include the Glucowatch™ (12) and TD Glucose Patch (13). Both devices allow the extraction of glucose through the skin for detection. Integ's device (14) involves glucose sampling using a needle cartridge and IR detection. SpectRX (15) has developed a painless sampling device based on laser microporation of the skin. The device allows glucose detection by conventional methods. However, neither of these devices is capable of continuous monitoring.

The development of a reliable long-term glucose biosensor intended for monitoring glucose levels in diabetics has proven to be a very challenging task. What started several decades ago from the advent of the Clark oxygen electrode (16) has now become the focus of many research laboratories. First, the various modes of glucose detection are reviewed followed by a discussion of glucose biosensors that show promise for use in diabetics. Lastly, a discussion of biosensor biocompatibility is presented, with special focus on the *in-vivo* sensitivity loss phenomenon observed for the glucose biosensor developed in the Wilson group.

2.2. Modes of Glucose Detection

Because of the specificity of enzyme-substrate reactions, enzymes are used as the recognition element in glucose biosensors. Furthermore, electrochemical detection has been the detection method of choice due to simplicity of sensor design. Glucose oxidase is most often employed because it is specific for glucose and consumes and generates species which can be detected electrochemically. The various modes of glucose detection using implantable glucose biosensors have been reported (7). Such sensors are based upon the amperometric detection of (a) oxygen, (b) hydrogen peroxide, or (c) a mediator. The fundamental enzymatic reaction is given below:

$$\text{Glucose} + O_2 \xrightarrow{GOx} \text{Gluconic Acid} + H_2O_2$$

Where Gox = Glucose Oxidase

Glucose is oxidized by oxygen catalyzed by glucose oxidase; hydrogen peroxide is produced in the process. Either oxygen consumption or hydrogen peroxide production may be used for glucose detection, since the kinetics of glucose consumption is proportionally related to oxygen consumption and hydrogen peroxide production. Figure 1.1 (reproduced from reference 7) is a schematic representing (a) the detection of oxygen.

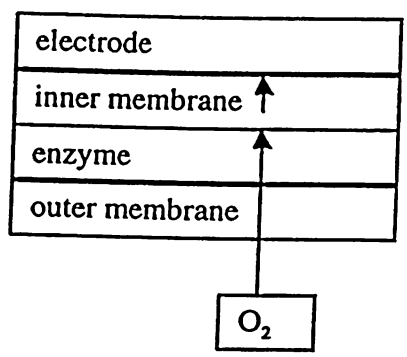

Figure 1.1. Schematic of a Glucose Biosensor Based on (a) Oxygen Detection Mode (Adapted from reference 7).

For this detection mode, the electrode is poised at a potential at which oxygen is reduced (i.e. -600mV Vs Ag/AgCl). The decrease in oxygen current observed at the electrode surface is proportional to the consumption of glucose in the enzymatic layer. However, a nonenzymatic reference electrode is required to produce an

amperometric difference signal between the basal oxygen and the oxygen consumption due to the enzymatic reaction. This requirement complicates the design and size of the glucose biosensor.

The second mode of detection, illustrated in Figure 1.2, is (b) hydrogen peroxide detection at the electrode surface. In this mode, the electrode is poised at a potential for oxidation of hydrogen peroxide (i.e. +600mV Vs Ag/AgCl). The increase in current due to hydrogen peroxide production is proportional to the amount of glucose present. Because of the high potential (+600mV) required to oxidize hydrogen peroxide, there is increased interference from electroactive species. Elimination of potential interferences requires a permselective inner membrane or a scavenger enzyme.

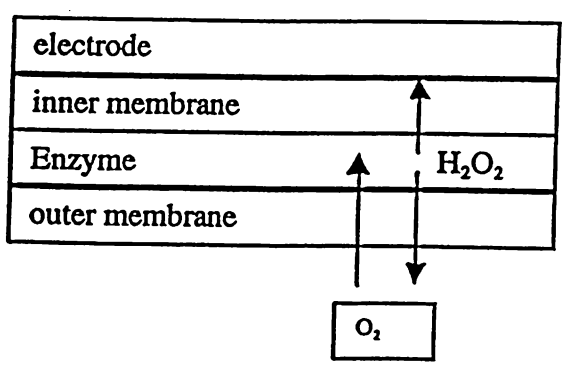

Figure 1.2. Schematic of a Glucose Biosensor Based on (b) Hydrogen Peroxide Detection (Adapted from reference 7).

The last mode of detection is based upon (c) mediator detection at the electrode surface. It takes advantage of the fact that the enzymatic reaction is a ping pong reaction and requires two steps: 1. reduction of the enzyme by glucose and 2. oxidation of the reduced enzyme by oxygen. In this mode, an electron acceptor mediator replaces oxygen and accepts the electrons from the reduced flavine adenine dinucleotide ($FADH_2$) moiety and transfers them to the electrode surface. This process, shown in Figure 1.3 (Adapted from reference 7), proceeds rapidly and efficiently. There are two advantages of this mode. First, the potential required to oxidize mediators is relatively low compared to the potential required to oxidize hydrogen peroxide. This can decrease interferences from endogenous species, provided that they do not react directly with the mediator. If the mediator reacts rapidly with the enzyme thus greatly increasing its turnover, the result will be an increase in the Michaelis constant. This, in turn, will increase the linear response of the sensor. However, mediators are frequently unstable and lead to sensors with limited lifetime. Competition between the mediator and oxygen for the reduced enzyme is also a serious problem because the mediator must necessarily be fixed over the electrode surface to prevent leaching out, whereas oxygen is able to freely diffuse.

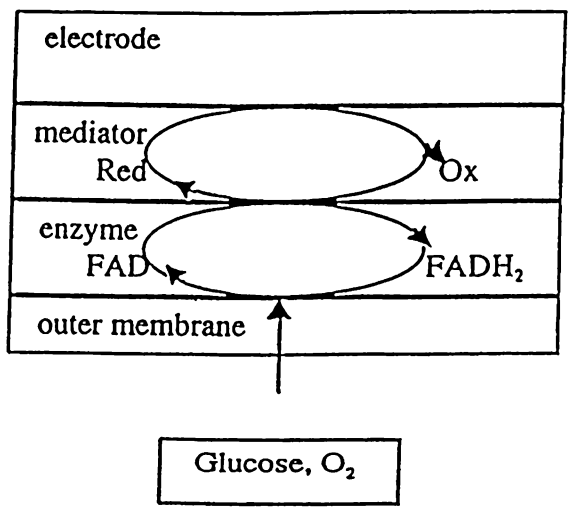

Red = reduced form of the mediator

Ox = oxidized form of the mediator

FAD = oxidized form of the coenzyme flavine adenine dinucleotide

$FADH_2$ = reduced form of the coenzyme flavine adenine dinucleotide

Figure 1.3. Schematic of a Glucose Biosensor Based on (c) mediator oxidation (Adapted from reference 7).

2.3. Glucose Biosensors

Glucose biosensors based upon all three modes of glucose monitoring have been developed for use in diabetic patients. Jansen et al. (17) have reviewed the various implantable devices. The least frequent approach to glucose monitoring is based on oxygen consumption and has been exploited by Gough et al. (18). Their sensor is based on a two-dimensional design. A flexible cylindrical gel, ~0.2cm diameter and 30cm long, containing immobilized glucose oxidase and catalase is formed at the end of a silicone rubber tube. The tube contains a potentiostatic O_2 sensor. The gel is formed by crosslinking a mixture of glucose oxidase and catalase and dog serum albumin with glutaraldehyde; catalase is added to prevent H_2O_2 accumulation which the investigators feel may inactivate the glucose oxidase. The exposed end is covered with a layer of cross-linked albumin to enhance biocompatibility. The potentiostatic O_2 sensors each contain one silver and two platinum electrodes mounted in a glass stub which are covered by an electrolyte gel layer and a thin silicone rubber membrane. The investigators then weld the electrodes to insulate multifilament lead wires and the assemblies are cemented into respective silicone rubber tubes. The electrical leads were terminated at the opposite end with waterproof connectors. Sensors were implanted intravenously in the superior vena cava of six dogs for 1-15 weeks. Biocompatibility, enzyme lifetime, O_2 availability, O_2 sensor stability, and biochemical interference were sited as not being limitations; the limitations

noted were due to mechanical and electrical unreliability. Although this sensor appears very promising, because it is implanted intravenously, the risk of thrombosis and infection is too great, especially with a sensor of this size.

Wilkins et al. (19,20) have also used this approach. Their system consists of two implantable sensors, a rechargeable glucose biosensor and an oxygen electrode which is identical to the glucose sensor but with no enzyme in the micro-bioreactor. The sensors are connected to a wearable electronics package and data logger and two transcutaneous refilling capillary tubes. Glucose oxidase is immobilized on dispersed carbon powder which is held in a liquid suspension. The construction of the biosensor allows spent immobilized enzyme to be removed from the sensor body and fresh enzyme suspension simultaneously injected via septa, without sensor disassembly or surgical access (21). According to the investigators, this approach makes it possible to extend the sensor's lifetime by *in-situ* sensor refilling. Short-term (4 hr.) acute *in-vivo* experiments were performed with the pair of sensors subcutaneously implanted in the posterior neck region in dogs. Chronic *in-vivo* experiments (25 days) were performed in four unrestrained dogs. The investigators secured the glucose monitoring system (the electronics package and data logger) in pockets of a wearable jacket on the dog's back. According to the investigators, both acute and chronic experiments demonstrate that the implantable biosensor signal adequately follows the blood glucose level with a delay of 3-10 minutes. They reported that for chronic experiments,

the biosensor signal decreased to 85% of its initial value after eight days of implantation. On day twelve, they refilled the sensor *in-vivo* with fresh enzyme suspension, and reported that the response to blood glycemia increased back to 100% of its initial value. As noted by the investigators, this approach is novel and seems very encouraging for long-term implantation of glucose biosensors. However, the investigators should carefully consider the day-to-day *in-vivo* stability of the sensor which might fluctuate widely over the chronic implantation period.

The most popular mode of glucose monitoring is based on hydrogen peroxide detection. This approach has been taken by Wilson et al. (10,22). The sensor design is given in Figure 1.4.

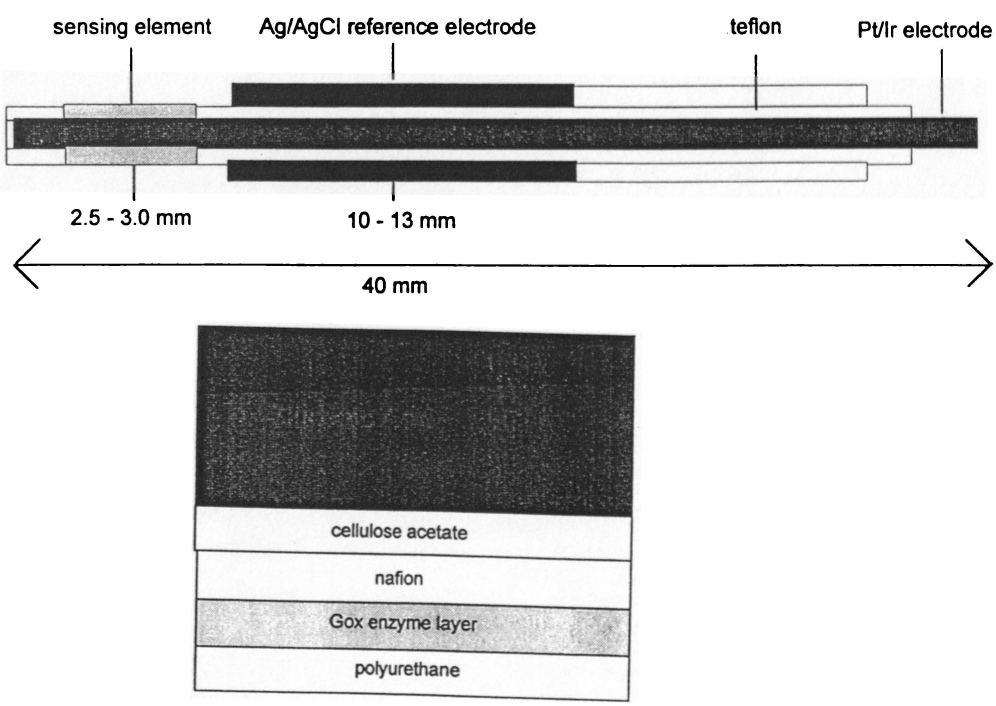

Figure 1.4. Design of Wilson Group Biosensor.

The sensor consists of a platinum-iridium wire coated with teflon (0.25mm o.d.), except for a 2mm cavity near its extremity, where glucose oxidase is immobilized on cellulose acetate, reticulated with glutaraldehyde, and covered by a polyurethane layer. The cathode consists of a silver/silver chloride wire wrapped tightly around the teflon coated wire. The external diameter of the glucose sensor is 0.45mm. Long-term (10 day) assessment of the sensor was determined by *in-vivo* implantation in rats. The sensors were implanted into the interscapular subcutaneous tissue of overnight-fasted rats using a 16 gauge cannula. After insertion into the tissue, the cannula was removed, leaving the sensor in place secured with adhesive plaster. The investigators reported that the sensitivity was significantly lower *in-vivo* than that observed *in-vitro* for the same sensors. According to the investigators, a longitudinal 5 day study of seven sensors tested on different days demonstrated a relative stability of the sensors' sensitivity (22). The investigators have also developed a user-friendly method for calibrating the sensor that also consists of a hypoglycemic alarm. This sensor functions well for short-term implantation. However, for long-term use, improvements in the stability and lifetime must be achieved.

Pickup et al. (23) have also chosen detection of hydrogen peroxide. The base of their electrode is a polyester-insulated platinum wire and the reference a similarly insulated silver wire, both 0.125mm diameter. Both wires are inserted into a nylon cannula of 0.625mm outer diameter, 0.35mm inner diameter, then cemented with

silastic medical grade elastomer. The investigators created a sensing layer at the tip of the electrode by applying an inner membrane of cellulose acetate followed by a cross-linked glucose oxidase membrane. An outer polyurethane layer was used. The sensor was withdrawn into a 21 gauge needle so that the sensing tip was level with the needle bevel, and secured at the other end with epoxy resin. The sensor was tested in humans. The sensor (inside a 21 gauge needle) was inserted subcutaneously. Seven of 14 implanted sensors showed no detectable change in current after glucose ingestion. For the seven sensors that did respond to glucose ingestion, the sensitivity *in-vivo* was significantly reduced compared to the pre-implantation sensitivity of these sensors. Clearly, nonresponse from half the sensors is of immediate concern and must be addressed.

Mediator detection has been used by Shichiri et al. (24). In this sensor, glucose oxidase and ferrocene carboxaldehyde are immobilized to cellulose diacetate on the surface of a needle-type hydrogen peroxide electrode. The surface is then covered with a hydrophobic polyurethane membrane followed by a biocompatible 2-methacryloyloxyethyl phosphorylcholine (MPC) membrane. This sensor was implanted in the subcutaneous tissue of a normal rat for seven days; measurements were only performed during glucose loading every day, while a polarographic voltage of +0.4V was loaded during the experimental periods. The investigators reported that the subcutaneous tissue glucose concentrations could be monitored for up to seven days without any *in-situ* calibrations, followed by 14 days

with one-point *in-situ* calibrations. This approach seems very promising for long-term glucose monitoring. However, the investigators must determine the reproducibility of the results as well as sensor stability upon continuous operation.

2.4. Biocompatibility

2.4.1.Tissue Response to Implanted Sensor

The ideal place to monitor blood glucose is of course in the blood (19). However, because of the threat of infection and thrombosis, it has been important to consider alternatives. The site would not only have to be safe, but it would need to accurately reflect the blood glucose concentration (26). The subcutaneous tissue has been the monitoring site of choice because it meets both these requirements and because of the ease of implantation (18,20,21). The biocompatibility issue arises from recognition of the profound differences between living tissue and nonliving materials. Biocompatibility issues are not whether there are adverse reactions to a biomaterial, but whether that material performs satisfactorily (that is, as intended) in the application under consideration. So, when host and material response are known, a final value judgement is then made that leads to the acceptance or rejection of the material (27).

When a device such as the sensor is implanted in the tissue, interactions between the sensor and tissue must be understood.

Figure 1.5, from reference (28), is an illustration of the non-specific immune response to implantation of a glucose sensor in the tissue; it is not clear whether or not the sensor causes a specific immune response (28).

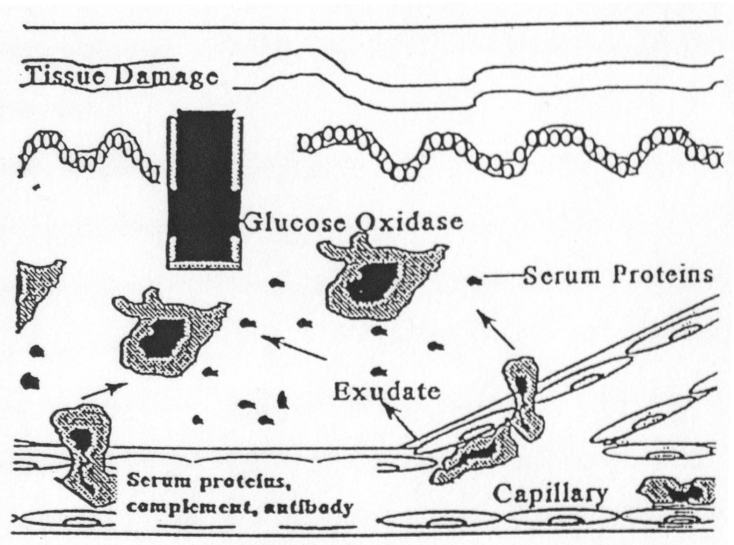

Figure 1.5. Schematic of Implanted Sensor-Tissue Nonspecific Interaction (From reference 28).

The following discussion is taken from material authored by Reichert and Saavedra (29). The initial event upon contact of a foreign material with body fluids is deposition of a layer of adsorbed protein. Protein adsorption occurs within minutes, and the composition and specific activity of the adsorbed protein layer

mediates subsequent interfacial events that lead to inflammation or thrombosis.

Acute inflammation is the short-term response to the presence of the implant and the associated trauma caused by the implantation procedure. Initially, plasma components move into the surrounding tissue bed as a result of vasodilation of the local capillaries and increased permeability of the capillary endothelium. Phagocytic leukocytes designed to degrade foreign objects attempt to engulf the sensor surface.

When a nonadsorbable material such as the sensor is implanted, a chronic inflammatory response is typically observed. It is characterized by the appearance of phagocytic foreign body giant cells at the implant site. After the cellular invasion phase subsides, fibroblast cells migrate into the inflammatory site. Fibroblasts initiate the production of granulation tissue-a highly vascular, reparative tissue that serves as a transient site of collagen formation. After about a week, granulation tissue eventually gives way to a collagenous tissue as remodeling of the wound site takes place; a smooth-surfaced implant will likely be completely encapsulated in a collagenous acellular, avascular fibrous sheath after several weeks of implantation.

The events that follow contact of blood with foreign surfaces leads to the formation of thrombus. One to two minutes after exposure to flowing blood, foreign surfaces are almost completely covered with a layer of blood plasma proteins and adherent platelets. The adsorption of specific proteins (e.g. hageman

factor) and the aggregation, lysis and release of platelet components stimulate the conversion of prothrombin to thrombin. Thrombin then catalyzes fibrin formation. Within minutes, a mature clot (thrombus), composed of a cross-linked fibrin network that entraps leukocytes, erythrocytes, and platelet fragments, is formed. The clot is subsequently invaded by phagocytes. The thrombus can either grow without limit or be dissolved by fibrinolysis and replaced by remodeled tissue, depending upon the implant (surface, shape, mechanical compliance and location, or the leaching of irritating chemicals). In the case of a nonremovable vascular device, such as an implant, the fibrin network is replaced with a layer of tissue termed the pseudo-, neo- or pseudoneointima that covers the surface exposed to blood flow.

The research presented in the following chapters deals with the biocompatibility of the sensor developed in the Wilson group (30,31). Therefore, it is worthwhile to mention some characteristics of sensor-tissue interactions observed for this sensor. The sensor was evaluated using the following biocompatibility tests (1): The Intracutaneous Implantation Test in the rat, the Intracutaneous Irritation Test by intradermal injection in the rabbit, the Confluent Fibroblast Cytotoxicity Test, the Ames Mutagenicity Test, and the Maximization Test in guinea pigs for sensitizing potential. Intracutaneous implantation showed neovascularization and infiltration of plasma cells and lymphocytes. The sensor met the requirements of the intracutaneous irritation

test. The sensor was not found to be cytotoxic, nor was it mutagenic. Also, sensitization was not found.

2.4.2. Sensor Response in Tissue: In-vivo Sensitivity Loss Phenomenon

A run-in time is observed upon implantation of the sensor *in-vivo* (32). This phenomenon consists of two components: background current stabilization and sensitivity loss. There is an initial dramatic loss of sensitivity and a subsequent progressive loss of sensitivity upon continued implantation. The sensitivity can be recovered upon explantation of the sensor and placement in buffer solution (31).

Sensors do not give accurate signals during the run-in period. However, a good correlation between the sensor output and the blood glucose can be made after the run-in period (usually 4-7 hrs. after implantation). According to Zhang and Wilson (33), the sensor output, once the sensitivity is calibrated, must reflect the blood glucose concentration correctly (within a clinically acceptable deviation, for example, 10%) for the desired time length. They reported that the run-in period should therefore be defined as the "true" time required for the sensor to achieve steady state. According to their report, to effectively evaluate the performance of a sensor, the results must demonstrate the stability of the *in-vivo* sensitivity which necessarily requires that more than one

sensitivity calibration and continuous monitoring for an extended period of time be emphasized to avoid misleading conclusions. The reduction of sensitivity decreases the life-time of the sensor. Although the cause of this phenomenon has not be determined, there are a number of explanations. This section will discuss in detail possible causes of the sensitivity loss.

Possible mechanisms of the *in-vivo* sensitivity loss have been reviewed (17,23,31). They include (a) altered glucose, oxygen or peroxide concentration at the implantation site, (b) inhibition of enzyme activity, and/or (c) a decrease in the access of analyte glucose and/or oxygen from the tissue to the enzymatic layer or product hydrogen peroxide to the electrode surface. Mechanisms for the alteration of glucose, oxygen, or hydrogen peroxide concentration at the implantation site are discussed below. Upon insertion of the sensor into the subcutaneous tissue, the tissue is damaged causing bleeding and possible changes in blood flow. This could restrict glucose transport from the blood to the interstitial fluid causing an apparent reduction in sensitivity. However, studies using a subcutaneously implanted wick (33) and microdialysis tubing (34) show subcutaneous glucose levels that are similar to blood glucose levels. Because the damage from needle insertion would be about the same as that for implantation of the wick or microdialysis tube, this doesn't seem to be a likely cause of sensor reduced sensitivity. Another possibility is that glucose is depleted around the sensor because the electrode actively consumes glucose that might be replaced only slowly by its restricted mass

transport through the interstitial fluid. However, this would not explain the recovery of sensor sensitivity after it is explanted (31). Inflammatory cells (mainly monocytes and macrophages) in the exudate fluid at the implantation site may alter the sensor's response by competing with the sensor for glucose (35). While this may contribute to the slow decrease in sensitivity, it is not likely the cause of the initial decrease in sensitivity. Reduction in oxygen partial pressure (PO_2) at the implantation site may also cause an apparent reduction in the sensor's response. However, since direct electron-transfer-mediated sensors (which are essentially oxygen-independent) also suffer reduced *in-vivo* sensitivity (36), it is likely that reduction in oxygen partial pressure would not explain the decrease in sensitivity observed. Finally, decomposition of hydrogen peroxide by catalase might lead to reduction in sensor sensitivity. However, placement of the sensor in buffer solution containing catalase does not alter the sensor's response (32).

It is also possible that the enzyme is inactivated or damaged when the sensor is implanted in the subcutaneous tissue. Inactivation could be due to proteolysis and/or pH changes. However, glucose oxidase has been shown to be very resistant to such factors (37). Inactivation may also be due to hydrogen peroxide accumulation (18). At any rate, if enzyme inactivation does occur, recovery of sensitivity clearly rules out irreversible enzyme inhibition.

Reduction in sensor sensitivity *in-vivo* could be caused by a decrease in access of glucose and/or oxygen from the tissue to the enzymatic layer or of hydrogen peroxide to the electrode surface. Thévenot et al. (38) have observed a decrease in sensor response due to adsorption of calcium chelates onto the platinum electrode. Adsorption of fibrin, biological molecules (i.e. proteins) or cells (i.e. macrophages) on the sensor's surface all have the potential to decrease access of glucose and oxygen to the enzyme layer by blocking the outer membrane. However, although fibrin formation has been observed on the surface of an implanted sensor (32), the sensor's sensitivity is recovered while the fibrin layer is still present. Adsorption of molecules or cells are likely to play a role. This mechanism seems plausible because adsorption of proteins on foreign surfaces and cellular invasion are part of the foreign body reaction to an implanted device. Also, both protein and cells can be removed upon sensor explantation and placement in buffer solution, which would allow the progressive recovery of sensitivity observed. Data supports the hypothesis that the decrease in sensor sensitivity observed *in-vivo* is apparently not due to a property of the *in-situ* environment in which the sensor is placed but to interactions between this environment and the sensor which lead to a modification of sensor sensitivity. It seems possible that this problem could be resolved by modification of the sensor's outer membrane to alter these interactions.

2.5. References

1. Biomatech **1996** and **1997** Reports; Biomatech, Chasse Sur Rhone France, Studies 378E601, 378E602, 378E603, 378E604, and 378E605.

2. Baier, R.E. J. Biomed. *Mater. Res.* **1969**; 3: 191-206.

3. Schichiri, M.; Kishikawaa, H.; Sakakida, M.; Kajiueara, K.; Hashiguchi, Y.; Nishida, K.; Uemura, T.; Konno, Y.; Ichinose, K. *Diabetes Res. Clin. Pract.* **1994**; 24 suppl.: S251-S259.

4. Gamburzev, S.; Atanasov, P.; Wilkins, E. *Sensors and Actuators* B, **1996**; 30: 179-183.

5. American Diabetes Association **1997** Diabetes Info: Diabetes Facts And Figures, www.diabetes.org/ada/c20f.html.p.1-12.

6. Fajans, S.S., "Classification and Diagnosis of Diabetes", in *Diabetes Mellitus, Theory and Practice*, Rifkin, H.; Porte Jr. D., Ed., Elsevier, **1990**, p.346.

7. Reach, G.; Wilson, G.S. *Anal. Chem.* **1992**; 64 (6): 381A-386A.

8. Page, S.R.; Peacock, I. *Diabetes Med.* **1993**; 10: 793-801.

9. The DCCT Research Group. Diabetes Control and Complications Trial (DCCT). *N. Eng. J. Med.* **1993**; 329 (14): 977-986.

10. Moatti-Sirat, D.; Capron, F.; Poitout, V.; Reach, G.; Bindra, D.S.; Zhang, Y.; Wilson, G.S.; Thrévenot, D.R. *Diabetologia* **1992**; 35: 224-230.

11.Clemens, A.H.; Hough, D.L. "Development of the Biostator(Glucose Clamp Algorithm" in *Artificial Systems for Insulin Delivery*, Brunetti, P., Ed., Raven, New York, **1983**, p.399-409.

12.Rao, G.; Glikfeld, P.; Guy, R.H. *Pharm. Res.* **1993**; 10 (12): 1751-1755.

13.Aronowitz, J. TD Glucose Patch, NASA-JDF Workshop on Physiological Analytes-Abstracts **April 7-8, 1998** Washington D.C.

14.TCPI Glucose Monitoring Website: http://www.techchem.com/nonevasi.html.

15.SpecTRX website: http://www.spectrx.com/glucose1.html.

16. Clark, L.C.; Lyons.C. *Ann. N. Y. Acad. Sci.* **1962**; 102: 29-45.

17.Gerritsen, M.; Jansen, J.A.; Kros, A.; Nolte, R.J.M.; Lutterman, J.A. *J. Invest. Surg.* **1998**; 11: 163-174.

18.Armour, J.C.; Lucisano, J.Y.; McKean, B.D.; Gough, D.A. *Diabetes* **1990**; 39: 1519-1526.

19.Yang, S.; Salehi,C.; Atanasov, P.; Wilkins, E. *Anal. Lett.* **1996**; 29(7): 1081-1097.

20.Salehi, C.; Atanasov, P.; Yeung, S.; Wilkins, E. *Anal. Lett.* **1996**; 29(13): 2289-2308.

21.Wilkins, E. Development of Rechargeable Biosensors for In-vivo Glucose Monitoring NASA-JDF Workshop on Non/Minimally Invasive Measurement of Physiological Analytes-Abstracts **April 7-8, 1998** Washington D.C.

22.Aussedat, B.; Thomé-Duret, V.; Reach, G.; Lemmonier, F.; Klein, J.C.; Hu, Y.; Wilson, G.S. *Biosen. Bioelec.* **1997**; 12 (11): 1061-1071.

23.Pickup, J.C.; Claremont, D.J.; Shaw, G.W. *Acta Diabetologia* **1993**; 30: 143-148.

24.Sakakida, M.; Nishida, K.; Shichiri, M. *Sensors and Actuators B* **1993**; 13-14: 319-322.

25.Jaffari, S.A.; Turner, A.P.F. *Physiol. Meas.* **1995**; 16: 1-15.

26.Updike, S.J. *Hospital Practice* March 15, **1996** p.15-16, editorial.

27.Black, J. "Biological Performance of Materials Fundamentals of Biocompatibility" in *Biomedical Engineering and Instrumentation Series*; Vol.8, Plonsey, R. and Katz, J.L., Eds. Marcel Dekker, New York, **1981**, pp.3-5.

28.Fintschenko, Y. *A Problem Driven Approach To The Minaturization and Automation of Enzyme-Based Assays and an Investigation of the Dissipation of Cyanazine and Bromide in Wetland Mesocosms*, Ph.D. Dissertation, The University of Kansas, **1997**.

29.Reichert, W.M.; Saavedra, S.S. "Materials Considerations in the Selection, Performance and Adhesion of Polymeric Encapsulants for Implantable Sensors," in *Materials Science and Technology - a Comprehensive Treatment*, vol. 14 - medical and Dental Materials, D.F. Williams, Ed. VCH, Weinheim, FRG, **1991**, pp. 303-343.

30.Wilson, G.S.; Zhang, Y.; Reach, G.; Moatti-Sirat, D.; Poitout, V.; Thévenot, D.R.; Lemmonnier, F.; Klein, J.C. *Clin. Chem.* **1992**; 38 (9): 1613-1617.

31.Thomé-Duret, V.; Gangnera, M.N.; Zhang, Y.; Wilson, G.S.; Reach, G. *Diabetes and Met.* **1996**; 22: 174-178.

32.Zhang, Y.; Wilson, G.S., Unpublished Data.

33.Fischer, U.; Ertle, R.; Abel, P.; Rebrin, K.; Brunstein, E.; Von Dorsche, H.H.; Freyse, E.J. *Diabetologia* **1987**; 30: 940-945.

34.Bolinder, J.; Ungerstedt, U.; Arner, P. *Diabetologia* **1986**; 35: 1175-1180.

35.Zhang, Y.; Bindra, D.S.; Barru, M.B.; Wilson, G.S. *Biosensors and Bioelectronics* **1991**; 6:653-661.

36.Claremont, D.J.; Sambrook, I.E.; Penton, C.; Pickup, J.C. *Diabetologia* **1986**; 29: 817-821.

37.Wilson, R.; Turner, A.P.F. *Biosen. Bioelec.* **1992**; 7: 165-185.

38.Labat-Allietta, N.; Thévenot, D.R. *Biosensors and Bioelectronics* **1998**; 13(1): 19-29.

3. Chapter 2: Suppression of Protein Adsorption for Improvement of Initial *In-Vivo* Sensitivity Loss

3.1. Background

As discussed in Section 2.4.2, the initial reduction of *in-vivo* sensitivity may be due to the adsorption of proteins on the sensor's surface when it is implanted *in-vivo* (1,2). Traditionally, polymers which have been used to prevent protein adsorption on various material surfaces have been polar but not charged. These include the hydrogels polyethylene oxide, PEO (3), and polyhydroxyethyl methacrylate, polyHEMA, (4). Reichert and Saavedra (5) have reported the various surface modifications used to decrease protein adsorption onto surfaces. Ratner et al. (6) have used RF-plasma deposited oligoglyme films (PEO-like surfaces) to inhibit protein adsorption and cell attachment onto contact lenses. Pretreatment of surfaces with biological molecules like albumin and heparin to improve biocompatibility has not proven to be very successful (7,8).

The idea of incorporating phosphoryl choline onto a material to provide biocompatibility was first proposed by Chapman in 1984 (9,10). He proposed that by mimicking the surface of the red blood cell, which is dominated by phosphoryl choline containing lipids, such polymers would resist protein adsorption similar to the erythrocyte. The phosphoryl choline (PC) moiety shown in Figure 2.1 is thought to be responsible for the erythrocyte's anti-protein adsorption characteristics. Due to the hydrophilic nature of the

phosphoryl choline head group, each is surrounded by approximately ten water molecules; the wettability attained prevents protein molecules from adsorbing to such polymer coated surfaces (9).

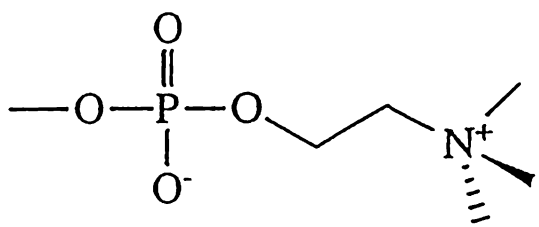

Figure 2.1. Structure of Phosphoryl Choline.

In 1993, Shichiri et al. (11) used a phosphorylcholine-containing polymer as an outer coating for a ferrocene-mediated needle type glucose biosensor for improved biocompatibility. They reported that the polymer 2-methacryloyloxethylphosphorylcholine-co-n-butyl methacrylate, poly (MPC-co-BMA), reduced protein adsorption and improved the *in-vivo* performance of their glucose biosensor.

Biocompatibles Ltd. has prepared phosphoryl choline-containing polymers and studied protein adsorption on various surfaces coated with the polymer (12). As seen in Figure 2.2, which was adapted from reference (12), protein adsorption can be reduced by 95%. In these

experiments, contact activation of fresh frozen plasma (FFP) by uncoated and methacryloyl phosphoryl choline (MPC)/lauryl methacrylate (LM) coated PVC, polycarbonate, and ultra high molecular weight polyethylene (UHMWPE) was determined using a commercially available activated Factor XII (FXIIa) kit produced by Shield Diagnostics (Dundee, Scotland).

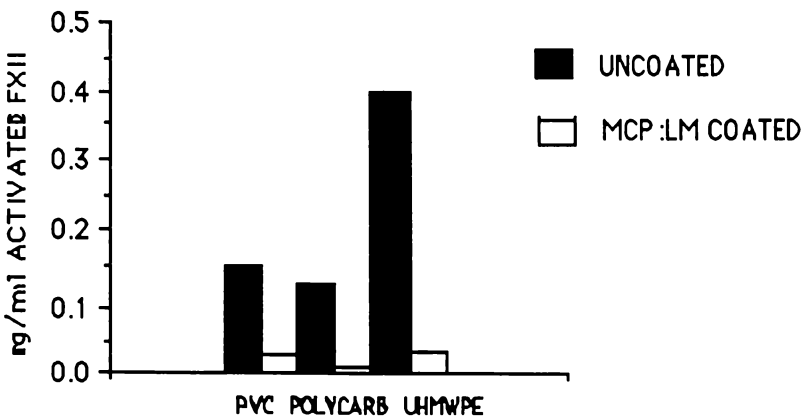

Figure 2.2. Coating of PVC (Polyvinyl Chloride), POLYCARB (Polycarbonate), and UHMWPE (Ultra High Molecular Weight Polyethylene) with MPC:LM Reduced the Amount of Activated FXII Measured in Fresh Frozen Plasma (FFP) Incubated with the Samples Relative to the Uncoated Material (Adapted from reference 12).

In this study, Poly[2-(methacryloyl oxyethyl)-2'-(trimethyl ammonium ethyl phosphate, inner salt]-co-(n-dodecylmethacrylate)(1:2) was used to prevent protein adsorption on the sensor's surface. The structure of the polymer is shown in Figure 2.3.

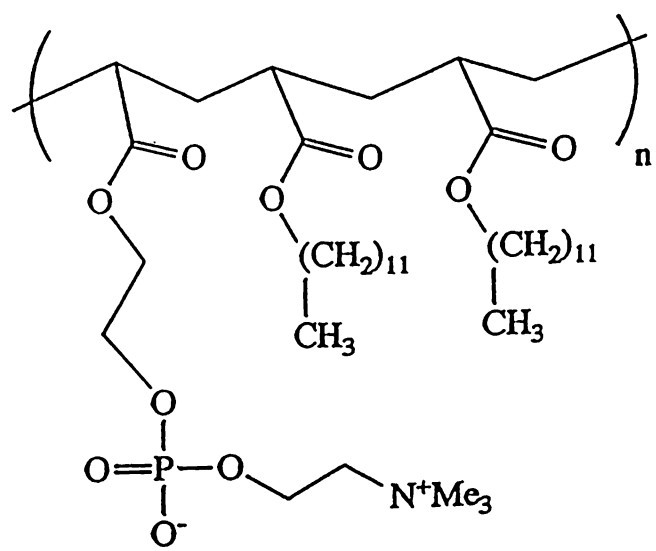

Figure 2.3. Structure of the Phosphoryl Choline Polymer.

The polymer was obtained from Biocompatibles Limited located in the United Kingdom. It was supplied as a purified white powder. The polymer is soluble in methanol, ethanol, and chloroform. The goal of this research was to coat glucose biosensors with the bicompatible PC polymer as an outer layer and in doing so achieve an improvement in the *in-vivo* sensitivity.

3.2. Experimental

3.2.1. Sensor Preparation: Materials and Methods

The 2300 STAT YSI Glucose Analyzer was purchased from Yellow Springs Instruments (Yellow Springs, OH). BD40 Chart recorders were from Kipp & Zonen (Bohemia, NY). Amperometric detectors were purchased from Bioanalytical Systems (West Lafayette, IN). Teflon-coated platinum/iridium (10% iridium) wire, wire o.d. of 0.17mm and overall o.d. of 0.25mm, was from Medwire (Mount Vernon, NY). Silver wire, o.d. of 0.05mm, was purchased from Johnson Matthey Alfa (Ward Hill, MA). Halothane, 2-Bromo-2Chloro-1,1,1-Trifluoroethane, was purchased from Sigma (St. Louis, MO). Both ketamine and xylazine were purchased from the University of Kansas Animal Care Unit.

Solutions were prepared as follows: 0.3M $FeCl_3$ from Aldrich (Wilwaukee, WI) in 1N HCl. 5% cellulose acetate solution: 5.0g of cellulose acetate (39.8% acetyl content, Aldrich) in 95g of solvent, 1:1 ethanol:acetone. 5% polyurethane solution: 5.0g of Tecoflex™ polyurethane, SG85A (Thermedics, Woburn, MA) in 95g of solvent, 94g tetrahydrofuran + 1g dimethylformamide. Nafion perfluorinated ion-exchange powder solution, 5% solution in a mixture of 10% water and lower aliphatic alcohols (Aldrich) was used as purchased. 0.1M phosphate buffer: 24.6g disodium phosphate, 4.4g potassium phosphate (monobasic), 0.2g sodium azide and 11.7g sodium chloride were dissolved in 2L of deionized distilled water and the pH was adjusted to pH 7.4 with 5M HCl or NaOH solutions. 8% glucose oxidase solution: 20mg glucose oxidase (approximately 200-250 U/mg, Biozyme Laboratories International, San Diego, CA) in 0.25ml phosphate

buffer. 4% bovine serum albumin solution: 20mg bovine serum albumin (Sigma) in 0.5ml phosphate buffer. 12% glutaraldehyde solution: 25% reagent glutaraldehyde (Aldrich) was diluted by adding an equal amount of deionized distilled water. 1.39M glucose (Sigma) solution, 75% ethanol solution, and 10% heparin (Sigma) solution were all prepared using deionized distilled water.

Teflon coated Pt/Ir wire was cut into 40mm lengths. A circular cut was made in the teflon coating 6mm from the tail end and the 6mm teflon sleeve was removed to expose the metal wire which serves as the lead contact. A 0.05mm Ag wire was wrapped onto the sensor body starting 2mm from the teflon edge (7mm from the exposed Pt/Ir tip), extending up to 6mm from the other end (the distal end). The total length of the silver coil was ~27mm. A Ag/AgCl layer was created on the distal half of the silver coil by oxidation in a solution containing $FeCl_3$ (ferric chloride). A sensing cavity was created at the distal end by cutting the teflon ~6mm from the end and pushing the teflon until ~2.5-3.0mm metal surface was exposed. The extra teflon was then cut and removed.

Inner Membrane: The distal end of the sensor was dipped into a solution of 5% cellulose acetate and withdrawn slowly in a vertical manner. The layer was dried for about 5 minutes and the dip-coating step was repeated two more times. A copper wire loop ~3-4mm diameter was filled with Nafion™ solution and the sensor was coated by passing the sensor through the loop (forth and back) in a horizontal direction. The motion of the sensor was perpendicular to the loop. The layer was dried for 7-8 minutes in air. The step was repeated two more times. The dip-coating of cellulose acetate was repeated

two more times. The Nafion™ loop-coating was repeated two more times. The sensor was kept in a clean environment for enzyme immobilization.

Enzyme membrane: 50µl of 8% glucose oxidase, 50µl of 4% bovine serum albumin, and 1.5µl of 12% glutaraldehyde were mixed together. 0.4µl of this solution mixture was added to one half of the sensing cavity with a microsyringe while keeping the sensor horizontal. The drop was allowed to dry and crosslink for 4-10 minutes until almost dry. Another 0.4µl of the same glucose oxidase solution mixture was delivered to the other half of the cavity and allowed to dry for 15-20 minutes. The sensor was soaked in deionized distilled water for 5-10 minutes and then dried completely (~30 minutes) for the outer membrane coating.

Outer Membrane: An ideal situation would be to use the PC polymer as an outer membrane for the biosensor. However, unlike polyurethane, the PC polymer does not provide a barrier to glucose flux necessary for a glucose diffusion-controlled response. The PC polymer does however allow oxygen to freely diffuse, another requirement of the outer membrane. Therefore, the glucose biosensor was prepared with the phosphoryl choline (PC) polymer coated on top of the polyurethane (PU) layer. The sensing element and AgCl was loop-coated with 5% polyurethane solution. The coating was dried for approximately 45 seconds to 1 minute. The sensor was placed in phosphate buffer solution for approximately 1-2 weeks until the response stabilized. After stabilization, the PC polymer was coated on top of the polyurethane layer. 10mg/ml PC polymer was dissolved in a 9:1 volume:volume mixture of hexane:ethanol; ethanol solvated

the polymer while hexane was added to prevent disruption of the underlying membrane layer(s) which was found to occur with use of ethanol alone. Sensors were loop coated with the PC polymer solution and air dried approximately 45 seconds at which time the solvent remaining in the loop had evaporated. The sensors were then placed in 0.1M phosphate buffered saline pH 7.4 for a stabilization period of 1-2 weeks.

3.2.2. *In-Vitro* Experiment: Set-up and Conditions, and Sensitivity and Linear Range Determination

The experiment was performed in a 37°C thermostated cell to which 5ml of 0.1M phosphate-buffered saline was added. Sensors were fixed in the cell using a rubber stopper, and a stir bar was added. The platinum/iridium working electrode lead wire and silver reference electrode lead wire were connected to the detector, which in turn was connected to a chart recorder. A constant voltage of +600mV was applied to the working electrode.

After a stable background current response was established, usually ~30 minutes, glucose was added to the cell. Glucose solution was added in 18µl increments so that after each increment the final concentration of glucose in the cell was 5mM, 10mM, 15mM, and 20mM, respectively. 90% of the steady state current achieved after each increment was recorded. A calibration curve was prepared by plotting the current values versus the corresponding glucose concentration values. The data was fit to a linear regression curve. The slope of the curve was the sensitivity of the sensor in nA/mM. The linear

range was from 1mM glucose to the glucose concentration at which the curve deviated significantly from a linear regression curve.

3.2.3. *In-Vivo* Experiment: Set-up and Conditions and Sensitivity Coefficient, Apparent Subcutaneous Glucose Concentration, and Extrapolated Background Current

In-vivo procedures were approved by the Internal Animal Care and Use Committee (IACUC) at the University of Kansas. Male Sprague Dawley rats weighing 250-450 grams were used in the experiments. Anesthesia was given first by placing the rat in an air-tight bowl containing halothane dabbed tissue. After the animal was down, an intramuscular injection of ketamine (.5ml) and xylazine (.2ml) mixture was administered. Subsequent injections of .35ml ketamine were given as necessary, approximately every hour, to maintain the animal under anesthesia. The rat was then placed on a thermostated pad maintained at 37°C. The back of the rat was shaved and the area was cleaned with 75% ethanol. The sensor was placed inside a 21-gauge needle and the needle and sensor were inserted into the subcutaneous tissue. The needle was removed, leaving the sensor in place. A potential of +600mV was then applied to the working electrode and the output current was monitored.

The sensor's output was allowed to stabilize for 2 to 4 hours. The basal blood glucose level was determined by clipping the end of the animal's tail and squeezing a few drops (~75µl) of blood into a microcentrifuge tube containing ~1µl of 10% heparin solution. The sample was centrifuged and the plasma glucose concentration was

determined using a glucose analyzer. This procedure was repeated until a stable glucose reading and sensor output was reached. Then, ~1ml of 25% glucose solution was injected intraperitoneally. Following glucose injection, blood glucose concentration and sensor output reached a new plateau. The pre-glucose and post-glucose steady states of the blood glucose level and of the sensor output current were used to calculate an *in-vivo* sensitivity coefficient (S.C.), expressed in nA/mM, as the ratio between the change in the sensor current and the change in glucose concentration and an extrapolated *in-vivo* residual current (I_o) which would be observed in the absence of glucose (13). The calculated apparent subcutaneous glucose concentration (A.S.G.C.) was obtained by subtracting from the sensor current observed at a given time (I), the *in-vivo* background current (I_o), and then by dividing the resultant current by the *in-vivo* sensitivity coefficient (S.C.). An *in-vivo* two-point calibration was used to determine the *in-vivo* sensitivity coefficient, apparent subcutaneous glucose concentration, and *in-vivo* background current (I_o) as follows:

$$S.C. = \Delta I / \Delta C$$

And

$$A.S.G.C. = (I - I_o)/S.C.$$

3.2.4. Electron Spectroscopy for Chemical Analysis (ESCA)

ESCA was performed on sensor materials as well as the sensor to determine whether or not the phosphoryl choline polymer membrane was present on the surface of the sensor, as expected. The experiments were performed at the National ESCA and Surface Analysis Center for Biomedical Problems (NESAC/BIO) at the University of Washington with NIH funds (RR-01296). The explanation of ESCA given below is taken from the book by Baker and Betteridge (14) which gives a good review of ESCA and from the book by Barr which discusses the principles and practice of ESCA (15). A schematic diagram of the components of a typical ESCA instrument is shown in Figure 2.4 (Adapted from reference 16).

ESCA, also called X-ray Photoelectron Spectroscopy or XPS, is based upon the photoelectron effect. X-rays are focused upon a specimen in the analysis chamber. Electrons can be expelled from any orbital if the associated ionization potential is less than the energy of the impacting x-rays. Ejected electrons possess a quantity of kinetic energy approximately equal in magnitude to the difference between the energy imparted by the x-ray photons and the orbital ionization potential. Electrons that are ejected within a solid angle of acceptance of a slit within the target chamber then enter the focusing electron analyzer through this slit. Once inside the analyzer, electrons take different paths depending upon their energies and the voltage applied to the analyzer plates. A spectrum is recorded by sweeping the voltage so that progressively less energetic electrons come into focus on the exit slit, through which

they can pass, be detected, and displayed. The equation which describes this process is BE = hν - KE, where BE is the orbital ionization potential or the energy with which the electron is bound to an atom (the value sought), KE is the kinetic energy of the emitted electron (the value measured) and hν is the x-ray energy for which h is Planck's constant and ν is the photon frequency (a known value). Energy values obtained can provide information about the nature and environment of the atoms from which the electrons came.

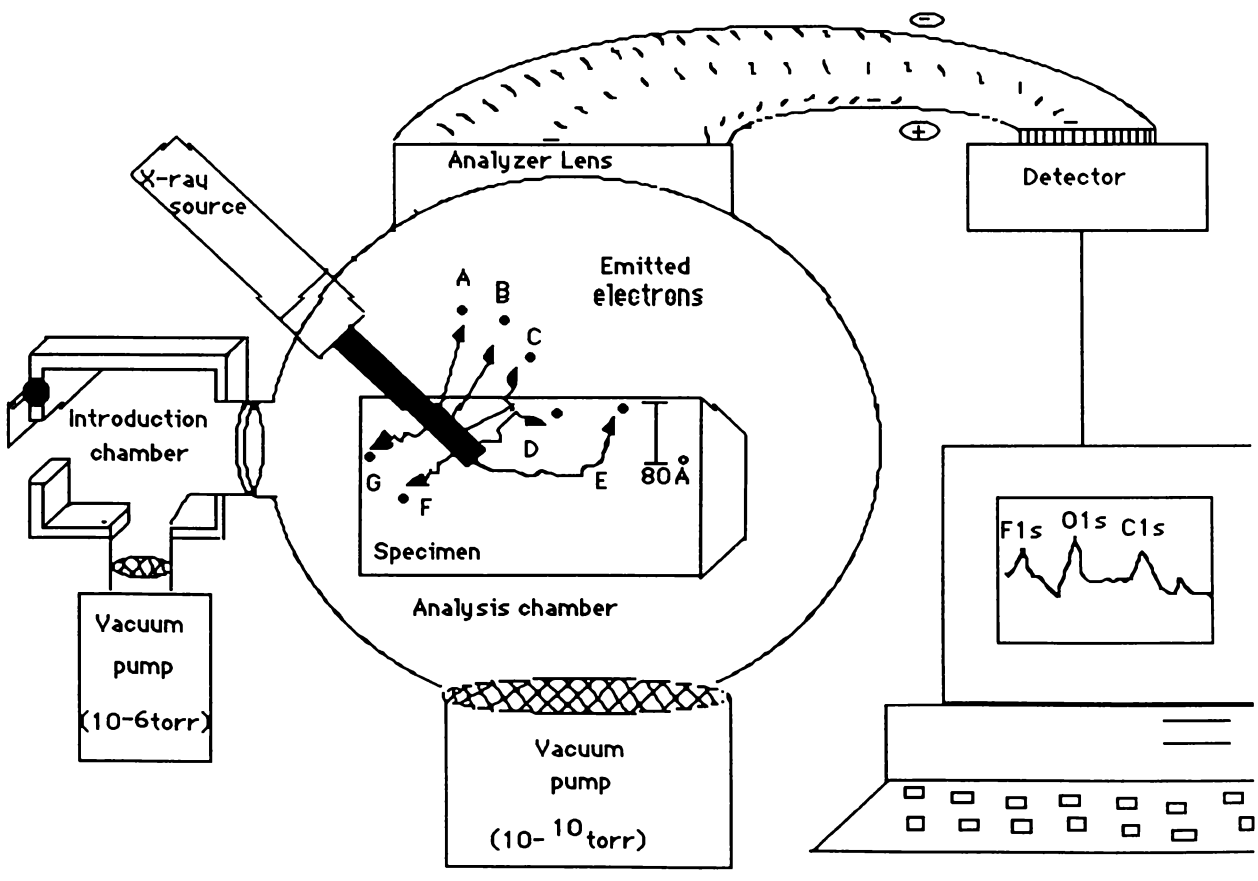

Figure 2.4. Schematic Diagram of a Typical ESCA Instrument (Adapted from reference 16).

Samples were packaged in pouches before shipment to the center for analysis. A total of 5 samples were sent for analysis. Table 2.1 describes the content of each sample. The sensors tested were bent as needed to facilitate mounting in the chamber. Spectra were taken from two or three points for each sample. The elemental composition of each sample was determined by surveying spectra over the energy region 0-1000 eV. High resolution spectra of the C(1s) peak were also taken.

Table 2.1

Description of samples analyzed by ESCA

SAMPLE #	SAMPLE CONTENT
A-1	Solid Tecoflex™ Polyurethane (PU)
A-2	5% PU dissolved in a mixture of 98% THF and 2% DMF
A-3	10mg/ml Phosphoryl Choline (PC) polymer dissolved in 9:1 hexane:ethanol by volume and coated on a bare Pt/Ir wire
A-4	Glucose biosensor with PC outer membrane
A-5	Glucose biosensor with polyurethane outer membrane which had been implanted in a rat for ~ 2 1/2 hrs.

The following ESCA experimental procedures and conditions were provided in a report from NESAC/BIO: Analysis were performed on a Surface Science Instrument (SSI) X-probe ESCA instrument which permits analysis of the outermost 20-100 Å of a sample in an elliptical area. The largest spot was used, with approximate

dimensions of 1700 μm by 1000 μm. The nominal take-off angle (the angle between the sample normal and the input axis of the energy analyzer) was 55° for all spectra, however, given the curvature of these samples it is reasonable to assume that photoelectrons from a range of take-off angles reached the detector. Typical pressure in the analysis chamber during spectral acquisition was 10^{-9} torr. An aluminum K $\alpha_{1,2}$ monochromatized X-ray source was used to stimulate photoemission. The energy of electrons emitted from the sample was measured with a hemispherical energy analyzer operating at a pass energy of either 150 eV (for the determination of elemental composition) or 50 eV (for C (1s) high-resolution acquisitions). Lower pass energies provide higher spectral resolution; higher energies permit more rapid data acquisition and more accurate quantitative analysis. SSI data analysis software was used to calculate the elemental compositions from peak areas and to peak fit the high resolution C (1s) spectra. A low energy electron gun was used for charge neutralization. In the case of high-resolution spectra, the binding energy scale for the reported peak energies was referenced by setting the CHx peak maximum in the C (1s) spectrum to 285.00 eV.

3.3. Results

3.3.1. Sensor *In-Vitro* Characteristics: Sensitivity, Linear Range, Stability and % Error

Standard curves and stability curves for the sensors used in this study are shown in Figures 2.5 and 2.6, respectively. The *in-vitro* data is summarized in Table 2.2. The results obtained for the sensors were similar to results obtained for typical sensors prepared with a polyurethane outer layer. The sensitivity of the six sensors ranged from 0.76 nA/mM to 10.1 nA/mM. The correlation coefficient was 0.99 for all sensors. The sensors were stable with ≤ 10% error over a two-week test period. In general, the sensitivity of the sensors decreased slightly after the PC coating, with the exception of sensor#3 which had an ~50% decrease in sensitivity. Sensors#1, #3, #4, #5, and #6 were linear up to 15mM glucose. However, Sensor#2 was only linear up to 9mM glucose. Generally, higher sensitivity sensors have poorer linear range. Reasonable % error was obtained for 4 out of 6 sensors: 26% for sensor#1, 27% for sensor# 2, 20% for sensor#5, and 13% for sensor#6. With the exception of sensor#3 and sensor#4, the sensors were stable with ≤ 27% error over a two week period during which the sensitivity of each sensor was tested several times, 2 to 6 days apart. The % error was calculated using the following equation:

$$\% \text{ Error} = \frac{S_B - S_F}{S_B} \times 100$$

Where S_B = sensitivity before PC coating

S_F = Sensitivity furthest from value before PC coating

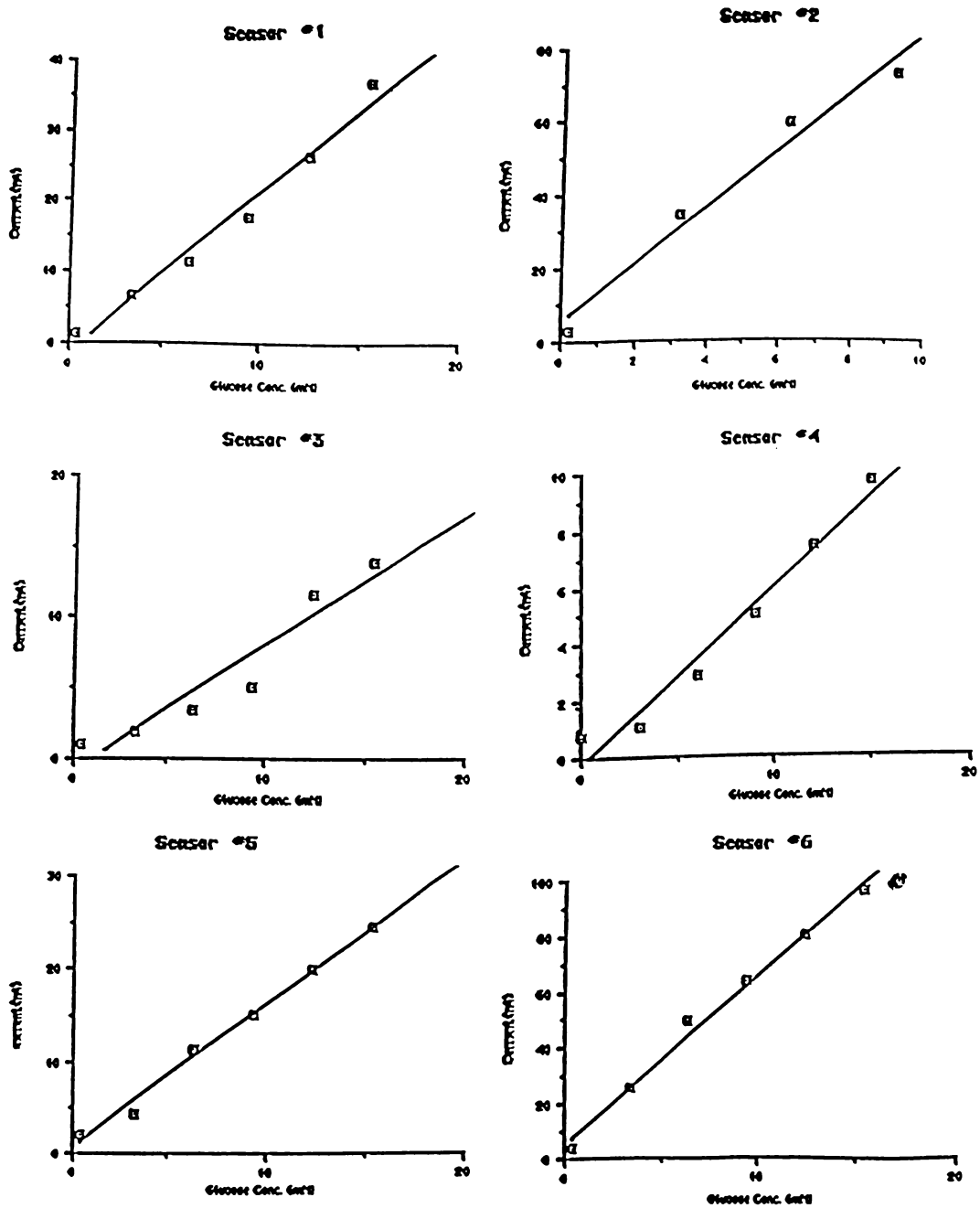

Figure 2.5. Standard Curves for Sensors before PC Outer Membrane.

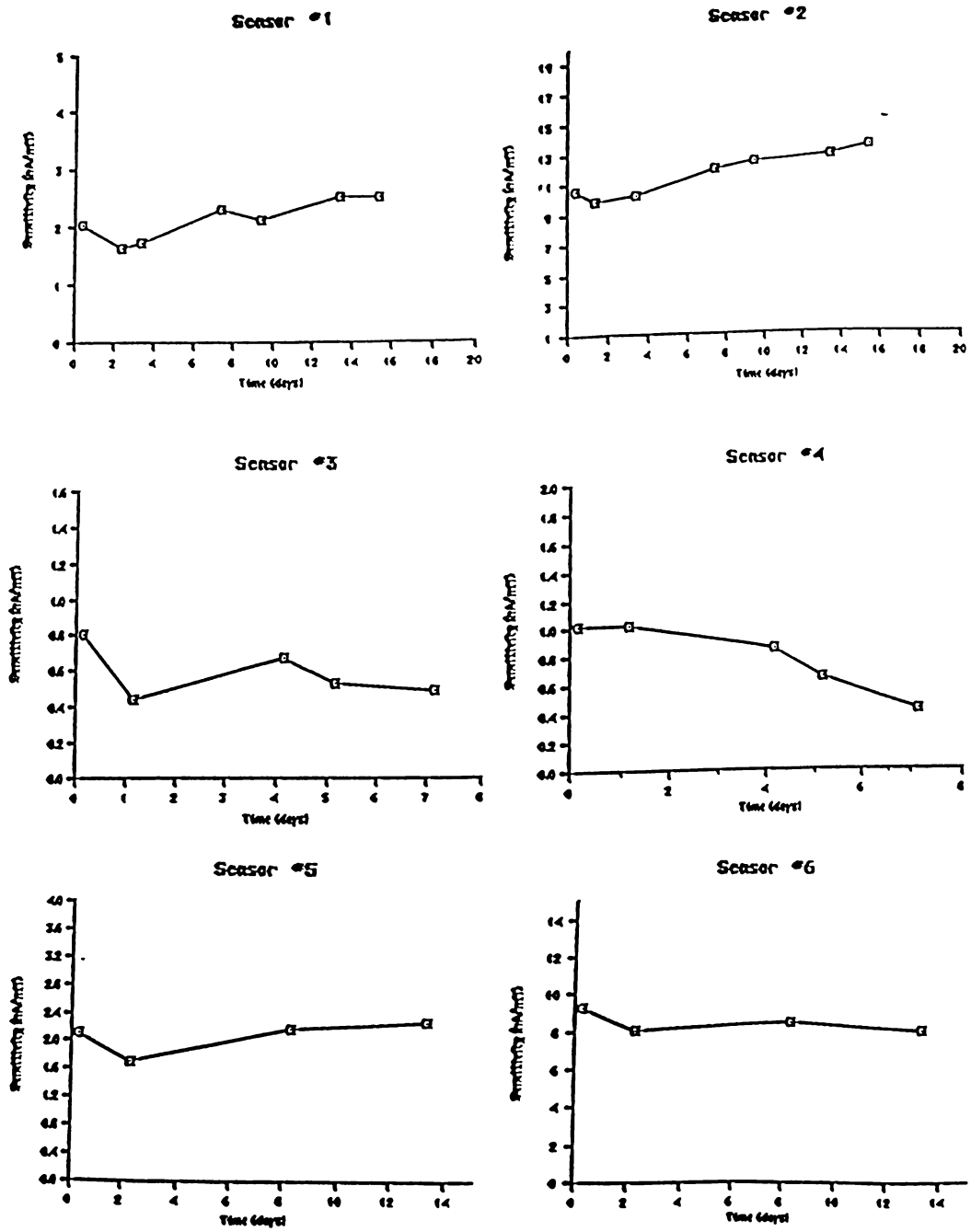

Figure 2.6. Stability Curves for Sensors Prepared with the PC Outer Membrane

Table 2.2

In-vitro data for 6 sensors prepared with the PC outer membrane

SENSOR#	SENSITIVITY BEFORE PC LAYER (nA/mM)	SENSITIVITY AFTER PC LAYER (nA/mM)	LINEAR RANGE (mM)	* 14 DAY STABILITY (nA/mM)	% ERROR
1	1.9	1.5	0-15	1.9±0.5	26
2	10.1	9.4	0-9	10.1±2.7	27
3	0.76	0.40	0-15	0.76±0.36	47
4	0.97	0.97	0-15	0.97±0.59	61
5	2.0	1.6	0-15	2.0±0.4	20
6	8.9	7.7	0-15	8.9±1.2	13

* n = 7 for sensor#1 and sensor#2

n = 5 for sensor#3 and sensor#4

n = 4 for sensor#5 and sensor#6

where n = number of measurements made

3.3.2. *In-vivo* Sensitivity

The *in-vivo* experiment was performed as described in Section 3.2.3. Two sensors were implanted in one rat: sensor#1 and sensor#2 were implanted in rat 1, sensor#3 and sensor#4 were implanted in rat 2, and sensor#5 and sensor#6 were implanted in rat 3. The *in-vivo* sensitivity was determined using the 2 point calibration method. Table 2.3 shows the *in-vivo* results.

Table 2.3

Results of *In-vivo* Experiments in which Glucose Biosensors were Coated with the PC Outer Membrane

SENSOR#	SENSITIVITY (nA/mM)			%CHANGE FROM *IN-VITRO* TO *IN-VIVO*	BACKGROUND CURRENT (nA)
	PRE-*IN-VIVO*	*IN-VIVO*	POST-*IN-VIVO*		
1	2.4	3.3	3.7	+27	-14.3
2	12.8	0.71	12.8	-95	4.4
3	0.45	4.0	0.44	+89	-34.5
4	0.38	9.6	0.94	+96	-87.5
5	2.2	0.10	0.86	-95	0.80
6	7.7	0.80	7.8	-90	-5.9

Half the sensors (sensors#2, #5, and #6) showed a decrease in sensitivity *in-vivo* compared to the pre-*in-vivo* sensitivity, while the other half (sensor#1, #3, and #4) showed an increase in sensitivity *in-vivo* compared to the pre-*in-vivo* sensitivity. The decrease in sensitivity by 90-95% *in-vivo* was similar to the decrease observed for sensors prepared with PU as the outer membrane. The sensors which showed an increase in sensitivity *in-vivo* increased by 27% for sensor #1, 89% for sensor #3, and 96% for sensor #4. For these sensors, the background currents calculated were large and negative compared to the usual *in-vivo* values of ~ 1 nA to 5 nA obtained for sensors prepared with the PU outer membrane.

3.3.3. Electron Spectroscopy for Chemical Analysis (ESCA)

Table 2.4 lists the expected atoms for each sample.

Table 2.4

Expected atoms for each sample analyzed by ESCA

SAMPLE#	SAMPLE CONTENT	EXPECTED
A-1	Solid Tecoflex™ Polyurethane (PU)	C, N, O
A-3	10mg/ml Phosphoryl Choline (PC) polymer dissolved in 9:1 hexane:ethanol by volume and coated on a bare Pt/Ir wire	C, N, O, P
A-4	Glucose biosensor with PC outer membrane	C, N, O, P
A-5	Glucose biosensor with polyurethane outer membrane which had been implanted in a rat for ~ 2 1/2 hrs	C, N, O

Only spectra for samples A-1, A-3, A-4, and A-5 are given in Figures 2.7, 2.8, 2.9, and 2.10, respectively, because the contents of sample A-2 evaporated before analysis. Although spectra were taken from two or three points for each sample, only one spectrum for each sample is given. Composition and peak fitting results are given in Tables 2.5, 2.6, 2.7, and 2.8 for samples A-1, A-3, A-4, and A-5, respectively. Binding energy values given in the tables have been

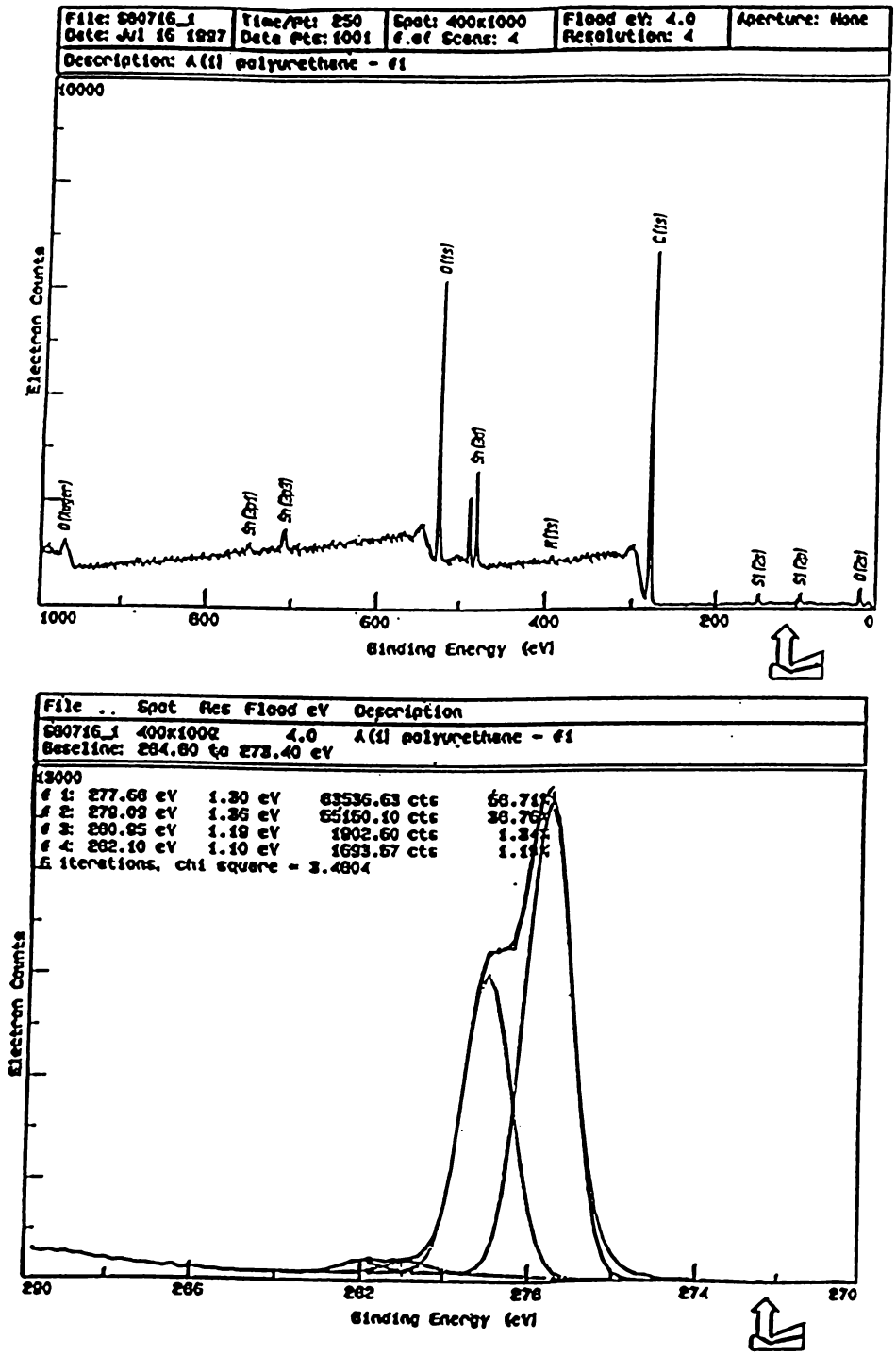

Figure 2.7. ESCA Spectrum for Sample A-1 (Polyurethane).

Table 2.5.

Composition and Peak Fitting Results for Sample A-1 (Polyurethane).

	Atomic Percent Surface Elemental Composition				
A(1)	C	O	Si	Sn	N
1	75.2	20.9	1.8	1.2	1.0
2	74.2	20.6	2.8	1.2	1.3

	C1s		
A(1)	BE (eV)	FWHM (eV)	Area (%)
1	285.0	1.30	58.7
	286.4	1.36	38.8
	288.3	1.19	1.3
	289.2	1.10	1.2
2	285.0	1.36	60.8
	286.4	1.37	36.5
	288.4	1.20	1.4
	289.4	1.16	1.3

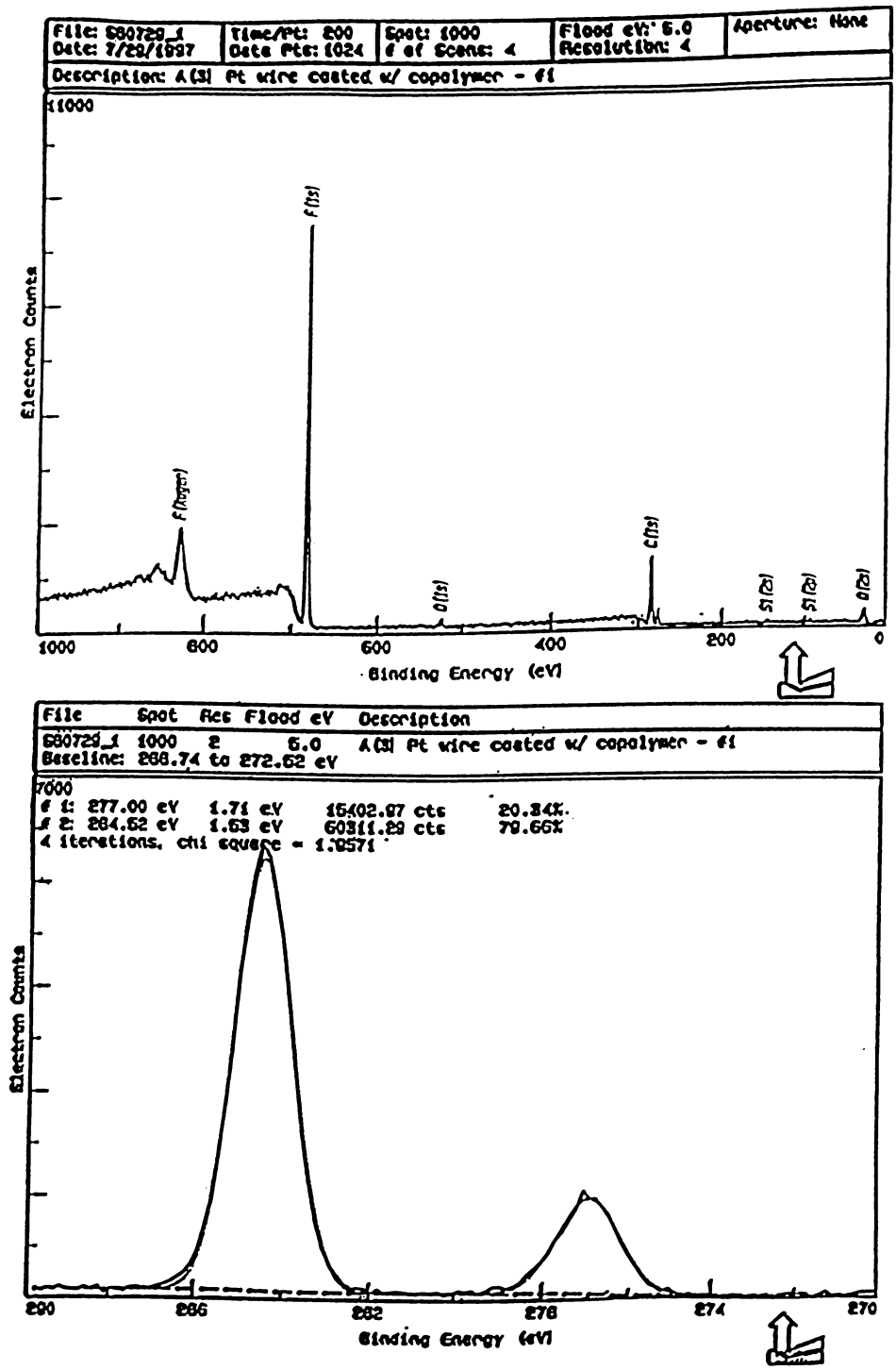

Figure 2.8. ESCA Spectrum for Sample A-3 (Phosphoryl choline polymer-coated wire).

Table 2.6.

Composition and Peak Fitting Results for Sample A-3 (Phosphoryl choline polymer-coated wire).

	Atomic Percent Surface Elemental Composition			
A(3)	C	O	F	Si
1	37.7	2.1	58.6	1.7
2	38.2	2.3	58.5	1.0
3	36.7	1.6	61.8	trace

	C1s		
A(3)	BE (eV)	FWHM (eV)	Area (%)
1	285.0	1.71	20.3
	292.5	1.53	79.7
2	285.0	1.83	23.2
	292.4	1.56	76.8
3	285.0	1.82	14.9
	292.5	1.55	85.1

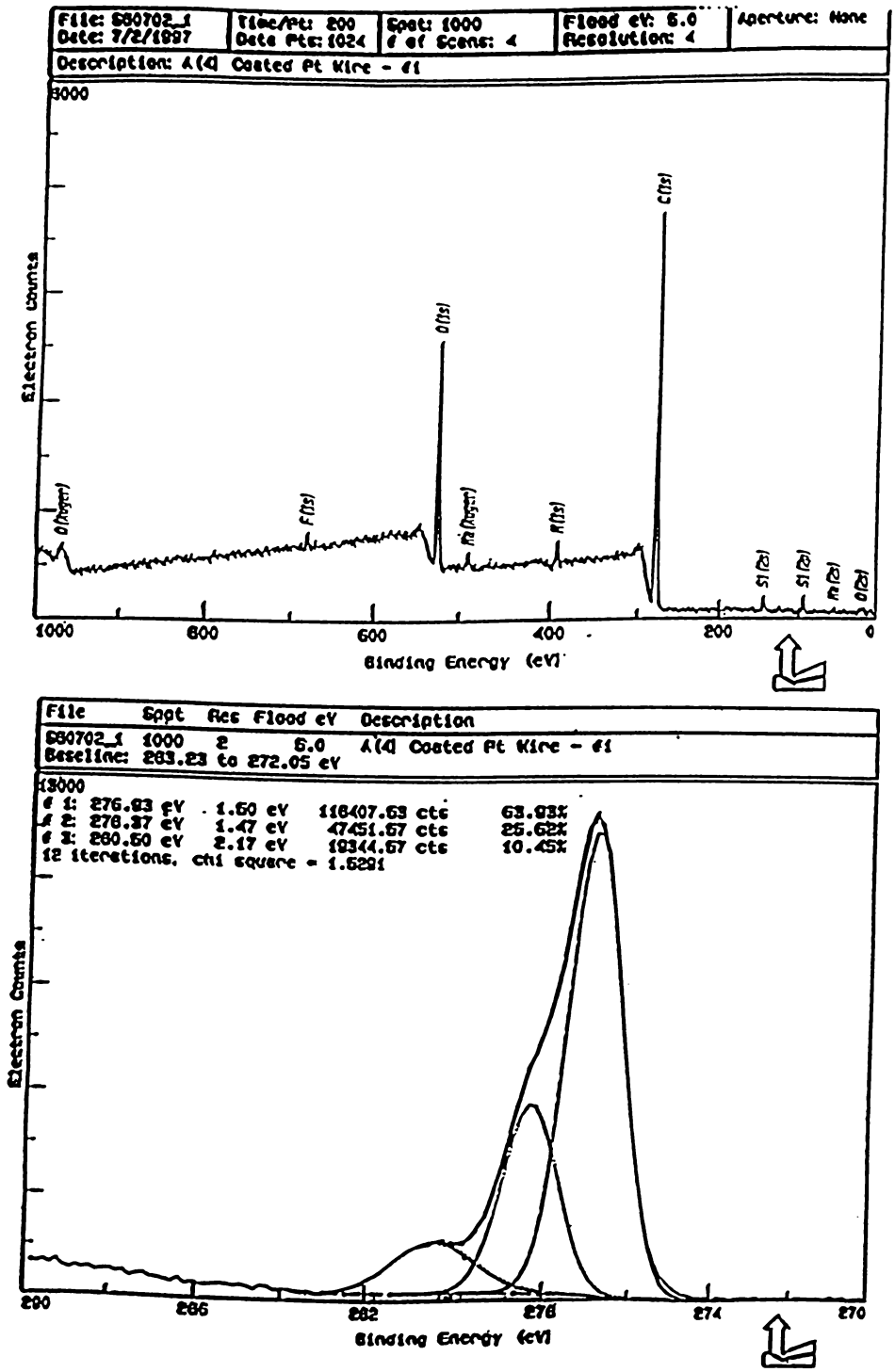

Figure 2.9. ESCA Spectrum for Sample A-4 (Phosphoryl choline polymer coated on sensor surface).

Table 2.7.

Composition and Peak Fitting Results for Sample A-4 (Phosphoryl choline polymer coated on sensor surface).

	Atomic Percent Surface Elemental Composition					
A(4)	C	O	Si	N	Na	F
1	73.2	19.3	3.8	2.4	1.2	trace
2	77.8	16.7	2.0	3.5	trace	trace
3	85.6	11.8	trace	2.6	nd	nd

	C1s		
A(4)	BE (eV)	FWHM (eV)	Area (%)
1	285.0	1.50	63.9
	286.4	1.47	25.6
	288.6	2.17	10.5
2	285.0	1.52	71.1
	286.6	1.58	20.8
	288.9	1.53	8.2
3	285.0	1.42	73.1
	286.5	1.46	18.9
	289.0	1.17	8.0

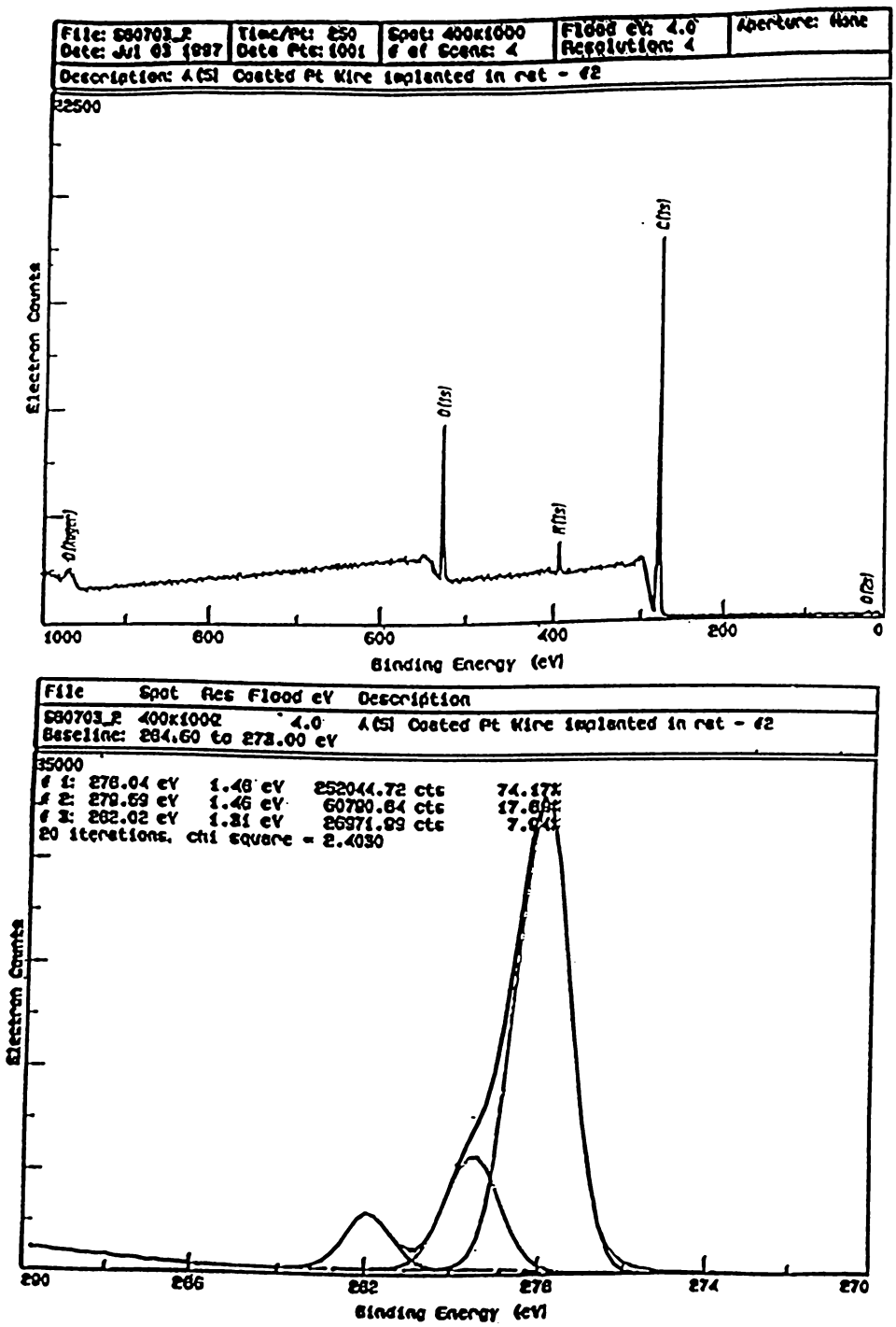

Figure 2.10 ESCA Spectrum for Sample A-5 (Implanted sensor).

Table 2.8.

Composition and Peak Fitting Results for Sample A-5 (Implanted sensor).

Atomic Percent Surface Elemental Composition			
A(5)	C	O	N
1	82.4	14.4	3.2
2	83.0	14.1	2.9

	C1s		
A(5)	BE (eV)	FWHM (eV)	Area (%)
1	285.0	1.48	74.2
	286.6	1.46	17.9
	289.0	1.31	7.9
2	285.0	1.44	75.6
	286.6	1.41	16.8
	289.0	1.25	7.6

corrected for charging, but the binding energy values in Figures 2.7, 2.8, 2.9, and 2.10 have not been corrected.

Sample A-1 consisted of Tecoflex™ polyurethane, the polymer normally used as the sensor's outer membrane. Figure 2.11 shows the structure of Tecoflex™ polyurethane.

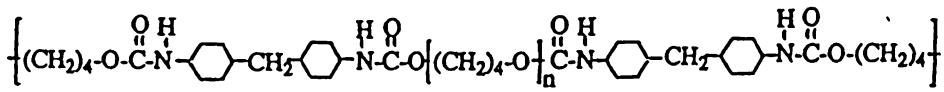

Figure 2.11. Structure of Tecoflex™ Polyurethane.

Tecoflex™ is a segmented polyurethane containing "soft" segments formed by polyether residues and "hard" cyclohexane segments formed by urethane and urea linkages (17). This polymer should therefore give rise to C, N, and O atomic spectra, as was the case, Figure 2.7 top spectrum. Small amounts of tin (Sn) and silicon (Si) were also detected, the former being presumably residual catalyst. The polymer can be identified by the ratio of the percent peak area due to different C bonds in the C (1s) high resolution spectrum (Figure 2.7 bottom spectrum). The hydrocarbon C-H bond, the lowest binding energy peak at 277.68eV, represents 58.71% of the total C (1s) peak area. The ether C-O bond, the second lowest binding energy peak at 279.09eV, represents 38.76% of the total peak area. The urethane C=O linkage, the highest binding peak at 282.10eV, represents 1.19% of the total peak area. The second highest peak at 280.95eV, which

represents 1.34% of the total peak area, was hard to fit. This spectrum, however, is consistent with that of Tecoflex™ polyurethane.

For sample A-3, a cavity was created on a teflon-coated platinum-iridium wire by stripping away 2.5-3 mm of teflon and coating the wire with 10mg/ml PC polymer dissolved in 9:1 hexane:ethanol by volume. According to Figure 2.3 and Table 2.4, the phosphoryl choline polymer should contain C, N, O and P atomic spectra. However, Figure 2.8 (top spectrum) reveals the presence of large amounts of F in the spectrum and a small C (1s) peak. Based upon this result, it was concluded that sample A-3 contained polytetrafluoroethylene (PTFE) or teflon. If this is the case, then the oxygen and silicon detected would be contaminants and the fluorine-to-carbon ratio is low. The C-F contribution is seen in the C (1s) high resolution peak envelope as the highest binding energy peak. Also, there is significant hydrocarbon contamination evident in the C (1s) envelope in the lowest binding energy peak. This result was unexpected. There should have been a large C (1s) peak and no F peak for the PC sample. This spectrum was consistent with that of polytetrafluoroethylene or teflon. Perhaps the sample was incorrectly positioned and the x-rays bombarded the teflon insulation covering the electrode instead of bombarding the sensing cavity which contained the PC polymer.

Sample A-4 consisted of a glucose biosensor prepared as described in Section 3.2.1. (PC layer on top of PU layer). The expected atoms for the PC polymer are C, N, O and P, as shown in Figure 2.9 top spectrum. All atoms except P were detected. This

may have been due in part because P represents such a small part of the polymer. Three different analyses of this sample were carried out. As seen in Table 2.7, the carbon and oxygen content vary significantly from point to point in this data set, as does the breakdown of the C(1s) peak fit results. In general, however, they are consistent with the PC polymer. There was some contamination from Si, Na, and F. The high-resolution C(1s) peak fit (Figure 2.10 bottom spectra) shows somewhat less hydrocarbon (the lowest binding energy peak at 276.93eV) and more C-O at 278.37eV and C=O at 280.50eV than expected. There may have been some contribution from the underlying polyurethane layer.

Sample A-5 contained a glucose biosensor (polyurethane outer membrane) which had been implanted ~2.5 hrs. *in-vivo*. This spectrum (Figure 2.10) is essentially the same as that of Figure 2.7 for sample A-1, but without the presence of Sn and Si contamination. Because proteins are thought to be the cause of the *in-vivo* sensitivity loss, it was hoped that by comparing these ESCA results with that of polyurethane which had not been exposed to tissue (sample A-1), evidence of protein adsorption might be observed. If proteins are adsorbed onto the polyurethane surface, we would expect to see an increase in the %C, %O, and %N for sample A-5 compared to sample A-1. We might also see contribution from the protein to the polyurethane C (1s) high resolution peak. While the %C and %N increased for sample A-5 compared to sample A-1 (~9% increase and ~69% increase, respectively), the %O decreased (~31% decrease). Also, it was difficult to unambiguously conclude that proteins

contributed to the high resolution C (1s) spectrum because of spectral overlap between the polyurethane membrane and the proteins.

3.4. Discussion

It was assumed that proteins are responsible for the sensitivity loss phenomenon. Based upon results obtained for sensors prepared with the PC polymer as an outer membrane, it is questionable whether or not the polymer will be useful for suppression of protein adsorption *in-vivo*.

There was some concern about the stability of the PC polymer as the outer membrane on the glucose biosensor. The presence of the PC polymer was confirmed by ESCA (Sample A-4); however, this was not proven for a statistically significant number of sensors. In fact, it is possible that at least for the sensors that showed 90-95% loss in sensitivity *in-vivo* that the PC polymer was not present on the surface. In this case, polyurethane would have been exposed to the tissue and the resulting loss in sensitivity *in-vivo* would have been expected.

There could have been two reasons for the increase in sensitivity *in-vivo* observed for the other half of the sensors. Firstly, uptake of water may have led to an increase in glucose permeability and a subsequent increase in sensitivity. However, because of the large increase in sensitivity *in-vivo* compared to the pre-*in-vivo* value and measurement of markedly lower post-*in-vivo* sensitivity values for sensors#3 and #4 after explantation, this explanation is not as likely as a nonlinear response *in-vivo*.

Evidence to support this explanation is the large negative background current observed. A large negative value calculated for the background current in conjunction with an increase in sensitivity is usually indicative of a nonlinear response.

ESCA results for the sensor which had been implanted in a rat for ~2 1/2 hours did not confirm the presence of proteins on the sensor's surface. Because the polyurethane membrane and proteins contain the same elements (C, N, and O), it may be difficult to determine the contribution from proteins to the polyurethane membrane. Perhaps another method like FTIR could be used to complement the ESCA analysis.

Thus, from these experiments it is still not clear whether or not the PC polymer prevents protein adsorption *in-vivo* as it has been shown to do *in-vitro*, assuming that proteins are responsible for the sensitivity loss. There are experiments which need to be carried out in order to help clarify some questions which still remain unanswered.

3.5. Future Work

ESCA analysis of at least 6 sensors coated with the PC polymer should be performed for statistically significant data. If all sensors indeed have the PC polymer coated on the outer surface, the issue of protein adsorption must be revisited. FTIR analysis of implanted sensors might clarify the PC polymer's role in protein adsorption *in-vivo*. If proteins are found present on the surface, then it can be concluded that the PC polymer will not be useful in

preventing protein adsorption *in-vivo*. If however, proteins are not present on the surface of the sensor either the polymer prevents protein adsorption and the possibility of conducting more *in-vivo* experiments exists, or the proteins are not detected.

If the analysis should reveal that the PC polymer isn't stable as an outer coating on the glucose biosensor, the situation is more complex. However, the possibility of improving the stability exists.

3.6. References

1. Gamburzev, S.; Atanasov, P.; Wilkins, E. *Sensors and Actuators B* **1996**, 30, 179-183.

2. Quinn, C.P.; Pishko, M.V.; Schmidtke, D.W.; Ishikawa, M.; Wagner, J.G.; Raskin, P.; Hubbell, J.A.; Heller, A. *American Journal of Physiology* **1995**, 269, E155-E161.

3. Lee, J.H.; Kopecek, J.; Andrae, J.D. *J. Biomed. Mater. Res.* **1989**, 23, 351-368.

4. Horbett, T.A.; Hoffman, A.S., *Bovine Plasma Protein Adsorption onto Radiation Grafted Hydrogels Based on HEMA and VP*, ACSS Adv. Chem. Ser., 145, 230, **1975**.

5. Reichert, W.M.; Saavedra, S.S. "Materials Consideration in the Selection, Performance and Adhesion of Polymeric Encapsulants for Implantable Sensors," in *Materials Science and Technology - a Comprehensive Treatment*, vol.14 - Medical and Dental Materials, D.F. Williams, Ed. VCH, Weinheim, FRG, **1991**; pp. 303-343.

6. Johnston, E.E.; Ratner, B.D.; Bryers, J.D. *Abstracts of Papers of the American Chemical Society* **1997**, 214 (iss Sep), pp. 303-PMSE.

7. Parzer, S.; Mannhalter, B.C. *J. Mater. Sci. Mater. Med.* **1993**, 4, 12-16.

8. Eberhart, R.C.; Munro, M.S.; Frautschi, J.R.; Lubin, M.; Clubb, F.J. Jr., Miller, C.W.; Sevastianov, V.I. "Influence of Endogenous Albumin Binding on Blood-Material Interactions" in *Blood in Contact with Natural and Artificial Surfaces*, vol. 516, E.F. Leonard, V.T. Turitto, and L. Vroman, Eds. New York Academy of Scienes, New York **1987**, pp. 78-95.

9. Hayward, J.A.; Chapman, D. *Biomaterials* **1984**, 5, 135.

10. Durrani, A.A.; Hayward, J.A.; Chapman, D. *Biomaterials* **1986**, 7, 121.

11. Sakakida, M.; Nishida, K.; Shichiri, M. *Sensors and Actuators B* **1993**, 13-14, 319-322.

12. Campbell, E.J.; O'Byrne, V.; Stratford, P.W.; Quirk, I.; Vick, T.A.; Wiles, M.C.; Yianni, Y.P. *ASAIO Journal* **1994**, 40 (3), M853-M857.

13. Velho, G.; Froguel, P.H.; Thévenot, D.R.; Reach, G. *Biomed. Biochim. Acta.* **1989**, 48 (11/12), 957-964.

14.Baker, A.D.; Betteridge, D. *Photoelectron Spectroscopy Chemical And Analytical Aspects*, Pergamon Press: **1972**, 1-6.

15.Barr, T.L. *Modern ESCA The Principles and Practice of X-Ray Photoelectron Spectroscopy*, CRC Press: **1994**, 5-69.

16.Ratner, B.D. *Cardiovascular Pathology* **1993**, 2(3), 87s-100s.

17.Bruck, S.D. *Properties of Biomolecules in the Physiological Environment*, CRC Press: **1980**, 68.

4. Chapter 3: Characterization and Identification of Leachate Molecules Extracted from Explanted Glucose Biosensors

4.1. Background

The bioengineering community seems to be in agreement that adsorption of proteins on the surface of a foreign material implanted *in-vivo* or exposed to serum or plasma is the first step in the initiation of thrombosis or the inflammatory response (1,2,3). However, as discussed below, it has become increasingly evident that some materials exposed to serum or plasma take up small molecules as well as protein. In 1989, Elbicki and Weber (4) studied the cyclic voltammetric (CV) response of ferrocene carboxylate and tris (2,2′-bipyridine) ruthenium dication at a glassy carbon electrode both in buffer and in human serum. Although the response was improved upon filtration of the serum using a 30 kDa filter, the investigators still observed a substantial decrease in current; it was necessary to use a 3-5 kDa filter to obtain a response similar to the one observed in buffer solution. The investigators concluded that small molecules were poisoning the electrode surface and that the low molecular weight cut-off filter protected the electrode from protein as well as small molecules present in the serum.

In 1993, Müller et al. (5) incubated modified polystyrene latex particles with human citrate plasma for 5 minutes at 37°C. The particles were washed with distilled water and dispersed in a

protein solubilizing solution. The solution was then analyzed by two-dimensional polyacrylamide gel electrophoresis (2-D PAGE). Countless numbers of spots were detected. The 3-D plot of PI (isoelectric point), molecular mass, and amount of protein revealed the presence of several peaks below 9 kDa.

Perhaps the most interesting report was by Kerner et al. (6) in 1993. They exposed an electroenzymatic glucose sensor to native plasma, plasma ultrafiltrate (molecular weight < 10 kDa) and dialyzed plasma (molecular weight > 12 kDa). Exposure of the sensor to native and ultrafiltrate plasma both produced large reduction in sensor sensitivity. However, exposure of the sensor to dialyzed plasma resulted in much improvement of sensor signals. Filtration of plasma does not eliminate interferences from small molecules as does dialysis; thus, the authors concluded that low molecular weight substances not retained by the outer polyurethane membrane caused the sensor inactivation.

The extraction of such small molecules from various materials exposed to plasma or serum should not go overlooked. A device such as a glucose biosensor might take up these small molecules, as well as protein. Although it is not obvious how the molecules affect the sensor's response, it is our belief that small molecules as well as protein may effect the sensor's sensitivity when it is implanted *in-vivo*. Therefore, the research presented in this chapter has been aimed at characterization and identification of all such biomolecules, which may potentially effect the sensor's response. With information about the molecules such as class, molecular

weight, and PI, the possibility of designing an appropriate outer membrane which could prevent the uptake of these molecules by the biosensor might exist. Such a membrane would have to retain certain qualities of the currently used polyurethane outer membrane. It would need to restrict glucose flux and allow oxygen to freely diffuse to maintain a glucose diffusion-controlled response. It would then incorporate some feature(s) to eliminate interferences from biomolecules based upon the molecules' characteristics. Such a membrane could be very beneficial to the development of a reliable, long-term glucose biosensor for treatment of insulin-dependent *diabetes mellitus*.

In this project, glucose biosensors with polyurethane outer membranes were prepared. The sensors were implanted *in-vivo* in rats, subsequently explanted, and soaked in phosphate-buffered saline to extract the biomolecules. A scheme for characterizing and identifying the molecules was developed; this chapter discusses the details of characterization and identification of the leachate molecules. We expect to find proteins in the sample as well as some small molecules. Determination of the molecular weight distribution, molecular classes, and the most abundant molecules will be of great interest. Also, Sections 4.3.9. and 4.4.7. discuss correlation between the sensitivity of the sensor and the amount of protein extracted. It is our belief that sensors which have relatively higher sensitivity to glucose will also take up relatively higher amounts of other biomolecules, i.e. proteins.

4.2. Strategic Scheme for Characterization and Identification

The scheme developed for characterization and identification of the extracted biomolecules is shown in Figure 3.1.

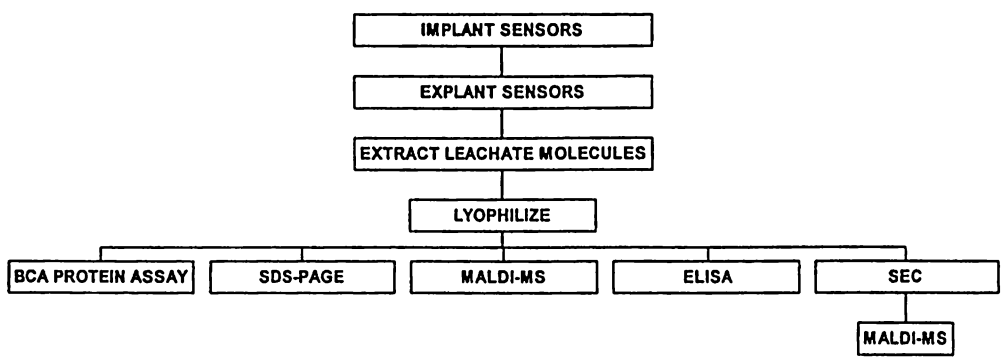

Figure 3.1. Scheme for the characterization and identification of biomolecules extracted from the glucose biosensor.

Following this scheme, it was expected that molecules would be taken up by the sensor during the implantation period and be removed from the sensor into the buffer during the extraction period. Samples were combined and lyophilized to improve detection. The first characterization involved determining the amount of protein present

in the sample, since proteins are known to coat foreign surfaces implanted *in-vivo* (7,8). Secondly, electrophoresis was performed to determine the molecular weight range of the molecules present in the sample. Thirdly, mass spectrometry was used to acquire accurate molecular weights. Immunoassay was then carried out for identification of specific target molecules such as albumin, fibrinogen, and immunoglobulins (IgG), which are all expected to be taken up by an implanted device (9,10,11). Size-exclusion chromatography was then used as an alternative method for determining the molecular weight distribution and it allowed the sample to be cleaned up so that further characterization and identification might be possible. Finally, MALDI-MS of chromatographic fractions was performed.

4.3. Experimental

4.3.1. Materials and Equipment

Lyophilization was performed using a Labconco model 75034 (Kansas City, MO) freeze dryer. The Bicinchoninic Acid (BCA) Protein Assay kit was purchased from Pierce (Rockford, IL). The BCA Protein Assay and ELISA were carried out in low-binding and high-binding, respectively, nonsterile 96 well polystyrene flat bottom plates from Corning Glass Works (Corning, NY). A Molecular Devices Kinetic Microtiter Plate reader and accompanying software (Menlo Park, CA) were used to analyze samples for ELISA and the BCA Protein

Assay. Electrophoresis equipment and chemicals were purchased from Biorad (Hercules, CA): Mini-Protean® II electrophoresis cell/accessories and computer controlled electrophoretic power supply (3000Xi), SDS-PAGE broad range standards (catalog# 161-0317), precast 12% polyacrylamide gels, 2-mercaptoethanol, bromophenol dye, and silver stain kit (containing fixative enhancer concentrate, silver complex solution, reduction moderator solution, image development solution, and development accelerator solution). 18 MΩ filtered water from a Barnstead Nanopure System was used. Other chemicals used were glycerol (Chemco, Topeka KS), TRIS-HCl (Fisher), sodium dodecyl sulfate, SDS (Sigma), glycine(Fisher), methanol (Fisher), and glacial acetic acid from Mallinckrodt Chemical (Paris, KY). The gel was scanned on a 312 nm variable intensity transluminator (Fisher Scientific). A Hewlett Packard (Rolling Meadows, IL) G2025A matrix-assisted laser desorption ionization mass spectrometer with an N_2 laser was used for mass analysis. Sinapinic acid matrix was from Sigma. Immunoassay chemicals are listed as follows: rabbit anti-rat albumin (Inter-Cell Technologies, Hopewell NJ), rabbit anti-rat fibrinogen (Accurate Chemical & Scientific Co., Westbury, NY), sheep anti-rat immunoglobulins (U.S.A. Boehringer Mannheim Corp., W. Germany), donkey anti-sheep IgG-peroxidase conjugate (Sigma Biosciences), goat anti-rabbit IgG-peroxidase conjugate (Sigma Biosciences), horseradish peroxidase (HRP) substrate consisting of a one to one volume solution of 3,3′,5,5′-tetramethylbenzidine (TMB) and hydrogen peroxide from Kirkegaard and Perry Laboratories, Inc. (Gaithersburg, MD). Rat IgG-reagent grade

from serum, fibrinogen fraction I from rat plasma, and rat albumin fraction V were all purchased from Sigma. Washing buffer was prepared from 2.28 gram Na_2HPO_4, 0.56 gram KH_2PO_4 and 17.56 gram NaCl dissolved in 2 L Nanopure water, pH adjustment to 7.4, and addition of 0.4ml Tween 20 (Sigma Chemicals). Blocking buffer was prepared from 0.4 gram bovine serum albumin (Sigma) dissolved in 200 ml washing buffer. Coating buffer (0.17 carbonate buffer) was prepared from 1.38 gram Na_2CO_3, 0.62 gram $NaHCO_3$ dissolved in 1L nanopure water and adjusted to pH 9.5. Biosep-Sec-2000 LC standards, Biosep-Sec-2000 (300 X 4.60 mm) analytical column, and Biosep-Sec-2000 (30 X 4.6 mm) guard column were all purchased from Phenomenex (Torrance, CA). The analytical column particles were 5 µm hydrophilic bonded silica. The column exclusion range was 1,000 Da to 300,000 Da. The UV-Vis spectrophotometric detector (SPD-6AV), liquid chromatograph (LC-6A), system controller (SCL-6A), and data analysis system (C-R4A) were all purchased from Shimadzu (Kyoto, Japan).

4.3.2. Extraction of Molecules from Sensor

The sensors were prepared as described in Section 3.2.1., but with no reference electrode and no phosphoryl choline membrane. Sensors were not polarized. Details of the *in-vivo* experimental procedure are covered in Section 3.2.3. Sample extractions were collected from a total of 24 glucose biosensors; 6 rats were used, with 4 sensors implanted in each rat. Since the immediate

sensitivity loss is of concern here, the sensors were implanted in the subcutaneous tissue for ~2 hrs.; after approximately 2 hrs. implantation, the sensor's output is usually fairly stable and therefore it was assumed that the uptake of molecules by the sensor was complete. The sensors were then explanted and placed in 500µl of 10mM phosphate-buffered saline (PBS) pH 7.4 contained in 1.5ml polyethylene tubes for 24 hrs.; sensors implanted in the same rat were placed together in 1 tube. After the 24 hr. extraction period, the sensors were removed and samples were combined together so that one sample contained extractions from 12 sensors. Two samples (referred to as sample 1 and sample 2) were obtained in this manner. The sensors were tested to ensure that the sensitivity was close to the pre-*in-vivo* value. The 24 hr. extraction period was chosen because at that time ~80% of the pre-*in-vivo* sensitivity was recovered and it was assumed that the majority of molecules had been extracted. The two sample solutions were stored in the freezer between -10°C to -20°C.

4.3.3. Lyophilization

Lyophilization was carried out to preconcentrate the samples. The samples were thawed at room temperature and refrozen in dry ice for ~30 minutes. Lyophilization was carried out overnight. The vacuum reached ~10 microns and the temperature was -100°C. Each sample was then reconstituted in 500 µl 0.1M PBS pH 6.8.

4.3.4. Bicinchoninic Acid (BCA) Assay

The Pierce BCA Assay (12) was used to determine the total amount of protein in the samples. The assay reaction is shown below in Figure 3.2.

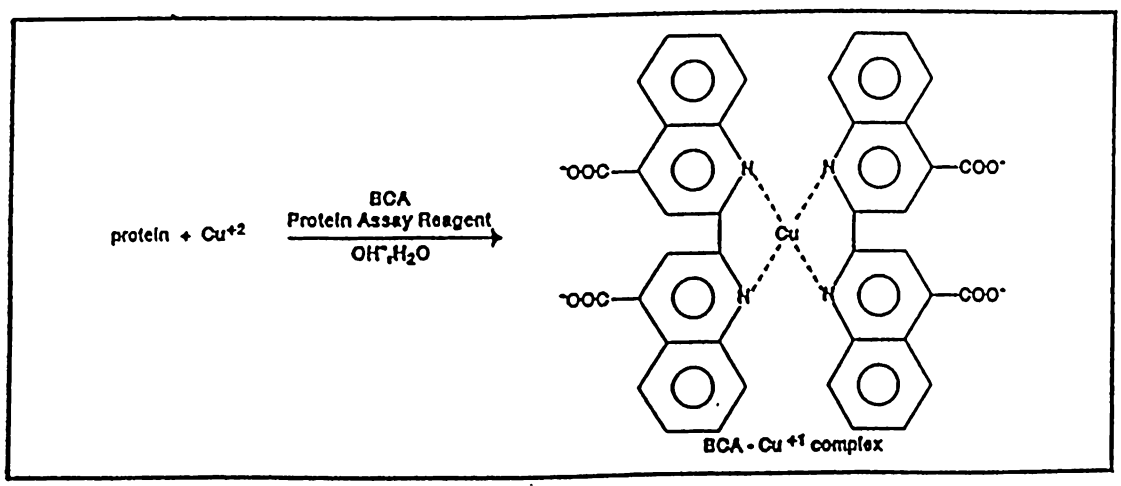

Figure 3.2. The Bicinchoninic Acid (BCA) Assay

Certain amino acids in proteins specifically cysteine, cystine, tryptophan, and tyrosine reduce copper II in alkaline medium to copper I; this is known as the biuret reaction. Two molecules of bicinchoninic acid then react with one cupric (copper II) ion to

form a complex which absorbs at 562nm. The detection limit of the assay is 10µg/ml protein.

Seven bovine serum albumin (BSA) standards of varying concentrations (2mg/ml to 31.25µg/ml) were prepared by diluting 200µl of the 2mg/ml stock BSA sample into 200µl deionized distilled water. Serial dilution was carried out and the last 200µl was discarded. BSA standards were 2000µg/ml, 1000µg/ml, 500µg/ml, 250µg/ml, 125µg/ml, 62.5 µg/ml, and 31.25µg/ml. Deionized water was used as the blank. Each well contained 200µl color solution and 10µl either sample solution (unknown samples), standard solution (standards), or deionized water (blanks). After addition of solutions, the plate was shaken three times then incubated at 37°C for 30 minutes. The plate was shaken three more times before detection of the complex at 550nm.

4.3.5. Sodium Dodecyl Sulfate-Polyacrylamide Gel Electrophoresis (SDS-PAGE)

Molecular weights of the sample components were determined using SDS-PAGE. The procedure followed was according to BioRad' s protocol. Required solutions were prepared as follows:

5X Electrode Running Buffer, pH 8.3: 9 gram Tris base
43.2 gram glycine
3 gram SDS
600 ml 18 MΩ filtered water

For a single electrophoretic run, 120ml 5X stock running buffer was diluted with 480ml of 18 MΩ filtered water (procedure taken from the Bio-Rad Mini-Protean®II electrophoresis cell instruction manual, with volumes of the 5X stock buffer and water doubled).

Stock Sample Buffer: 4.8ml distilled water
1.2ml of 0.5M Tris HCl, pH 6.8
1.0ml glycerol
2.0ml of 10% (w/v) SDS
0.5ml of 0.1% (w/v) bromophenol blue

(0.5M Tris HCl, pH 6.8: 6 gram Tris base dissolved in ~ 60ml deionized water, adjusted to pH 6.8 with 1 N HCl, and made to 100ml with deionized water).

Sample Buffer: 475µl stock sample buffer
25µl β-mercaptoethanol

Samples were prepared by mixing the solutions as shown in Table 3.1. The standard solution was prepared according to Bio-Rad's protocol by mixing 20 µl sample buffer and only 1 µl standard solution, since the proteins contained in the standard are concentrated. However, since the unknown sample is not as concentrated as the standard solution, 20 µl of unknown sample solution was mixed with 20µl sample buffer.

Table 3.1

Preparation of Samples for SDS-PAGE

SAMPLE	SAMPLE BUFFER VOLUME (µl)	STANDARD OR UNKNOWN SAMPLE VOLUME (µl)
Standard	20	1
Unknown	20	20
Blank	20	–

After preparation, standard, unknown, and blank samples were heated at ~82°C for 10 minutes and cooled for ~10 minutes. Running buffer was added to the cell and 5µl standard, unknown, or blank solution was loaded per well (samples were prepared according to Bio-Rad's protocol with modification of the heating temperature from 95°C to 82°C, and heating time from 5 minutes to 10 minutes). Blanks were placed in the outer wells and in between standard and unknown wells to prevent contamination upon addition of solution to wells. Separation was carried out at 200V constant voltage setting with a run time of 45 minutes. The gel was carefully removed and placed in the following solutions for silver staining according to Bio-Rad's protocol:

Step 1: Fixative Enhancer (30 minutes)

200ml methanol

40ml acetic acid

40ml fixative enhancer concentrate

120ml of 18MΩ filtered water

Step 2: 18 MΩ Filtered Water (20 minutes)

Step 3: 18 MΩ Filtered Water (20 minutes)

Step 4: Staining (~20 minutes), mixed in order given below

70ml of 18MΩ filtered water

10ml silver complex solution

10ml reduction moderator solution

10ml image development solution

100ml development accelerator solution

Step 5: Stop Step (15 minutes)

10ml acetic acid

200ml of 18MΩ filtered water

Step 6: High Purity Water (5 minutes)

18MΩ filtered water

The gel image was captured with a transluminator connected to a Macintosh computer, using the BIT image program. Molecular weights were calculated using the gel reader program.

4.3.6. Matrix-Assisted Laser Desorption Ionization-Mass Spectrometry (MALDI-MS)

MALDI-MS was performed with an N_2 laser operating at 337nm. Sample solutions were prepared with 75% sinapinic acid matrix for analysis.

4.3.7. Enzyme-Linked Immunosorbent Assay (ELISA)

Identification was carried out using ELISA. For these experiments, the sandwich format was used. A schematic diagram depicting the principle of the sandwich ELISA is shown in Figure 3.3. (adapted from reference 13). The sample is adsorbed on the surface of the solid phase. The primary antibody which recognizes one or more epitopes on the sample molecule is then added followed by the enzyme-labeled secondary antibody which is specific for the FC portion of the primary antibody. Detection is achieved upon addition of enzyme substrate; conversion of the substrate to product produces a measurable chemical or physical change.

In the following experiments, ELISA was used to determine whether or not the sample contained albumin, fibrinogen, and immunoglobulins. Detection was based upon absorbance. TMB is a

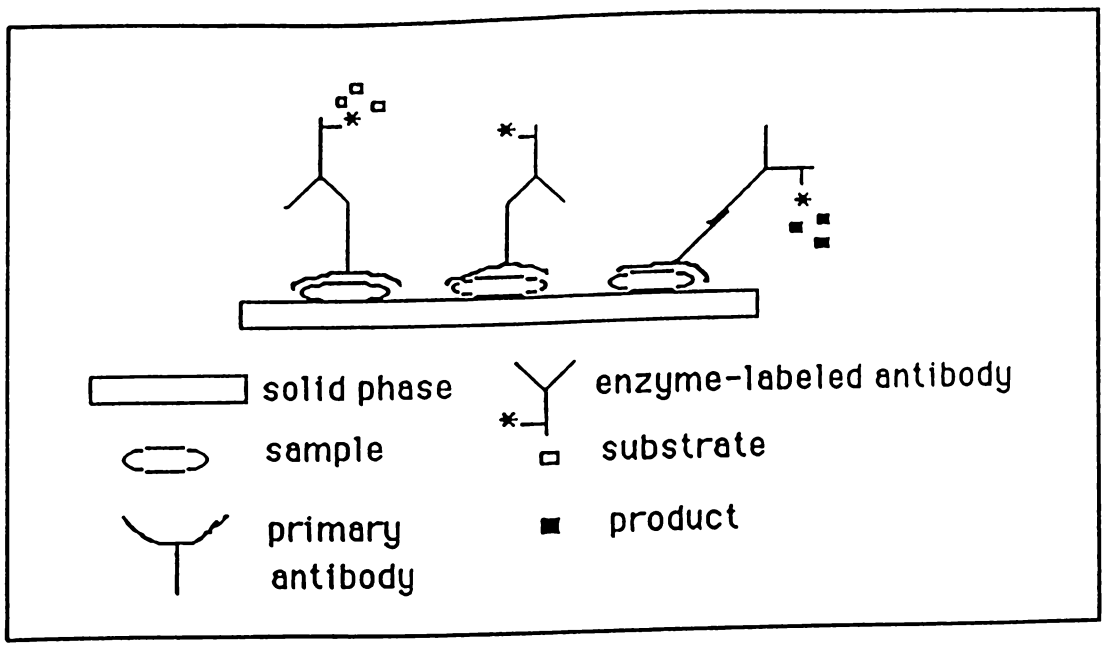

Figure 3.3. Principle of the Sandwich ELISA (Adapted from reference 13).

chromagen that yields a blue color when oxidized with hydrogen peroxide (catalyzed by HRP). Affinity constants and detection limits were determined by preparing an antibody titration curve using fixed antigen concentration and varying antibody concentration. Three separate plates were used in the analyses for albumin, fibrinogen, and immunoglobulins. The procedures used for analysis of the sample for each protein is given below.

Albumin Detection:

100µl of 5µg/ml rat albumin fraction V in coating buffer was added to standard and blank wells. For sample wells, 1µl sample was mixed with 800µl coating buffer and 100µl of this mixture was added. The plate was incubated for 2 hrs. at 37°C. The wells were washed 4 times with washing buffer. Next 100µl blocking buffer was added to each well, and the plate was incubated for 1 hr. The plate was washed with washing buffer 4 times. 200µl rabbit anti-rat albumin was added to the first standard wells and serially diluted by 100µl to give a concentrate range from 40µg/ml to 9.5×10^{-6} µg/ml. 1µl of rabbit anti-rat albumin was added to 1ml blocking buffer. 100µl of this solution was added to sample wells to give a final concentration of 4µg/ml. The plate was incubated for 1 hr. and washed 4 times with washing buffer. 1µl goat anti-rabbit IgG-peroxidase conjugate was added to 15ml blocking buffer and 100µl of this solution was added to each well. The plate was incubated for 1 hr. and washed 4 times with water. 6ml TMB substrate was mixed with 6ml H_2O_2 substrate and 100µl was added to each well. 50µl of 1M HCl was added to each well after the color changed upon substrate addition. The absorbance at λ = 450-650nm was read for each well. An antibody titration curve was produced by plotting blank corrected absorbance versus antibody concentration.

Fibrinogen Detection:

The preparation of wells was carried out similarly to that for albumin detection, but with the following changes: The antigen fibrinogen fraction I was coated on the plate. 39µl sample was added to 400µl coating buffer. 100µl of this mixture was added to sample wells. Rabbit anti-rat fibrinogen was the primary antibody. Standard solutions prepared with this antibody ranged in concentration from 40µg/ml to 1.9 X 10^{-5} µg/ml. 20µl rabbit anti-rat fibrinogen was added to 15 ml blocking buffer. 100µl of this mixture was added to sample wells.

Immunoglobulin Detection:

The preparation of wells was carried out similarly to that for albumin detection, but with the following changes: 100µl of 3µg/ml rat IgG antigen in coating buffer was added to standard and blank wells. 39µl sample was added to 400µl coating buffer. 100µl of this mixture was added to sample wells. The primary antibody was sheep anti-rat IgG. The sheep anti-rat IgG standard solutions ranged in concentration from 40µg/ml to 7.6 X 10^{-5} µg/ml. For the sample, 1µg/ml sheep anti-rat IgG was added to the wells. The enzyme-labeled antibody was donkey anti-sheep IgG-peroxidase conjugate.

The affinity constant (Ka) was determined from the antibody titration curves using the following equation:

$$Ka = 1/[Ab]$$

Where [Ab] is the antibody concentration at 1/2 the maximum absorbance.

Detection limits were determined by drawing a straight line through the linear part of the curve and extrapolating from the lowest point on the linear part of the curve. Albumin, fibrinogen, and immunoglobulins were identified by absorbance detected in their respective sample wells, the approximate amounts determined using the appropriate antibody titration curve.

4.3.8. Size-Exclusion Chromatography (SEC)

Isocratic separation of the samples was carried out with 0.1M phosphate-buffered saline pH 6.8 as the mobile phase. The conditions of the separation are shown in Table 3.2.

Table 3.2

Conditions of SEC Separation

λ (nm)	TEMPERATURE (°C)	FLOW RATE (ml/min)	INJECTION VOLUME (µL)	PRESSURE (psi)	RUN TIME (min)
280	ambient	0.35	20	540-569	22

Standards were separated under the same conditions as the sample, but with 1µl injection volume and a run time of ~15 minutes. The sample peak fractions were collected separately and frozen. SEC fractions were analyzed by MALDI-MS.

4.3.9. Sensor Sensitivity Versus Amount of Protein Extracted

These experiments were performed to determine correlation between sensor sensitivity and the amount of protein extracted. Eight sensors numbered 56, 58, 59, 60, 63, 65 and 66 were prepared according to Section 3.2.1. with a polyurethane outer membrane. The sensitivity of the sensors was stabilized. The sensors were then implanted in rats for 2 hrs., without polarization of the electrode, (sensors 56, 59, 60, and 61 were implanted in rat 1 and sensors 58, 63, 65, and 66 were implanted in rat 2). The sensors were explanted and placed in separate tubes containing 1ml of 0.1M phosphate-buffered saline pH 7.4 for 2 hrs. (sensors implanted in rat 1) or 24 hrs. (sensors implanted in rat 2). The eight sample extractions were lyophilized and reconstituted in 100µl phosphate buffer. All eight samples were analyzed by BCA Protein Assay. The sensitivity of each sensor was tested after the 2 hr. or 24 hr. extraction period and compared to the amount of protein extracted from that sensor. The sensors were grouped together by the extraction period (either 2 hrs. or 24 hrs.). It was expected that higher sensitivity sensors would take up more protein. It was also expected that the

longer extraction time of 24 hrs. would allow for more protein to be extracted compared to the 2 hr. extraction time.

4.4. Results

4.4.1 BCA Assay of Sample 1 and Sample 2

The standard BCA curves for sample 1 and sample 2 are given in Figures 3.4 and 3.5, respectively. Sample 1 contained ~375µg/ml total protein while sample 2 contained ~420µg/ml total protein.

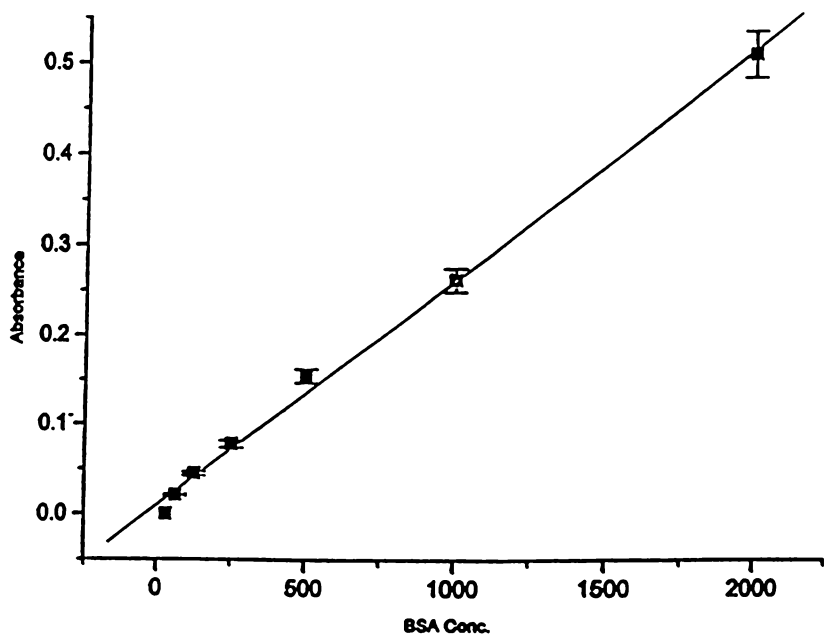

Figure 3.4. BCA Assay standard Curve for Sample 1.

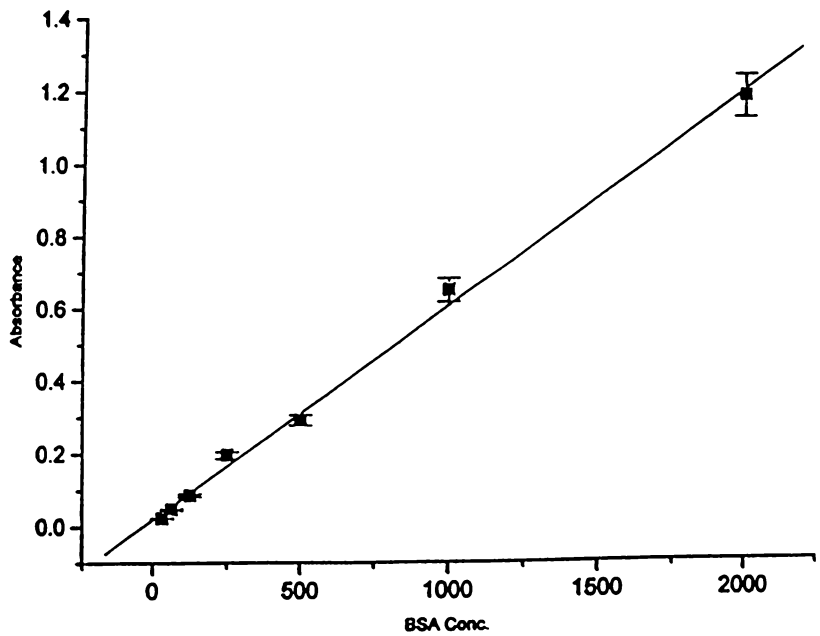

Figure 3.5. BCA Assay Standard Curve for Sample 2.

4.4.2. SDS-PAGE

Table 3.3. lists the molecular weights of the bands detected for sample 1 and sample 2 using silver staining. The bands covered a wide molecular weight range: 6kDa to 340kDa. A total of 5 bands were seen for sample 1 and 10 bands were seen for sample 2. Sample 1 contained bands at 14.4kDa, 66kDa, 82kDa, 97kDa, and 179kDa. Sample 2 contained the same bands that sample 1 contained plus additional bands at 6kDa, 55kDa, 103.2kDa, 122kDa, and 340kDa.

Table 3.3.

Approximate Molecular Weight of Bands Detected for Sample 1 and Sample 2 by SDS-PAGE and Silver Staining

SAMPLE 1	SAMPLE 2
—	6,000
14,400	14,400
—	55,000
66,000	66,000
82,000	82,000
97,000	97,000
—	103,000
—	122,000
179,000	179,000
—	340,000

4.4.3. MALDI-MS

Both sample 1 and sample 2 were analyzed by MALDI-MS. Unfortunately, no peaks were detected for sample 1. However, as shown in Figure 3.6, there were 2 peaks detected for sample 2. Peak 2 at m/z = 33236.6Da is believed to be the +2 charge of peak 3 at m/z = 66224.4Da. These peaks were thought to be due to serum albumin. The lower molecular weight peaks are due to the matrix.

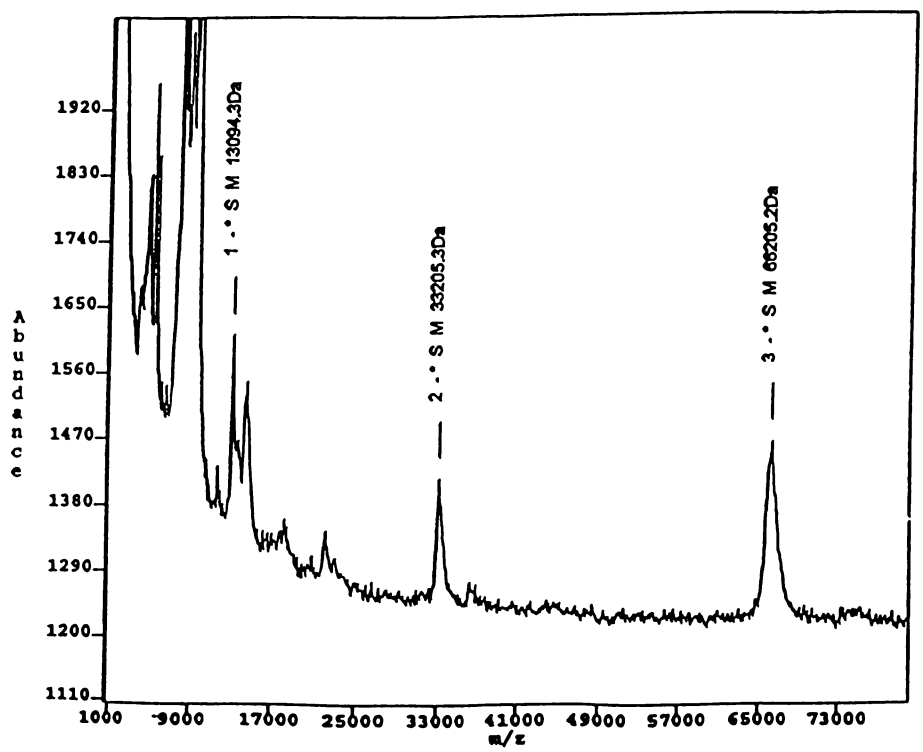

Figure 3.6. MALDI-MS of Sample 2.

4.4.4. ELISA

Sample 2 was analyzed for serum albumin, fibrinogen, and immunoglobulins using ELISA. The antibody titration curves for rabbit anti-rat albumin, rabbit anti-rat fibrinogen, and sheep anti-rat immunoglobulins are shown in Figures 3.7, 3.8, and 3.9, respectively. Table 3.4 shows the Ka and detection limit of the antibodies. The Ka and detection limit determined for rabbit anti-rat albumin (RaXRt albumin) were 9.9 X 10^9 M^{-1} and 1.6ng/ml,

respectively. The absorbance in the sample well was 2.885 which correlates to a concentration of approximately 316ng/ml albumin in the sample. The Ka and detection limit for the rabbit anti-rat fibrinogen (RaXRt fibrinogen) were 4.7 X 10^9 M^{-1} and 10ng/ml, respectively. The absorbance in the sample well was 1.681, correlating to a concentration of 32ng/ml for fibrinogen. The Ka and detection limit for the sheep anti-rat immunoglobulins (ShXRt immunoglobulins) were 2.7 X 10^9 M^{-1} and 6.5ng/ml, respectively. The sample well had an absorbance of 3.041 correlating to an immunoglobulin concentration of approximately 562ng/ml in the sample.

Taking the approximate amount of each protein detected and dividing by 12 (the total number of sensors used), there is approximately 26ng/ml albumin, 2.7ng/ml fibrinogen, and 47ng/ml immunoglobulins extracted from each sensor. The total amount of protein determined for sample 2 was ~420µg/ml. The total amount of protein due to albumin (316ng/ml), fibrinogen (32ng/ml), and immunoglobulins (562ng/ml) was ~910ng/ml, less than 1% of the total protein detected. Since these proteins are the most abundant in the plasma, it was expected that they would account for the majority of protein detected. However, the total amount of protein may have been grossly overestimated due to interference in the BCA Protein Assay from endogenous molecules which can reduce Cu^{+2} to Cu^{+1} (i.e. sugars, ascorbic acid, uric acid, amino acids) (12).

Table 3.4

Ka, Detection Limit, and Sample Concentration obtained using ELISA

ANTIBODY	AFFINITY CONSTANT Ka (M^{-1})	DETECTION LIMIT (ng/ml)	SAMPLE 2 CONCENTRATION (ng/ml)
RaXRt albumin	9.9×10^9	1.6	Albumin 316
RaXRt fibrinogen	4.7×10^9	10	Fibrinogen 32
RaXRt Immunoglobulins	2.7×10^9	6.5	Immunoglobulins 562

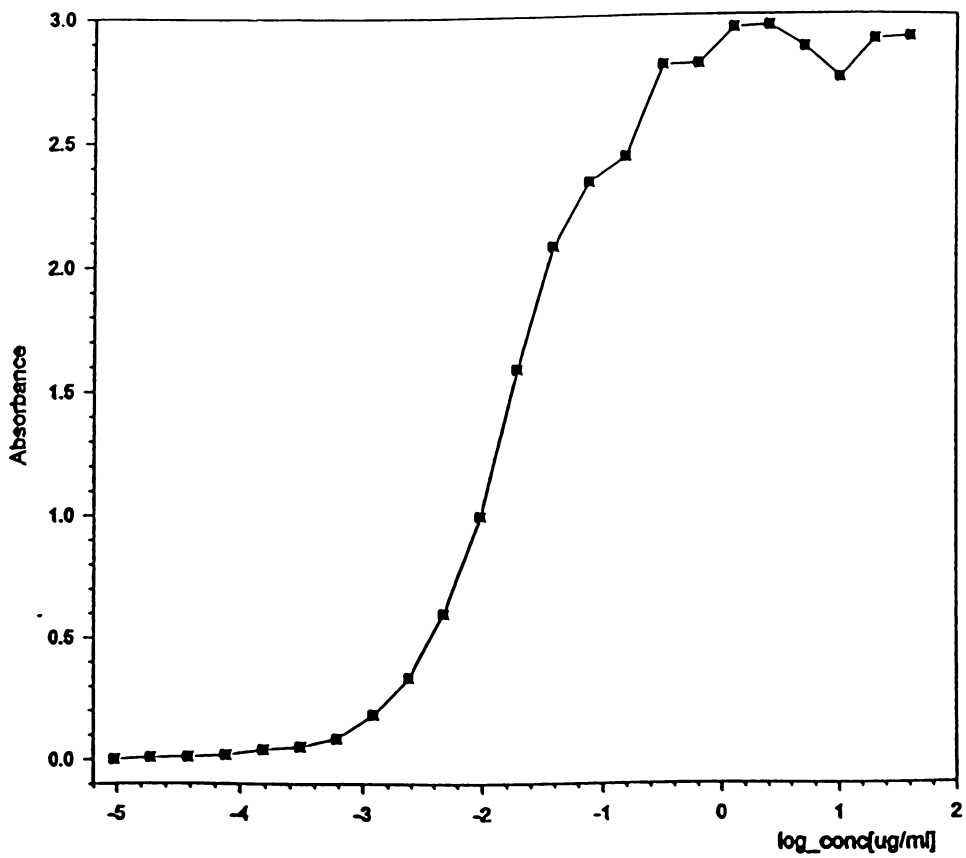

Figure 3.7. Antibody Titration Curve for Rabbit Anti-Rat Albumin.

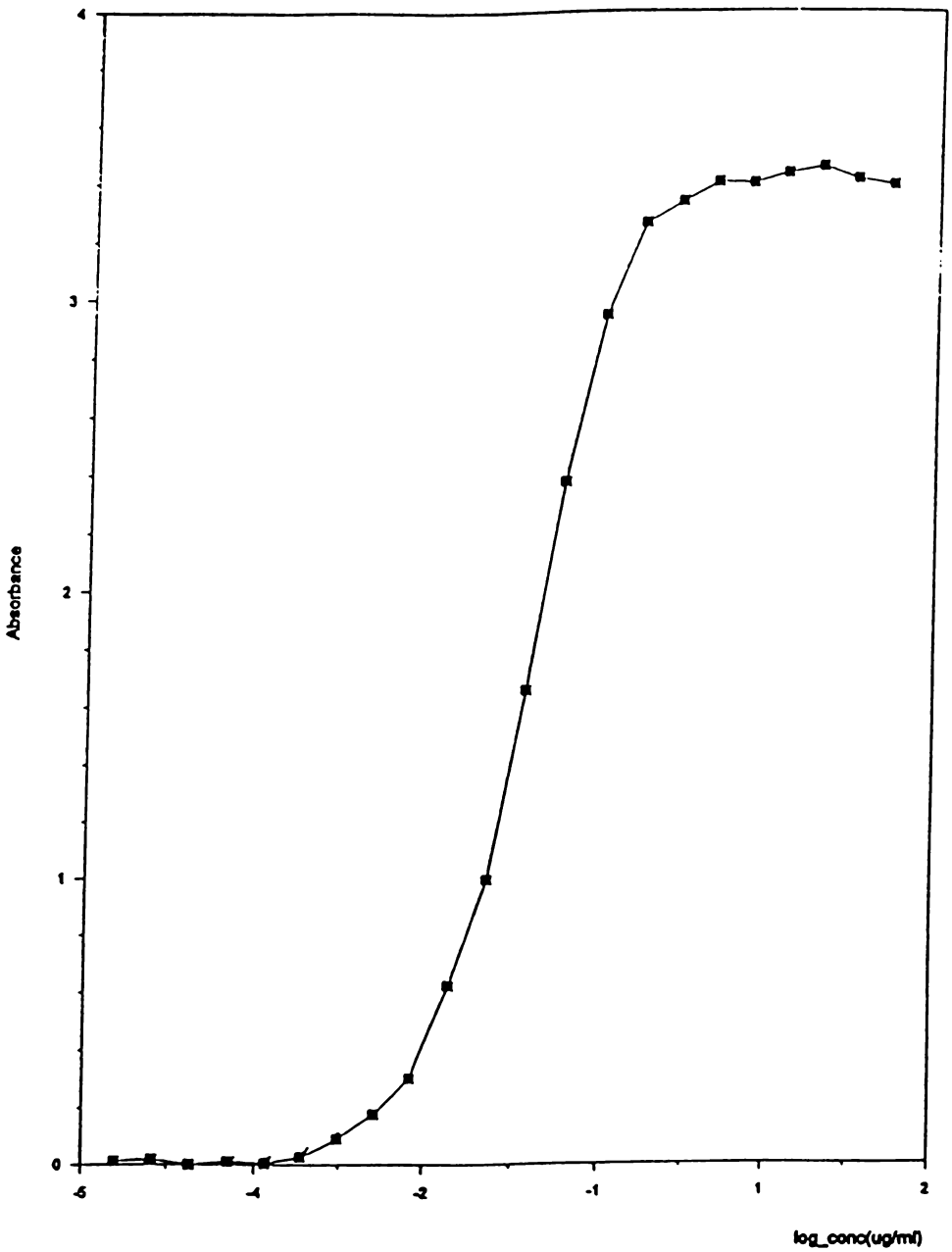

Figure 3.8. Antibody Titration Curve for Rabbit Anti-Rat Fibrinogen.

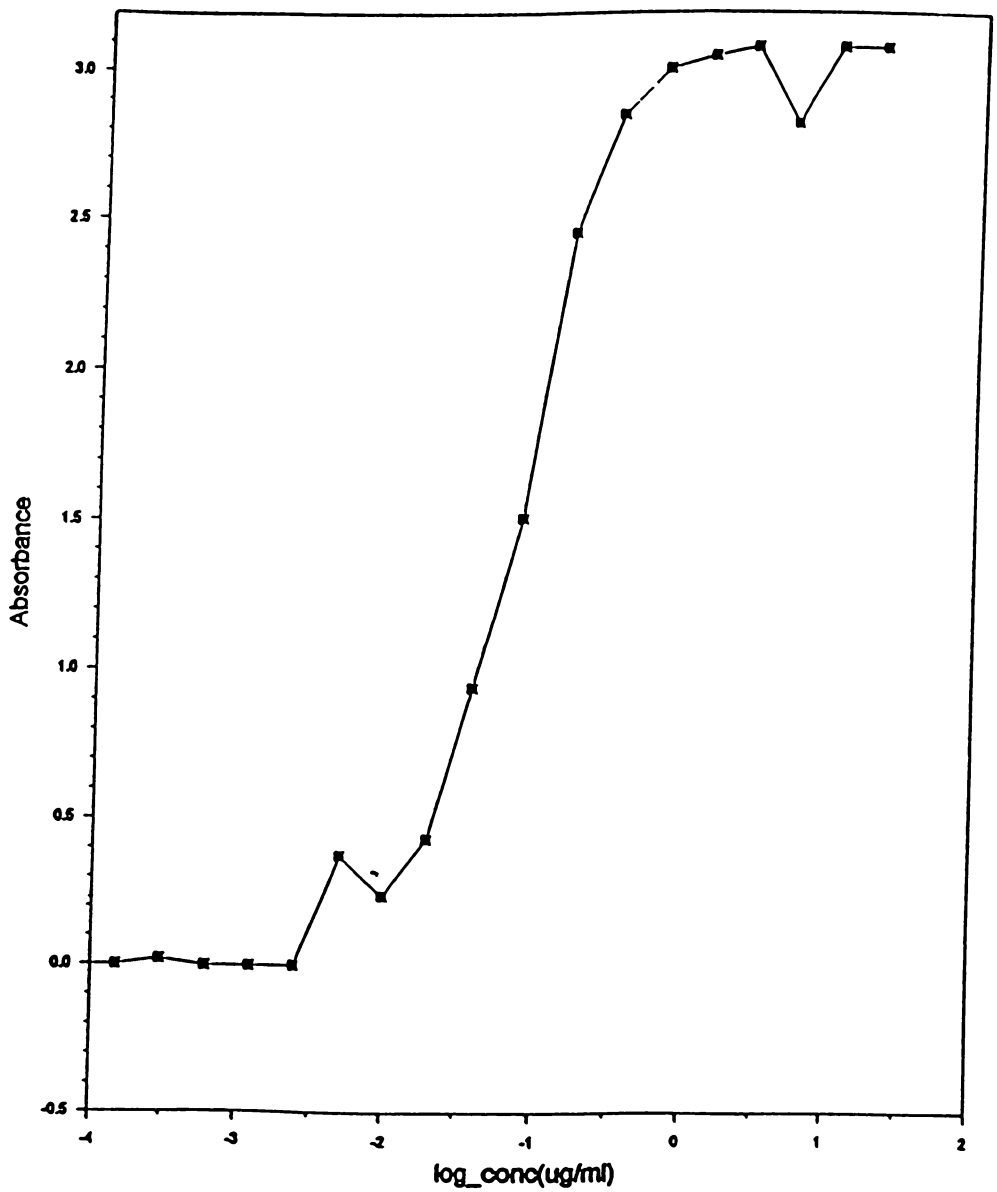

Figure 3.9. Antibody Titration Curve for Sheep Anti-Rat Immunoglobulins.

4.4.5. SEC

Peak retention time and corresponding molecular size for standard molecules is given in Table 3.5. The separation of standards is shown in Figure 3.10. The chromatograms of sample 1 and sample 2 are given in Figures 3.11 and 3.12, respectively. Referring to Table 3.5, sample 1 contained two prominent peaks at 6.500 min. and 9.176 min. These peaks correspond to molecular weights of approximately 280,000 Da and 14,000 Da, respectively.

Table 3.5

Retention Time and Molecular Size of Standards

PEAK NUMBER	RETENTION TIME (min)	MOLECULAR SIZE (Da)
1	6.278	670,000
2	6.584	150,000
3	7.659	44,000
4	8.611	17,000
5	10.633	244.2

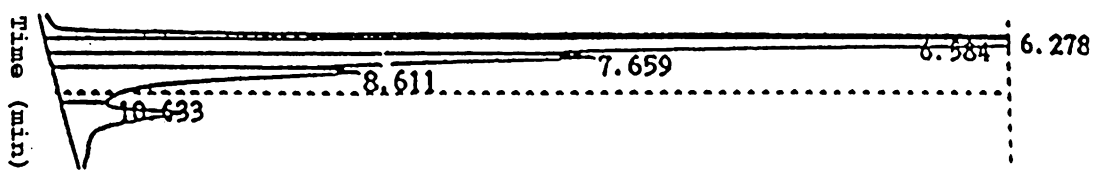

Figure 3.10. Chromatogram of SEC Standards.

Sample 2 contained six peaks. Peaks at 6.513 min., 7.594 min., 9.024 min., 9.793 min. and 10.537 min correspond to approximately 280,000 Da, 50,625 Da, 14,400 Da, 7000 Da and 1025 Da, respectively. A peak corresponding to a molecular weight greater than 300,000 Da was detected.

4.4.6. MALDI-MS

Chromatographic fractions of sample 1 and sample 2 were analyzed by mass spectrometry. Only sample 1 fraction at 9.176 min. revealed peaks. Figure 3.13 shows the resulting spectrum. Several low molecular weight peaks ranging from 922.6 Da to 1147.1 Da were

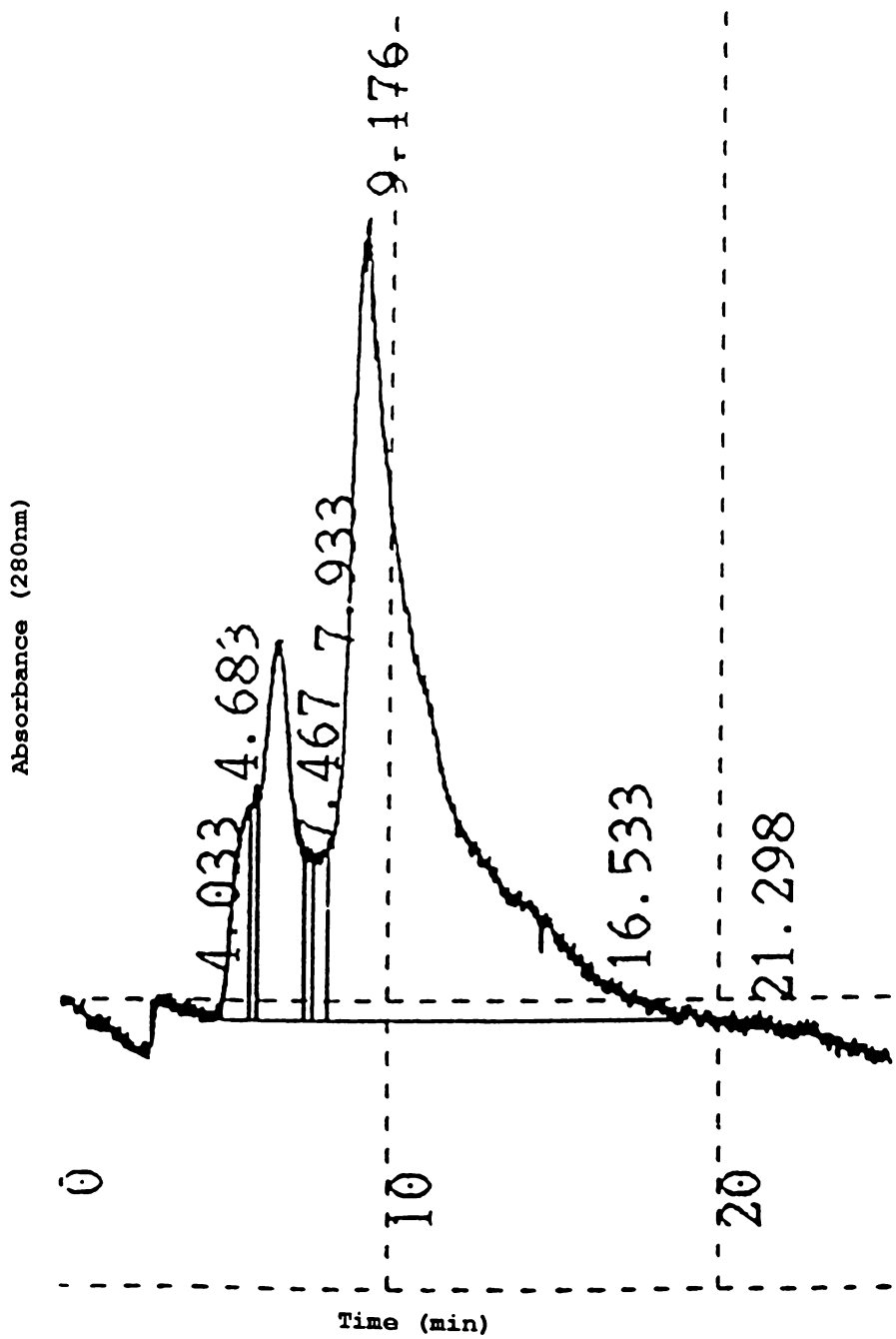

Figure 3.11. Chromatogram of Sample 1.

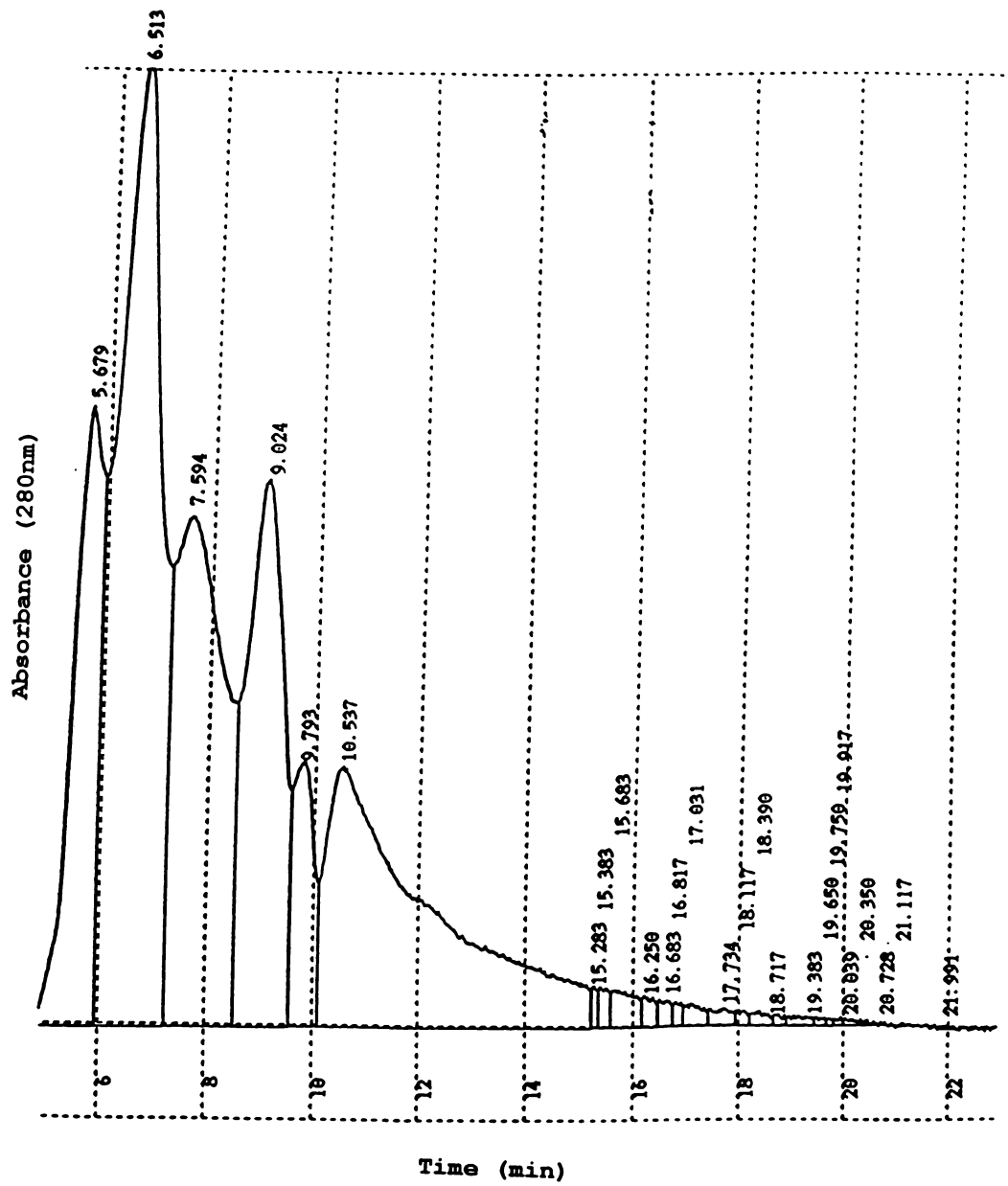

Figure 3.12. Chromatogram of Sample 2.

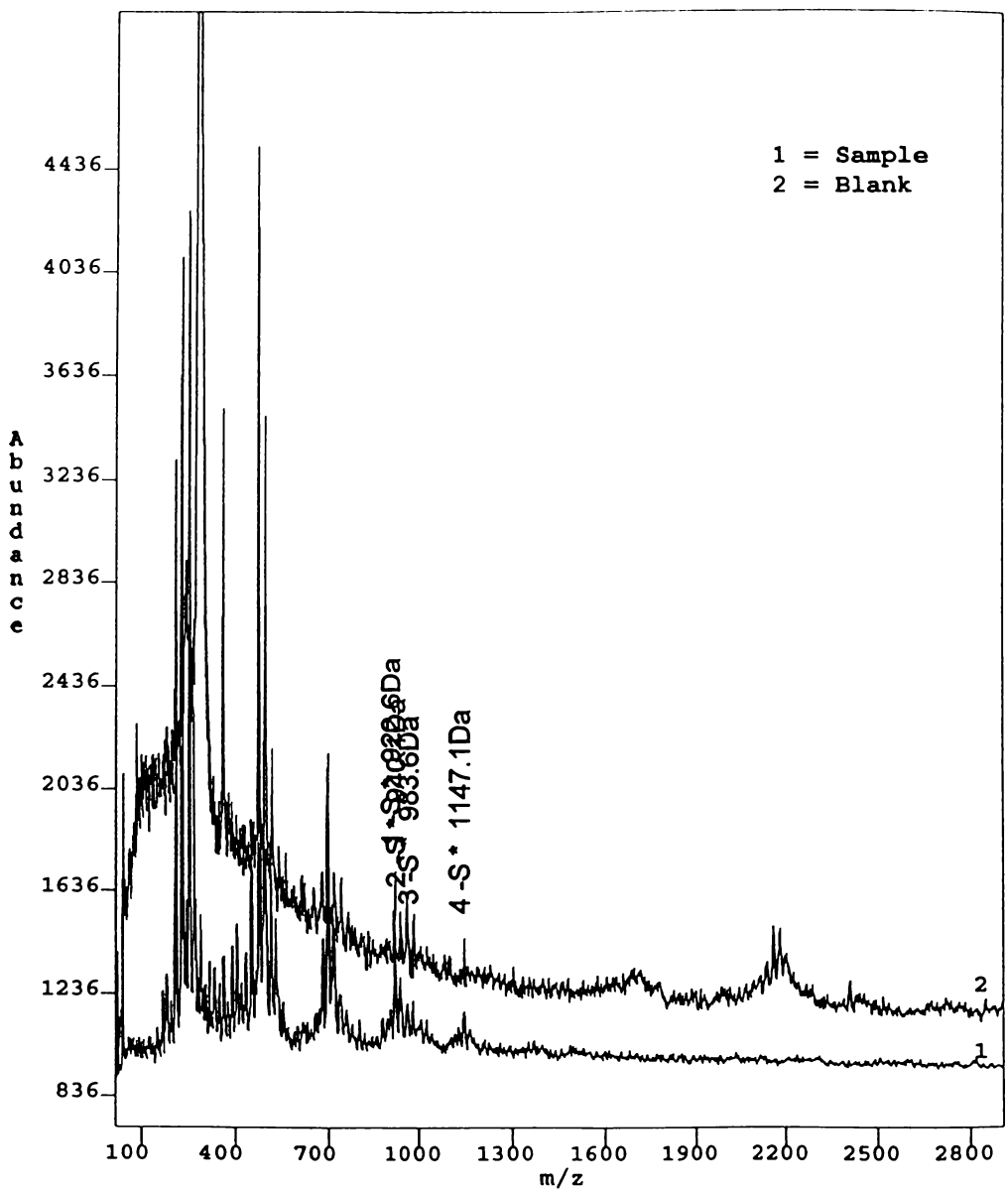

Figure 3.13. MALDI-MS of Sample 2 SEC Fractions.

detected. These peaks were so small that it is possible that they could have been due to the matrix.

4.4.7. Sensitivity Versus Amount of Protein Extracted

Table 3.6 shows the results of the BCA Protein Assay for the eight sensors whose sensitivity values were compared to the corresponding amount of protein extracted. The sensors were divided into either the 2 hr. extraction group or the 24 hr. extraction group, and then listed in order of increasing sensitivity. Sensitivities which ranged between 0.02nA/mM to 0.36nA/mM were considered low, and sensitivities which ranged between 1.6nA/mM and 3.3nA/mM were considered average. There is no significant difference between the amount of protein extracted from the sensors in the various groups.

4.4. Discussion

It is well known that any foreign object implanted into the body becomes immediately coated with a layer of protein; the glucose biosensor is no exception. From these experiments it has been shown that µg/ml levels of protein adsorb on the surface of the glucose biosensor when it is implanted in the subcutaneous tissue of rats. However, the total protein values determined may have been grossly overestimated and therefore should be rechecked. The total amount of protein in the higher molecular weight SEC sample fractions, >

Table 3.6.

Sensitivity Versus Amount of Protein Extracted

GROUP # (sensor #)	SENSITIVITY (nA/mM)	PROTEIN EXTRACTED (µg/ml) R = 0.99 SD = ± 13µg/ml
2 hr. extraction		
60	0.02	41
59	2.9	50
56	3.3	70
24 hr. extraction		
58	0.03	63
63	0.03	66
65	0.36	58
66	1.6	73

5,000 Da and presumably proteins, can be determined using the BCA Assay. Large discrepancies between the total amount of proteins detected for the sample before and after SEC separation would indicate that other reducing agents may have effected the BCA Assay results. The original sample may also be filtered and the BCA Assay used to analyze the filtrate. Using the BCA Assay result for sample

2, the protein surface coverage on each sensor can be estimated as follows:

420 μg total protein/12 sensors = **35 μg protein/sensor**

sensor surface area = W x π x L = 0.250mm x π x 40mm = **31mm^2**

protein surface coverage = 35μg protein/sensor x sensor/31mm^2

= 1.1 μg protein/mm^2

Because there are very few proteins present in the tissue, most of the proteins that would adsorb onto the surface of tissue implants would come from the plasma. Therefore, it would be expected that materials exposed to plasma or serum would have more proteins adsorbed onto their surfaces than would be materials exposed to the tissue (i.e. subcutaneous implantation). Bundy et al. (14) reported that between 22μg/cm^2 (0.22μg/mm^2) and 36μg/cm^2 (0.36μg/mm^2) total protein was eluted from the surface of various plastic and metal materials exposed to diluted serum for 3 days. This report is 3 to 5 times higher than Bundy's reported values. It seems likely that the calculated amount of 1.1μg/mm^2 is probably an overestimation of the protein surface coverage. Assuming that the average protein molecular weight is 66,000g/mol:

$1.1X10^{-6}$ g/mm^2 x mol/66,000g x $6.022X10^{23}$ molecules/mol

= $1.0X10^{13}$ molecules/mm^2

The approximate number of monolayers of protein adsorbing on the sensor can be calculated assuming that the proteins are

approximately 50 Å (5×10^{-6} mm) in diameter and denature once adsorbed onto the sensor surface. The surface area covered by 1 molecule is:

$$\pi r^2 = \pi\left(\frac{5 \times 10^{-6} \text{ mm}}{2}\right)^2 = \mathbf{1.96 \times 10^{-11}\ mm^2}$$

The number of molecules contained in 1 monolayer is:

$31mm^2$ (sensor surface area)/1.96×10^{-11} mm^2 (monolayer of molecules) = **1.6×10^{12} molecules/monolayer**

The number of monolayers adsorbing on the sensor is:

$1.0X10^{13}/1.6X10^{12}$ = **6.3 monolayers**

There are approximately 6 monolayers of protein on each sensor according to these calculations. Again, this calculation is probably overestimated.

There doesn't appear to be a correlation between the sensitivity of the sensor and the amount of protein extracted. It was assumed that sensors which had lower sensitivity to glucose would also have lower amounts of protein adsorbed on their surfaces compared to sensors which had a higher sensitivity to glucose. The hypothesis is that sensors with higher sensitivity to glucose probably have either a greater number of pores or larger pores through which protein might be adsorbed. However, this data is preliminary;

sensors with a wider sensitivity range (i.e. 1nA/mM to 10nA/mM) might show a correlation.

SDS-PAGE analysis and SEC revealed that the sensor takes up predominantly large molecules. However, according to SEC results, sample 2 contains molecules as low as 1025Da. MALDI-MS may have revealed low molecular weight peaks at ~900Da and 1100Da. These results draw attention to the need to be concerned about the effect of small molecules as well as protein on the response of the sensor. Table 3.7 lists some possible identities of the sample components based upon molecular weight data and the presence of the molecules in blood or tissue. Bands at 340,000Da, 179,000Da, and 66,000 have been determined by ELISA to contain fibrinogen, immunoglobulins (IgG), and serum albumin, respectively. Other possible proteins include coagulation factors, proteoglycans, and interleukins. The low molecular weight peaks fall in the range of peptides. Possible molecules include the hormones oxytocin and vasopressin.

Traditionally, surface characteristics of the implant such as charge, tension, morphology, and wettability have been thought to play a key role in the determination of the kinds of molecules which adsorb to surfaces (3). Instead of focusing on the characteristics of the implant as is often the case, this research dealt with trying to understand more about the molecular components taken up by the sensor that may potentially effect the sensor's response when it is implanted *in-vivo*. There must be some explanation as to why certain molecules are taken up by the sensor. It is apparent that molecular weight restrictions are not of underlying importance in the

determination of the kinds of molecules taken up by the sensor, since a very wide range of molecules are extracted from the sensor, as low as ~900Da to greater than 300,000Da. It must be noted however that degradation of proteins, specifically fibrinogen (15) is known to occur on surfaces and this degradation may be responsible for some of the low molecular weight species detected in the sample. Also, all molecules extracted may not have been detected.

The molecules detected by ELISA were albumin, fibrinogen, and immunoglobulins. The most obvious link between these molecules is their abundance in the plasma: albumin at 40g/l, fibrinogen at 2-3g/l, and Immunoglobulins at 8-17g/l (16). These molecules are reported to adsorb on many materials that have been implanted *in-vivo* or exposed to whole blood, plasma, or serum (9,10,11).

Table 3.7

Possible Identities of Molecules Extracted from the Glucose Biosensor

MOLECULAR WEIGHT (Da)	POSSIBLE IDENTITIES
340,000	*Fibrinogen, Factor V, Factor VIII, proteoglycans
179,000	*Immunoglobulins (IgG), Complement Components, Proteoglycans
122,000	Complement Components, Proteoglycans
103,200	Complement Components, Proteoglycans
97,000	Complement Components, Proteoglycans
82,000	Factor XII, Plasminogen, Haptoglobin, Complement Components, Proteoglycans
66,000	*Serum Albumin
55,000	Factor IX, Factor X, Factor VII
14,400	Interleukins-2, -3, -5, -7, -9, Angiogenin, Proteoglycans
6,000	Epidermal Growth Factor, Transforming Growth Factor, Proteoglycans
1100	Vasopressin
900	Oxytocin

*** bands identified by ELISA**

Molecules which are less abundant in the plasma, but which play an important role in the foreign body response may also be

likely to be taken up by the sensor. Such molecules include the coagulation factors and interleukins. Although most are present at levels much lower than 1g/l (16), their roles in the foreign body response make them good candidates for up take by the sensor.

Proteoglycans are also likely candidates to be taken up by the sensor. They maintain an essential environment for cell adhesion, migration, and proliferation (17). Proteoglycans consist of protein cores substituted with highly sulfated glycosaminoglycan (GAG) chains. Many proteoglycans are "sticky" in solution (18), a characteristic observed for both samples.

The low molecular weight species detected could have been peptides. Oxytocin and vasopressin, peptide hormones, fall into this molecular weight range. Both hormones are vasodilators. Since vasodilation does occur during acute inflammation, these molecules might be present in the sample.

4.6. Future Work

These experiments led to the conclusion that smaller molecules maybe just as important as protein in potentially effecting the sensor's response. Therefore, experiments designed to study this interaction should not be biased toward the detection of or elimination of protein.

For future work, determination of the significance of biomolecular class should be addressed; it will be important to perform both qualitative and quantitative characterization of the sample molecules. Classes of biological molecules which should be

tested include proteins, sugars, amino acids, lipids, and proteoglycans. Because the molecules might be present at low levels, ELISA will probably be a good detection method.

Another characteristic that might turn out to be important is molecular charge. This can be studied using 2D-electrophoresis. The prominent electrophoretic band at 14,400Da was significantly more intense than the other bands. In both sample 1 and sample 2, the intensity of this band was comparable to the intensity of standard bands which contained approximately 2000µg/ml of each standard molecule. Because this band is so much more prominent than the others, it would be beneficial to identify it. It would also be beneficial to identify the molecule(s) giving rise to the prominent SEC peaks. Electrospray Mass Spectrometry (ESMS) might be used to further separate SEC sample fractions. Enzymatic digestion followed by proteolytic mapping could be used to identify the proteins. Small molecules can interfere with the BCA Protein Assay. Therefore, the original samples should be filtered and the filtrate analyzed by BCA Assay. A significant signal would suggest interference from small molecules. Based upon the classes of molecules detected, further characterization can be carried out.

4.7. References

1. Poot, A.A.; Beugeling, T.; "protein Adsorption in Relation to Platelet Adhesion and Contact Activation" in *Modern Aspects of Protein Adsorption on Biomaterials*, Missirlis, Y.F. and Lemm, W., eds., Klumer Academic, **1990**; p.29.

2. Rolfe, P.; Martin, M.; Williams, D.; Walters, R.; Lamakoshi, K.; Tanaka, S. "In-Vivo Sensors-Haemocompatibility" in *In-Vivo Chemical Sensors Recent Developments*, Alcock, S.J. and Turner, A.P.F., eds., Cranfield, **1993**; p.167-178.

3. Anderson, J.M.; Marchant, K.K. *CRC Critical Reviews in Biocompatibility* **1985**, 1 (2), 111-204.

4. Elbicki, J.M.; Weber, S.G. *Biosensors*, **1989**, 4, 251-257.

5. Blunk, T.; Hochstrasser, D.F.; Müller, B.W.; Müller, R.H. *Proceed. Intern. Symp. Control. Rel. Bioact. Mater.* **1993**, 20, 284-285.

6. Kerner, W.; Kiwit, M.; Linke, B.; Keck, F.S.; Zier, H.; Pfeiffer, E.F. *Biosensors and Bioelectronics* **1993**, 8, 473-482.

7. Baier, R.E. *J. Biomed. Mater. Res.* 1969, 3, 191-206.

8. Hoffman, A.S., "Modification of Material Surfaces to Affect How They Interact with Blood" in *Blood In Contact with Natural and Artificial Surfaces*, Leonard, E.F.; Turitto, V.T.; Vroman, L., Ed., Proc. N. Y. Acad. of Sci., **1987**; p.96.

9. Brash, J.L.; Thibodeau, J.A. Journal of Biomedical Materials Research **1986**, 20, 1263-1275.

10. Horbett, T.A. *J. Biomed. Mater. Res.* **1981**, 15, 673-695.

11. Gendreau, R.M.; Winters, S.; Leininger, R.I.; Fink, D.; Hassler, C.R.; Jakobsen, R.J. *Applied Spectroscopy* **1981**, 35 (4), 353-357.

12. Smith, P.K.; Krohn, R.I.; Hermanson, G.T.; Mallia, A.K.; Gartner, F.H.; Provenzano, M.D.; Fujimoto, E.K.; Goeke, N.M.; Olson, B.J.; Klenk, D.C. *Anal. Biochem.* **1985**, 150, 76-85.

13. Fintschenko, Y. *A Problem Driven Approach To The Miniaturization and Automation of Enzyme-Based Assays and an Investigation of the Dissipation of Cyanazine and Bromide in Wetland Mesocosms*, ph.D. Dissertation, The University of Kansas, **1997**.

14. Hallab, N.J.; Bundy, K.J.; Óconner, K.; Clark, R.; Moses, R.L. *Journal of Long-Term Effects of Medical Implants* **1995**, 5(3), 209-231.

15. Brash, J.L.; Chan, B.M.C.; Szota, P.; Thibodeau, J.A. *J. Biomed. Mater. Res.* **1985**, 19, 1017-1029.

16. Anderson, L.O.; Lundén, R., "The Composition of Human Plasma", in *Plasma Proteins*, Blombäck, B.; Hanson, L.Å., Ed., John Wiley and Sons, **1979**; p.20.

17. Jollès, P. *Proteoglycans*, Birkhäuser Verlag Basel, Switzerland, **1994**; p.2.

18. Johnson, P.Y.; Blake, *D.A. J. Chromatogr. B* **1997**, 688, 27-33.

5. Chapter 4: Investigation of Sensor/Macrophage Interaction

5.1. Background

5.1.1.The Macrophage

Free macrophages are found in the blood as monocytes, cells 12-16μm in diameter. The blood monocytes derive from a specific marrow precursor, the monoblast. Monocytes migrate from the blood to the tissue in small numbers at a regular rate. There is a significant increase in the numbers that migrate into inflamed areas, where they rapidly enlarge and mature into macrophages (1). Mature macrophages are generally 15-30μm in diameter (2). Macrophages are mononuclear phagocytes, cells that are designed to digest foreign material (i.e. microorganisms) during inflammation. During phagocytosis, peritoneal macrophages show great increases in respiration: 7.0±0.3μloxygen/mg protein x hr. (over threefold increase) and oxidative activity toward glucose $280\pm20X10^{-3}$μmoles/mg protein x hr. (tenfold increase) over resting cells, for $1X10^{6}$ cells containing .2mg protein (3). Monocytes attach to the foreign surface and then differentiate into macrophages. These cells secrete a number of enzymes (i.e. lysozyme and proteases) and reactive oxygen species (i.e. superoxide, hydroxyl radical, and hydrogen peroxide) which work to degrade the foreign material. Macrophages also secrete wound-healing molecules, i.e. collagenase (4). They have a turnover rate of 24 hours in the tissue.

5.1.2. Experimental Design

In terms of biocompatibility, studying the sensor/tissue interaction is very important. As discussed previously in Section 2.4.2., cells may effect the sensor's response in a number of ways. If cells adhere to the surface of the sensor, the sensor's response may be effected by cell blockage of analyte flux to the sensor, or decreased enzyme activity due to pH changes or proteolysis from cellular enzymes or reactive oxygen species, or competition for glucose and/or oxygen. Competition between the cells and sensor for glucose and/or oxygen may occur even if cells aren't directly attached to the sensor's surface. In this situation, either the cells may not grow in the immediate vicinity of the sensing area or the sensor may suffer a reduced response due to reduced availability of analyte. We believe that there might be some degree of competition between the sensor and cells, particularly during the inflammation phase of the foreign body reaction to the implanted sensor. Such an interaction might explain the slow reduction in sensitivity with time observed *in-vivo* for the glucose biosensor. Cell-culture toxicity tests have shown that the sensor is not toxic to fibroblasts (5). Thus, it appears that the sensor does not interfere with the function of the host. However, no tests have been performed so far to establish whether the tissue interferes with sensor function. Therefore, this study was designed to examine this question. *In-vitro* cell culture was chosen because it seems to

provide an effective and feasible way to examine the glucose sensor/tissue interaction. To our knowledge, this is the first reported attempt to combine a glucose sensor with cells in culture so that the sensor's response can be tested while in cell-culture.

This experiment was designed to study macrophage cell growth in culture with sensors containing enzyme (active sensors). Inactive sensors, which do not contain enzyme, served as controls; these sensors are not expected to effect cell growth because of the absence of the enzyme. However, active sensors might effect cell growth if the sensor depletes glucose and/or oxygen from the cells. If cell growth is impaired in wells containing active sensors, the hypothesis that competition occurs will be supported. If it turns out that cells do not grow on or in the immediate area of the active sensor because of competition, this will be advantageous for sensor function.

A comparative calculation of glucose consumption by the sensor and cells is given below:

There will be **$1.7X10^{-5}$ mol glucose at the beginning** of the cell-culture (1.5ml of 11mM glucose solution).

Glucose consumption by the sensor:

Assumption: sensitivity = 2nA/mM and 10% of the current due to hydrogen peroxide is detected at the electrode surface

$$I\ t = n\ F \text{ moles consumed}$$

$I = 2nA/mM \times 11mM = 22nA \qquad 22nA/.1 = 2.2X10^{-7}A$

$(2.2X10^{-7})\ t = (2)(9.65X10^{4})$(moles consumed)

Moles consumed = $1.14X10^{-12}$ mol glucose/s = **$9.8X10^{-8}$ mol glucose/day**

($9.8X10^{-8}$ mol glucose per day/$1.7X10^{-5}$ mol glucose)(3 days)(100%) =

1.7% of total glucose

Glucose consumption by macrophages:

Assumption: there are .2mg protein/$1X10^{6}$ cells consuming $280X10^{-3}$ µmol glucose/mg protein x hr and there are $5X10^{5}$ cells present at the beginning of the cell-culture

($2.8X10^{-7}$ mol glucose/mg x hr)(.2mg protein/$1X10^{6}$ cells) =

$5.6X10^{-14}$ mol glucose/hr. x cell

($5.6X10^{-14}$ mol glucose/hr. x cell)($5X10^{5}$ cells) =

$2.8X10^{-8}$ mol glucose/hr. = **$6.7X10^{-7}$ mol glucose/day**

($6.7X10^{-7}$ mol glucose per day/$1.7X10^{-5}$ mol glucose)(3 days)(100%) =

12% of total glucose

From this calculation of bulk glucose consumption, macrophages consume more glucose than does the sensor. It seems likely that macrophages will not be effected by the presence of the sensor, but that the cells may effect the sensor's response. However, surface interactions may lead to a different observation. The main concern is being able to grow the cells effectively. We hoped that cell growth would not be effected by the process chosen for sensor fixation into the cell-culture plate or by the process of sterilizing the cell-culture plate.

5.2. Experimental

5.2.1.Materials and Methods

Materials for sensor preparation and testing were reported in Section 3.2.1. All sensors were prepared and tested in a clean room purchased from Clean Air Products (Minneapolis, MN). 24-well oxygen-treated polystyrene plates, purchased from MatTek (Ashland, MA) were gifts from Professor James M. Anderson, M.D., Ph.D., at Case Western Reserve University (Cleveland, OH). E6000® containing tetrachloroethylene (0.01lb/gl volatile organic compound, low toxicity) industrial strength adhesive and sealant was purchased from Eclectic Products, Inc. (Pineville, LA). Liquid Nails® (44.54% volatile by volume) multipurpose sealant containing the following organic solvents: ethylbenzene, toluene, xylene, and polybutene, was purchased from Macco Adhesives (Cleveland, OH). The ethylene oxide (EtO) gas (Pennigas® mixture: 12% ethylene oxide + 88% dichlorodifluoromethane w/w) was purchased from Pennsylvania Engineering Co. (Philadelphia, Pennsylvania). The EtO chamber was a gift from Professor Paul Kitos, Ph.D., at the University of Kansas. The cell-culture experiment was carried out in Professor Anderson's laboratory. RPMI 1640 medium, antibiotic/antimyotic mixture, and PBS containing calcium and magnesium cations were from Life Technologies (Grand Island, NY). May Grünwald stain was from Sigma Chemical Co. (St. Louis, MO). Blood for serum was obtained from an unmedicated, overnight-fasted donor, passed through a 0.2μm filter

from Nalgene (Rochester, NY), and stored at -80°C until use. Human monocytes were isolated from the venous blood by a nonadherent, density centrifugation method, which has been previously described (6). Isolated monocytes were judged >97% viable by trypan blue exclusion, and >80% pure by staining for nonspecific esterase and peroxidase. Monocytes were suspended in the following: RPMI 1640 medium (containing amino acids, vitamins, salts, phenolsulfonphthalein indicator, and 2,000mg/l glucose) mixed with 25% autologous serum and an antibiotic/antimiotic mixture (10,000U/ml penicillin G sodium, 10,000µg/ml streptomycin sulfate, 25µg/ml amphotercin B as Fugizone in 0.85% saline) (7).

5.2.2.Sensor Preparation

Active sensors were prepared as described in Section 3.2.1 with polyurethane outer membrane. Due to the high humidity in the clean room, 3% polyurethane solution was used as the outer coating instead of 5% polyurethane solution. Increasing humidity causes faster solvent evaporation, which in turn causes pores for analyte passage to close more rapidly; this increases the chances of nonresponsive sensors. To balance out this effect, the % polymer used was lowered. Sensor dimensions were slightly different from the dimensions given in Section 3.2.1. The length of the sensor was 42mm ± 1mm, the length of the sensing cavity was 2mm-3mm ± 0.2mm, the length of the Ag/AgCl reference electrode was 12.5mm ± 4mm, the length of the Ag reference contact lead was 12.5mm ± 4mm, and the

length of the Pt/Ir working contact lead was 6.0mm ± 0.5mm. Inactive sensors were prepared in a manner similar to active sensors, but without the enzyme layer. A total of 18 active sensors and 5 inactive sensors were prepared, although only 5 of each were used in the cell culture study; sensors with low (less than 0.40nA/mM) or high sensitivities (greater than 10nA/mM) were rejected.

5.2.3.Sensor Stabilization and Subsequent Fixation in 24-Well Plate

After preparation, the response of active sensors was stabilized in phosphate-buffered saline (PBS) for 16 days, during which time each sensor's response to glucose was tested 2-4 times. Because of the large number of sensors to be tested, measurements were made several days apart for most sensors. The sensors' response was tested *in-vitro* as described in Section 3.2.2., but at ambient temperature instead of 37°C, since it was not possible at the time to determine the response of the sensors at 37°C once they were fixed in the wells of the plate. Five active sensors with sensitivity values ranging between 1-6nA/mM were chosen for fixation in the 24-well plate. On day 16, a hole approximately 3mm-4mm in diameter was drilled through the outerside of ten wells of the plate as close to the bottom part of the well a possible using a 3mm-4mm diameter drill bit that had been sterilized with ethanol. The debris was wiped away using Kimwipes® and one sensor was inserted through the hole and placed flat at the bottom in each of the ten

wells. Five active sensors and 5 inactive sensors were fixed in the plate. Solution leakage was a big problem. Therefore, to inhibit leakage from the wells, it was advantageous to seal the hole on both the inside and the outside with strong sealants. E6000®, which did not appear to affect cell growth from a previous test experiment, was used as the inner sealant. Liquid Nails®, another strong sealant, was used as the outer sealant. After application to the wells, the sealants were allowed to dry overnight (>12 hrs.). Figure 4.1 shows the position of the sensor inside the well at an angled view of the top/side of the plate. Figure 4.2 is a schematic of the 24-well plate. It shows placement of the active and inactive sensors in the wells. Active sensors were designated as A251, A253, A258, A261, and A262. Inactive sensors were designated as I251, I253, I258, I261, and I262.

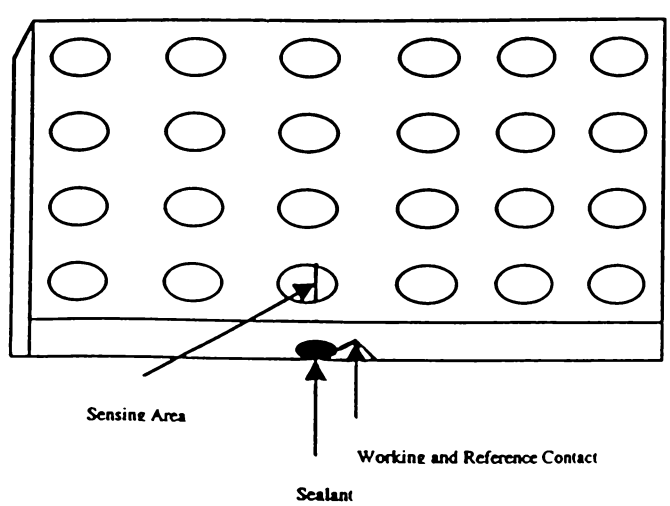

Figure 4.1. Top/side Angled View of a Sensor Fixed Inside a Well.

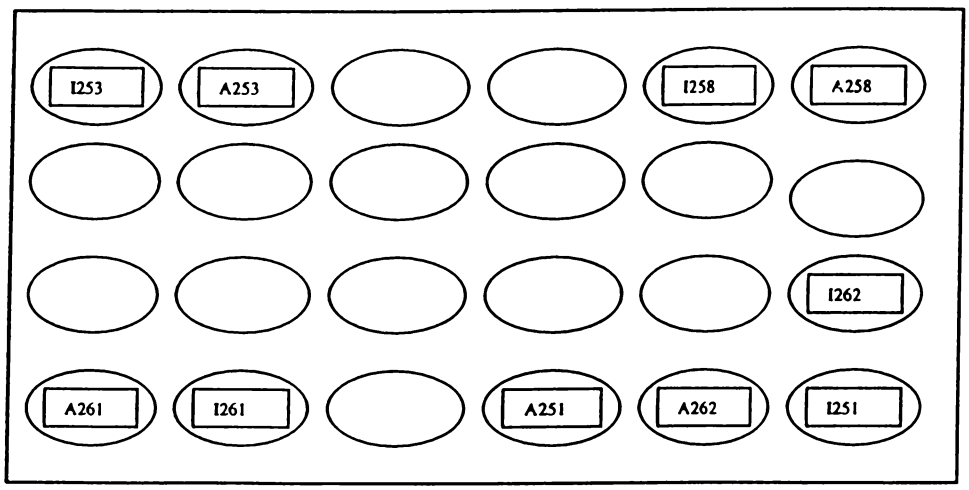

Figure 4.2. Schematic of 24-Well Plate Containing Active and Inactive Sensors.

5.2.4. Characterization of Active Sensors in 24-Well Plate: Sensitivity, Linear Range, and Stability

Active sensors were characterized by their sensitivity, linear range, and stability determined using calibration curves. During testing, 2.5ml of PBS was added to the well. The working electrode was polarized to +600mV vs Ag/AgCl. After an approximate 45 minute

to one hour stabilization period, glucose was injected into the well in 9µl increments, corresponding to final glucose concentrations of 5mM, 10mM, 15mM, and 20mM glucose. After each injection, the solution was mixed using a pipette. The solution was mixed several times until a stable sensor output was achieved. A calibration curve was prepared by plotting the glucose concentration (mM) against the corresponding 90% stabilized output current and fitting the data to a linear regression line. The sensitivity in nA/mM was determined from the slope of the line; the linear range was from 1mM glucose up to the glucose concentration at which the line deviated significantly from the linear regression line; stability was determined by comparing the sensitivity before fixation in the well to the subsequent sensitivity after fixation in the well. A sensitivity profile was prepared for each sensor by plotting the sensitivity (nA/mM) against time (days after sensor preparation).

5.2.5.Well Leakage Test

To ensure that wells would not leak during the cell-culture, the wells containing sensors were filled with PBS and placed in a 37°C incubator for 24 hrs. on days 21 and 23 after sensor preparation.

5.2.6.Sensor Sterilization

Sterilization was performed on day 26 after sensor preparation. The 24-well plate and cover were placed inside a

polystyrene bag. The bag was then placed in a chamber containing ethylene oxide (EtO) at about 1 atm pressure for 24 hrs. The bag was removed on day 27 after sensor preparation and the plate was allowed to outgas for 2 days. The plate was shipped to Case Western Reserve University on day 29 after sensor preparation for the cell-culture experiment. A total of 5 days was allowed for residual EtO to escape before the cell-culture experiment was begun.

5.2.7.Cell Fixation and Culture

On day 32 after sensor preparation, monocytes were added to each of the ten wells at a concentration of $5X10^5$ cells per well. Cells were incubated for 2 hrs. at 37°C in a humidified atmosphere of 95% air and 5% CO_2.. Nonadherent cells were removed by rinsing the wells with warmed (37°C) PBS containing calcium and magnesium cations. The remaining adherent cells were covered with 1ml of fresh medium and incubated with 25% heat-treated (56°C water bath for 1 hr.) autologous serum in RPMI. The cells were cultured for 3 days at 37°C in a humidified atmosphere of 95% air and 5% CO_2.

5.2.8.Cell Fixation and Staining

The 3 day cell-culture was completed on day 35 after sensor preparation. The cells in each well were rinsed twice for 5 minutes each with warmed PBS and fixed with methanol. May-Grünwald stain was added 50µl per well. Wells were washed briefly with PBS. Then,

Giemsa stain (8), diluted 1:14 in deionized distilled water, was added for 17 minutes, 50µl per well, and wells were rinsed twice with distilled water and allowed to air dry.

5.2.9.Microscopy and Cell Counting

Stained cells were viewed by light microscopy and photographed. Images (X2, X10, and X20) of the sensing area, tip, and reference were taken for all sensors. The number of cells within 5mm of either side of the sensing area (~9.8 mm^2 total area) was counted 3 times (using X10 images) for each of the ten wells containing active and inactive sensors. This distance of 5mm was chosen because it was the shortest distance for which counting was feasible; the sensing area accounted for ~2.0 mm^2, approximately 1/5 of the total area for which the cells were counted. The average number of cells counted for each well was recorded.

5.2.10:Statistical Analysis

The Wilcoxon Rank Sum Nonparametric Test (9) was used for statistical analysis of the data. This test is based on independent random samples. To use the test, all observations are ranked, assigning a rank of 1 to the smallest, 2 to the second smallest, and so on. The sum of the ranks, called a rank sum, is then calculated for each sample. If the distributions are identical, we would expect the sample rank sums, designated T_1 and T_2, to be nearly

equal. In contrast, if one rank sum is much larger than the other, then the data suggest that the population distributions are shifted to the left or right of one another. The null hypothesis (H_0) tested was H_0: **A = I**, that is the relative frequency distributions for inactive (I) and active (A) sensor populations are identical. In other words, there is no difference between cell growth in wells containing active sensors compared to cell growth in wells containing inactive sensors. This null hypothesis was tested against the following alternative hypothesis **Ha: A < I**, cell growth in wells containing active sensors is impaired compared to cell growth in wells containing inactive sensors. The hypothesis was tested at $\alpha = 0.05$ (95% confidence level).

5.3.Results

5.3.1.Sensor characteristics: Sensitivity, Linear Range, and Stability Before and After Fixation in the Well

All sensors were tested over a 25 day test period, but not necessarily on the same days. The response of sensor #251 was tested on days 1, 7, 10, 17, 18, 21, and 25 after preparation. The stability profile is shown in Figure 4.3. Table 4.1. summarizes the sensor's response and changes in the response after fixation in the well. The sensitivity increases from 0.49nA/mM ± 0.040nA/mM on day 1 to 2.08nA/mM ± 0.13nA/mM on day 10, presumably stabilized. Upon fixation of the sensor into the well, the sensitivity dropped by

~13%, 8.65%, and 6.25% on days 17, 18, and 21, respectively, from the stabilized value. On day 25, the sensitivity increased by 26.2% compared to the value measured before fixation in the well.

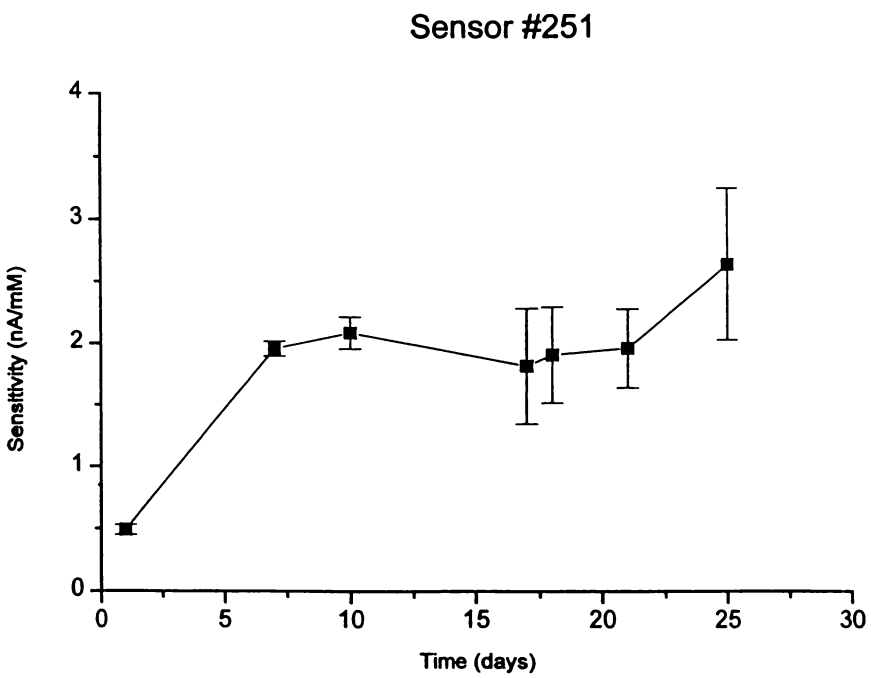

Figure 4.3. Stability Profile of Sensor #251.

Table 4.1. Summary of Sensor #251 Response.

DAYS AFTER PREPARATION	SENSITIVITY, nA/mM** (CORRELATION COEFFICIENT)	~ % CHANGE IN SENSITIVITY AFTER FIXATION IN THE WELL
1	0.49 ± 0.040 (0.99)	———
7	1.95 ± 0.06 (0.99)	———
10	*2.08 ± 0.13 (0.99)	———
17 (after well fixation)	1.81 ± 0.47 (0.97)	-13.0%
18	1.90 ± 0.39 (0.98)	-8.65%
21	1.95 ± 0.32 (0.99)	-6.25%
25	2.63 ± 0.61 (0.97)	+26.2%

*stabilized sensitivity

**0-10mM glucose

Figure 4.4 shows the response of sensor #251 (a) and the calibration curve (b) on day 10, seven days before fixation in the well. Figure 4.5 shows the response of sensor #251 (a) and the calibration curve (b) on day 17, one day after fixation in the well. On day 10, the response to glucose increased and then leveled off after each glucose injection, as expected. Using 3 points, the data fit a linear regression curve with a correlation coefficient of 0.99. The sensitivity, slope of the line, was 2.08nA/mM ± 0.13nA/mM. The sensor was linear from 1mM to 20mM glucose (Figure 4.4 (b) inset). During the measurement on day 17, after fixation in the well, the response quickly increased, slowly decreased, and then leveled off (Figure 4.5 (a)). The sensitivity and linear range were reduced by ~13% and 50%, respectively (Figure 4.5 (b)), compared to the measurement on day 10.

(a)

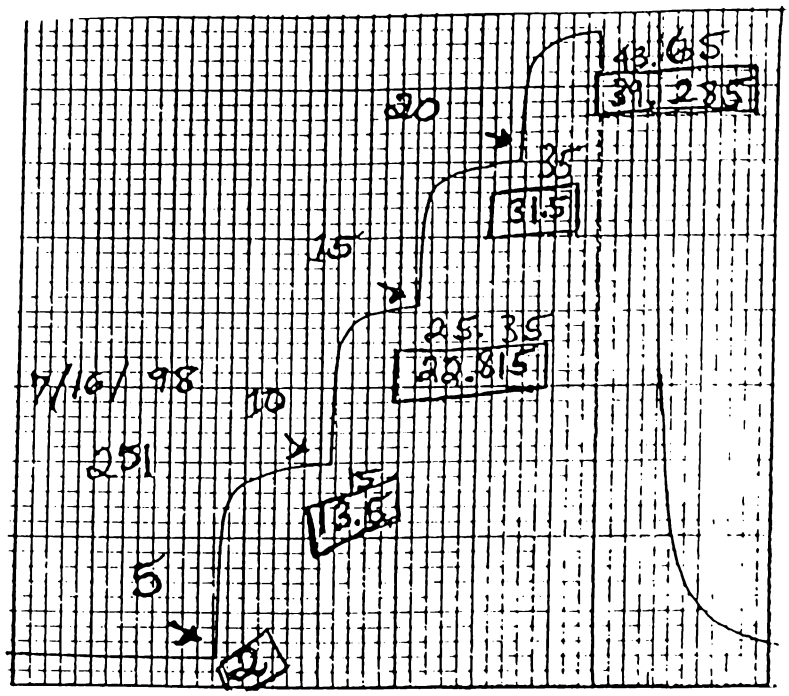

Sensor #251 at Day 10

(b)

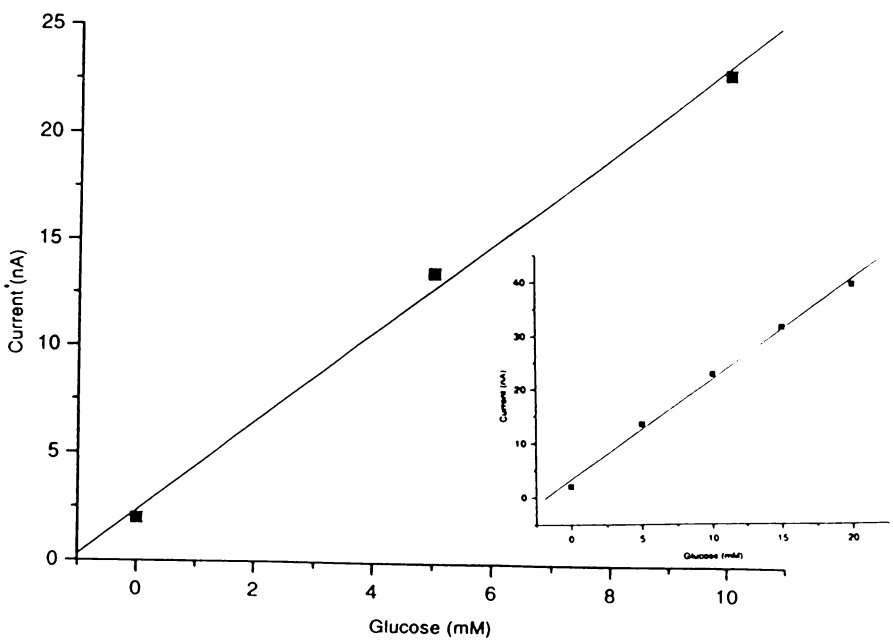

Figure 4.4. Response of Sensor #251 (a) and calibration curve for sensor #251 (b) at Day 10.

(a)

(b)

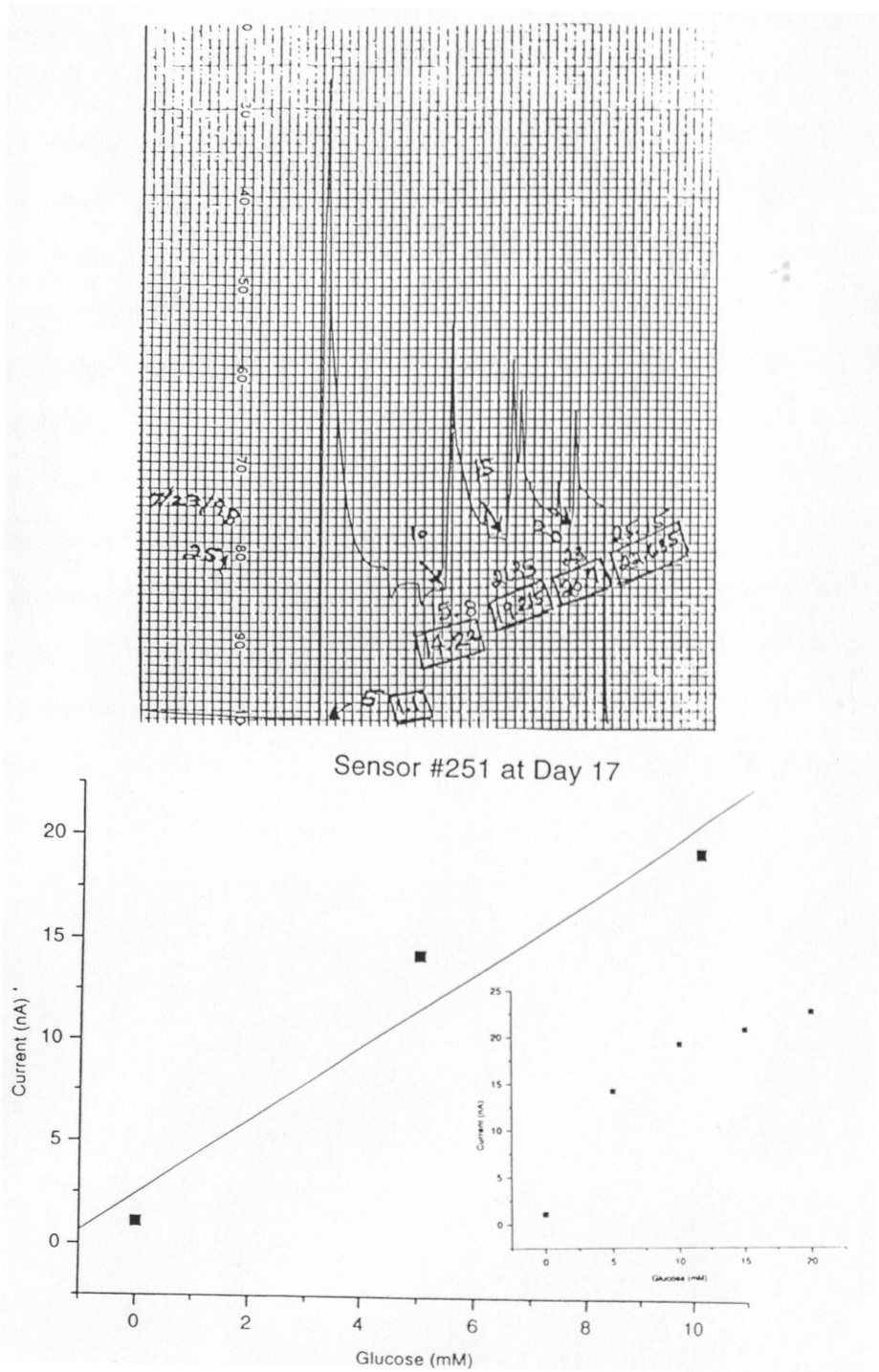

Figure 4.5. Response of Sensor #251 (a) and Calibration Curve for Sensor #251 at Day 17.

Figures 4.6, 4.7, 4.8, and 4.9 show the sensitivity profiles of sensor #253, 258, 261, and 262, respectively. Tables 4.2, 4.3, 4.4, and 4.5 summarize the response of sensors #253, 258, 261, and 262, respectively, over the 25 day test period. The sensors showed similar characteristics to sensor #251 before and after fixation in the well. The last sensitivity value measured before fixation in the well was stable within ~6% of the previous value measured, with the exception of sensor #253 which was stable to within 15%. All sensors were linear from 1mM to 20mM glucose before well fixation. Afterwards, on day 17, the sensitivity decreased by ~63.1%, 25.8%, 64%, and 61.4% for sensors #253, 258, 261, and 262, respectively. On day 25, the last measurement, sensors #253 and #258 appeared to be stabilized. The other sensors' response increased. After fixation in the well, the sensors were linear only up to 10mM glucose.

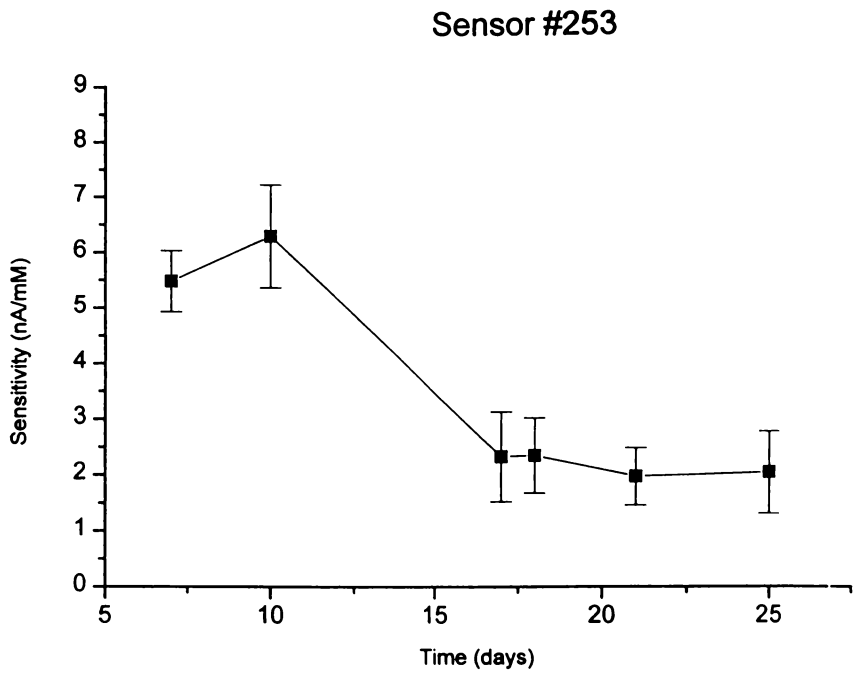

Figure 4.6. Stability Profile of Sensor #253.

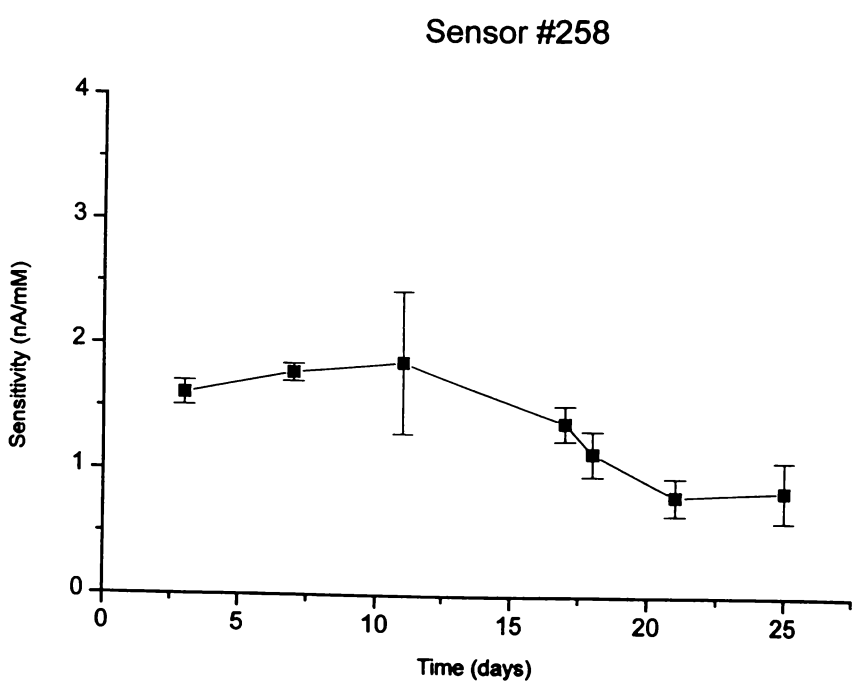

Figure 4.7. Stability Profile of Sensor #258.

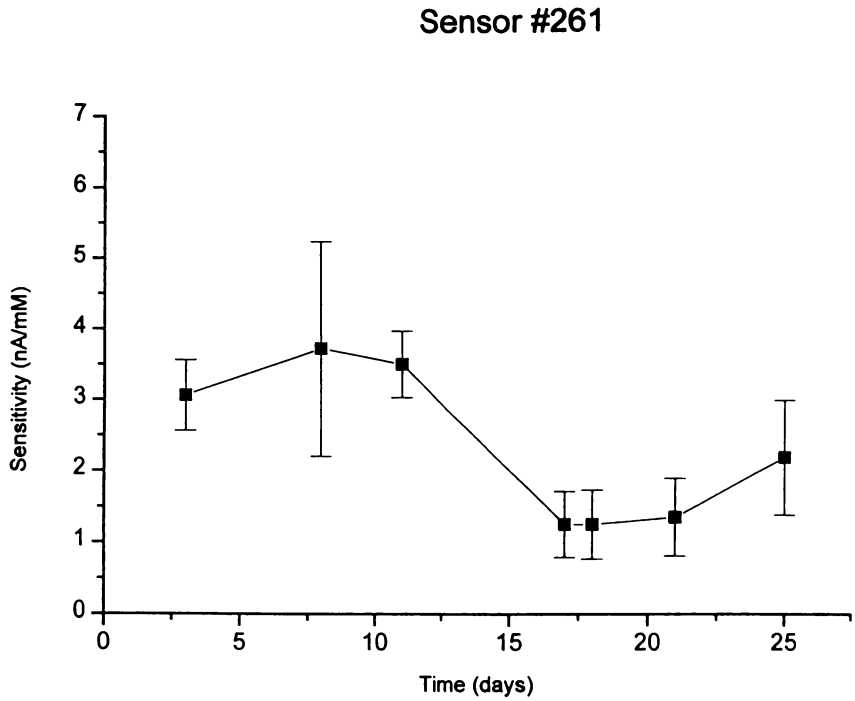

Figure 4.8. Stability Profile of Sensor #261.

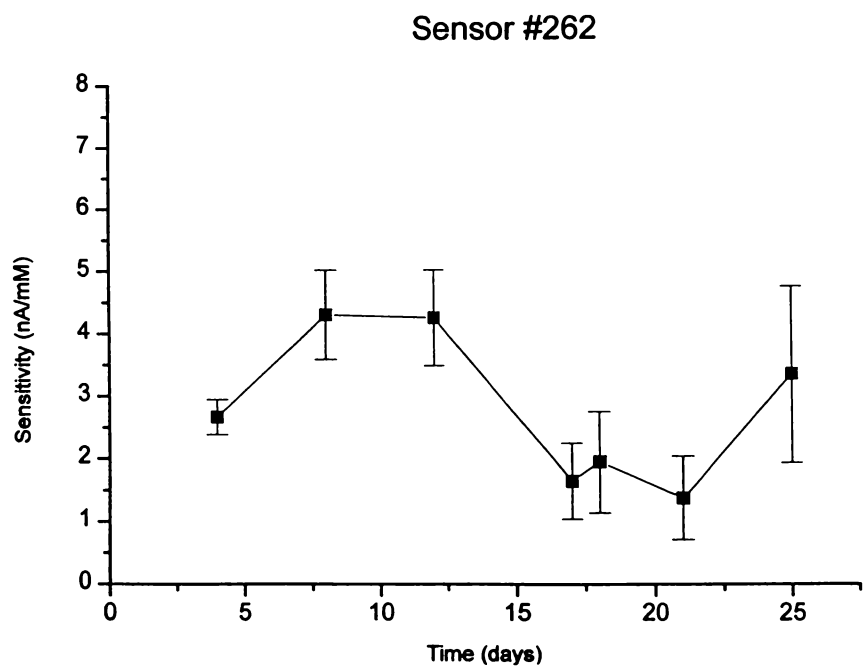

Figure 4.9. Stability Profile of Sensor #262.

Table 4.2. Summary of Sensor #253 Response.

DAYS AFTER PREPARATION	SENSITIVITY, nA/mM** (CORRELATION COEFFICIENT)	~ % CHANGE IN SENSITIVITY AFTER FIXATION IN THE WELL
7	5.48 ± 0.55 (0.99)	———
10	*6.29 ± 0.93 (0.99)	———
17 (after well fixation)	2.32 ± 0.80 (0.94)	-63.1%
18	2.34 ± 0.67 (0.96)	-62.8%
21	1.97 ± 0.51 (0.97)	-68.7%
25	2.04 ± 0.73 (0.94)	-67.6%

*stabilized sensitivity **0-10mM glucose

Table 4.3. Summary of Sensor #258 Response.

DAYS AFTER PREPARATION	SENSITIVITY, nA/mM** (CORRELATION COEFFICIENT)	~ % CHANGE IN SENSITIVITY AFTER FIXATION IN THE WELL
3	1.61 ± 0.098 (0.99)	———
7	1.78 ± 0.07 (0.99)	———
11	*1.86 ± 0.57 (0.96)	———
17 (after well fixation)	1.38 ± 0.14 (0.99)	-25.8%
18	1.14 ± 0.18 (0.99)	-38.7%
21	0.80 ± 0.15 (0.98)	-57%
25	0.084 ± 0.24 (0.96)	-55%

*stabilized sensitivity **0-10mM glucose

Table 4.4. Summary of Sensor #261 Response.

DAYS AFTER PREPARATION	SENSITIVITY, nA/mM** (CORRELATION COEFFICIENT)	~ % CHANGE IN SENSITIVITY AFTER FIXATION IN THE WELL
3	3.06 ± 0.50 (0.99)	———
8	3.72 ± 1.52 (0.92534)	———
11	*3.50 ± 0.47 (0.99)	———
17 (after well fixation)	1.25 ± 0.46 (0.94)	-64%
18	1.25 ± 0.48 (0.93)	-64%
21	1.35 ± 0.54 (0.93)	-61%
25	2.18 ± 0.80 (0.94)	-37%

*stabilized sensitivity **0-10mM glucose

Table 4.5. Summary of Sensor #262 Response.

DAYS AFTER PREPARATION	SENSITIVITY, nA/mM** (CORRELATION COEFFICIENT)	~ % CHANGE IN SENSITIVITY AFTER FIXATION IN THE WELL
4	2.67 ± 0.28 (0.99)	———
8	4.31 ± 0.72 (0.99)	———
12	*4.25 ± 0.77 (0.98)	———
17 (after well fixation)	1.64 ± 0.60 (0.94)	-61.4%
18	1.94 ± 0.80 (0.93)	-54.4%
21	1.37 ± 0.66 (0.90)	-67.8%
25	3.33 ± 1.41 (0.92)	-21.6%

*stabilized sensitivity **0-10mM glucose

5.3.2.Microscopy

After the 3 day cell-culture experiment, the cells were fixed and stained. Microscopic images (X10 magnification) of the wells which contained active sensors (A) and inactive sensors (I) were taken. Table 4.6 shows the average number of cells counted within 5mm of either side of the sensing area (9.8 mm^2 total area) for all sensors. The number of cells counted ranged from 31 ± 2 cells to 209 ± 3 cells.

Table 4.6.

Summary of Cells Counted ~5mm from Sensing Area.

SENSOR#	NUMBER OF CELLS COUNTED/9.8mm^2 (n = 3)
A251	87 ± 2
I251	209 ± 3
A253	127 ± 5
I253	54 ± 3
A258	31 ± 2
I258	42 ± 2
A261	61 ± 5
I261	46 ± 7
A262	44 ± 1
I262	114 ± 7

A = active sensors, I = inactive sensors, n = number of times cells were counted

Figures 4.10, 4.11, 4.12, 4.13, and 4.14 are images of active sensors #251, 253, 258, 261, and 262, respectively. Figures 4.15, 4.16, 4.17, 4.18, and 4.19 are images of inactive sensors #251, 253, 258, 261, and 262, respectively. Not only did the number of cells counted in the sensing area vary widely, but cell growth throughout the well wasn't confluent for any of the wells; the number of cells growing around the tip and reference areas varied widely from well to well. Also, the sensor's surface could not be observed well with this technique. Therefore, cell attachment and growth on the surface of the sensor could not be determined.

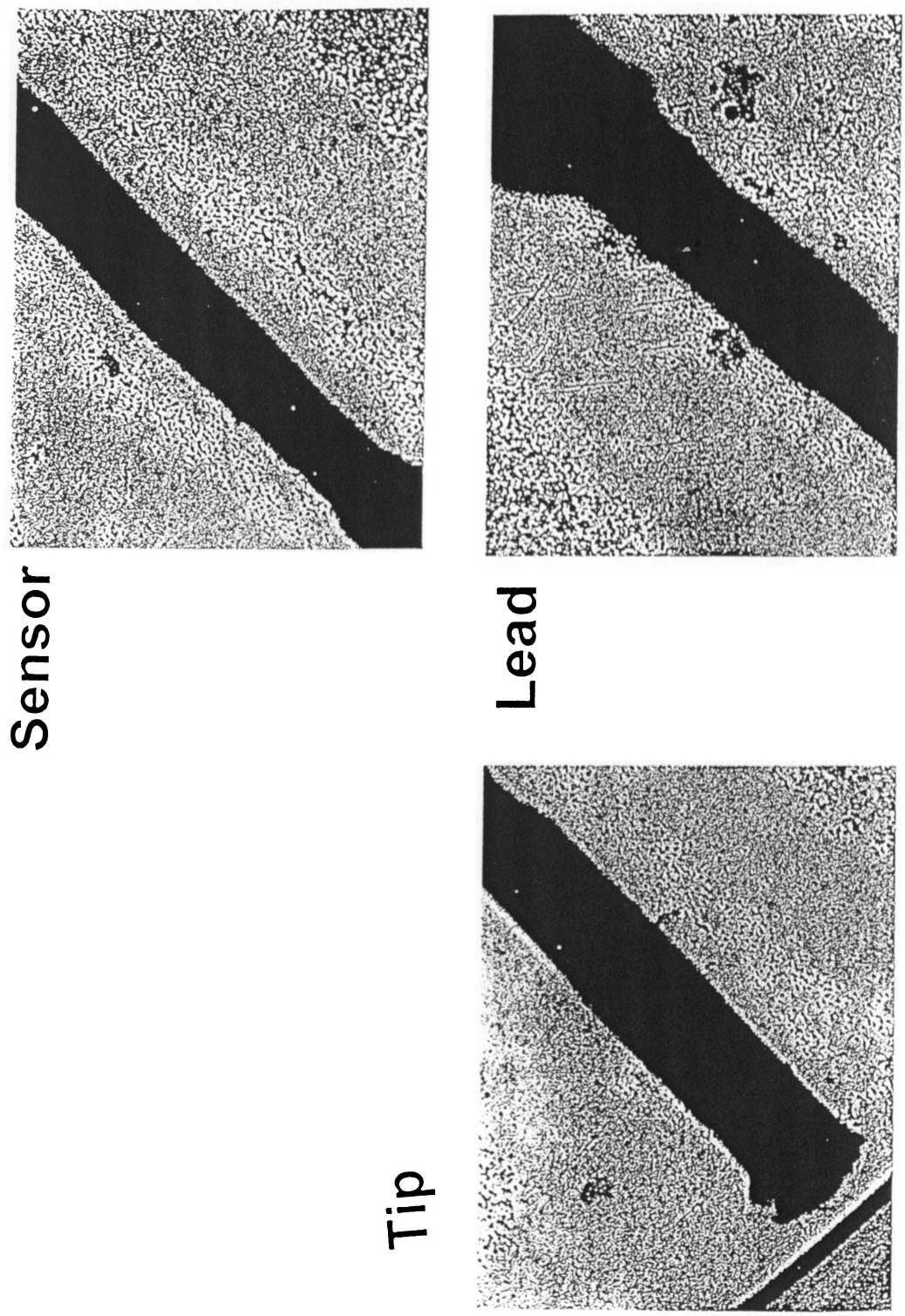

Figure 4.10. Microscopic Image (X10) of Sensor #251A.

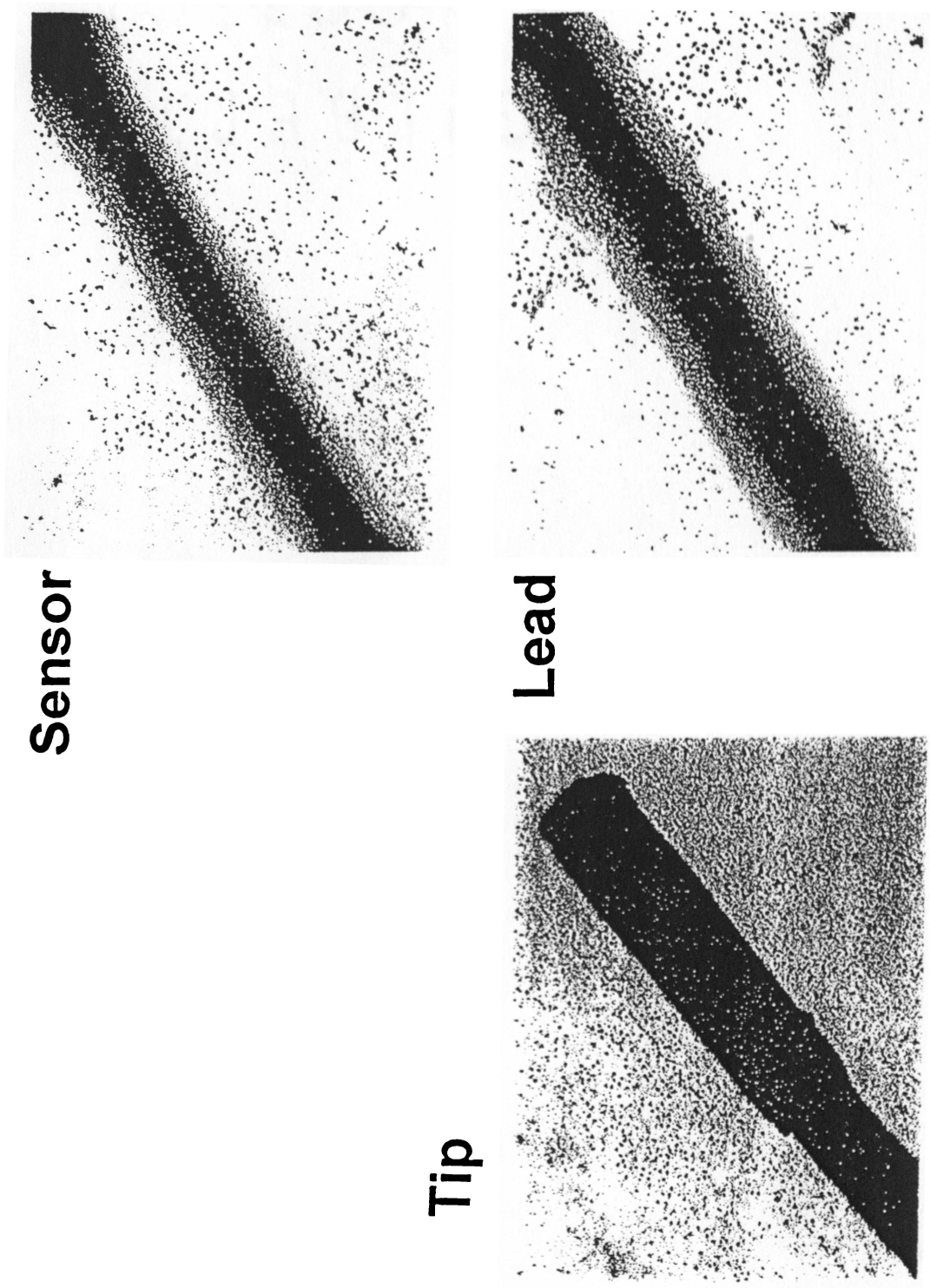

Figure 4.11. Microscopic Image of Sensor #253A.

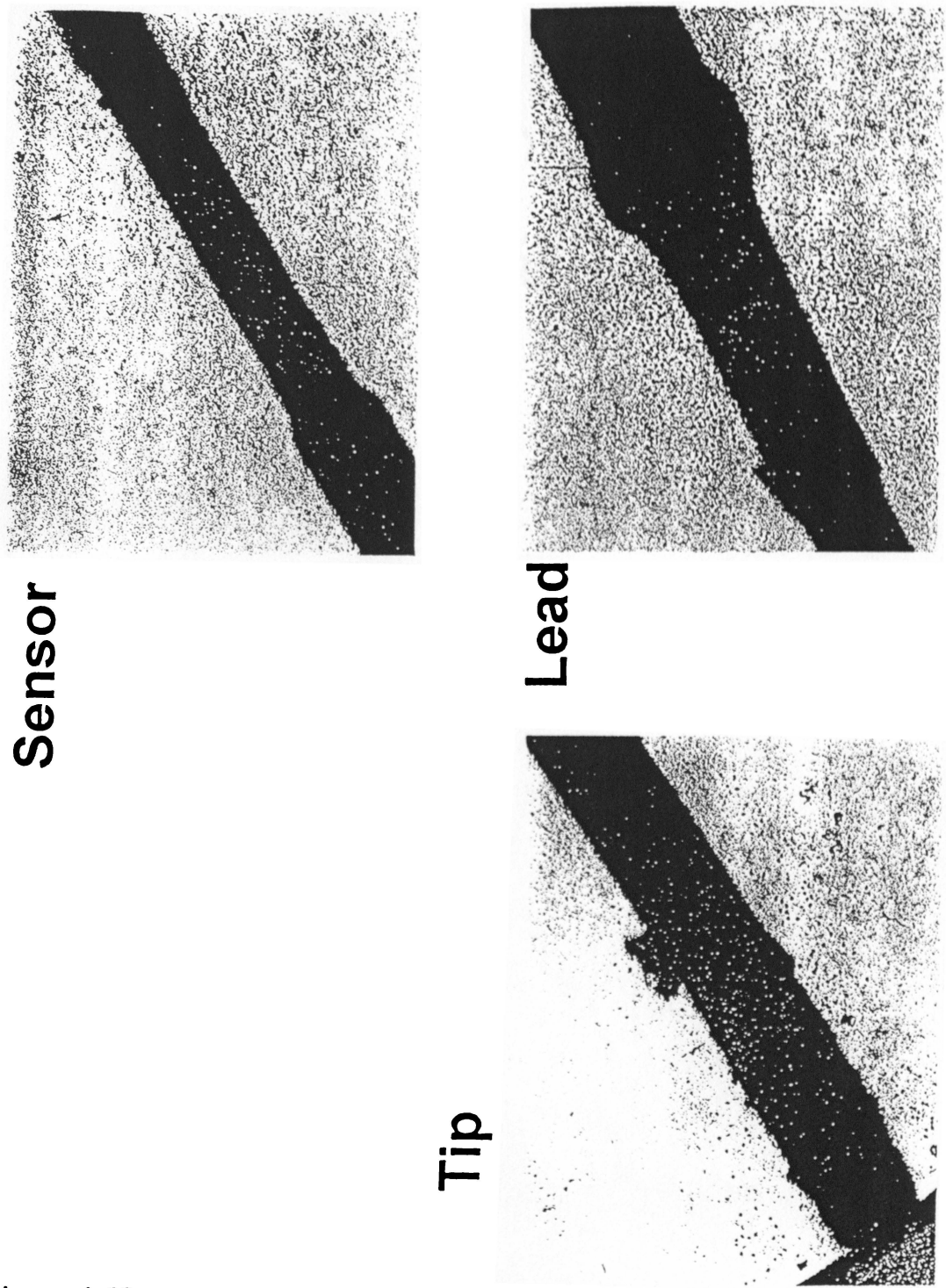

Figure 4.12. Microscopic Image of Sensor #258A.

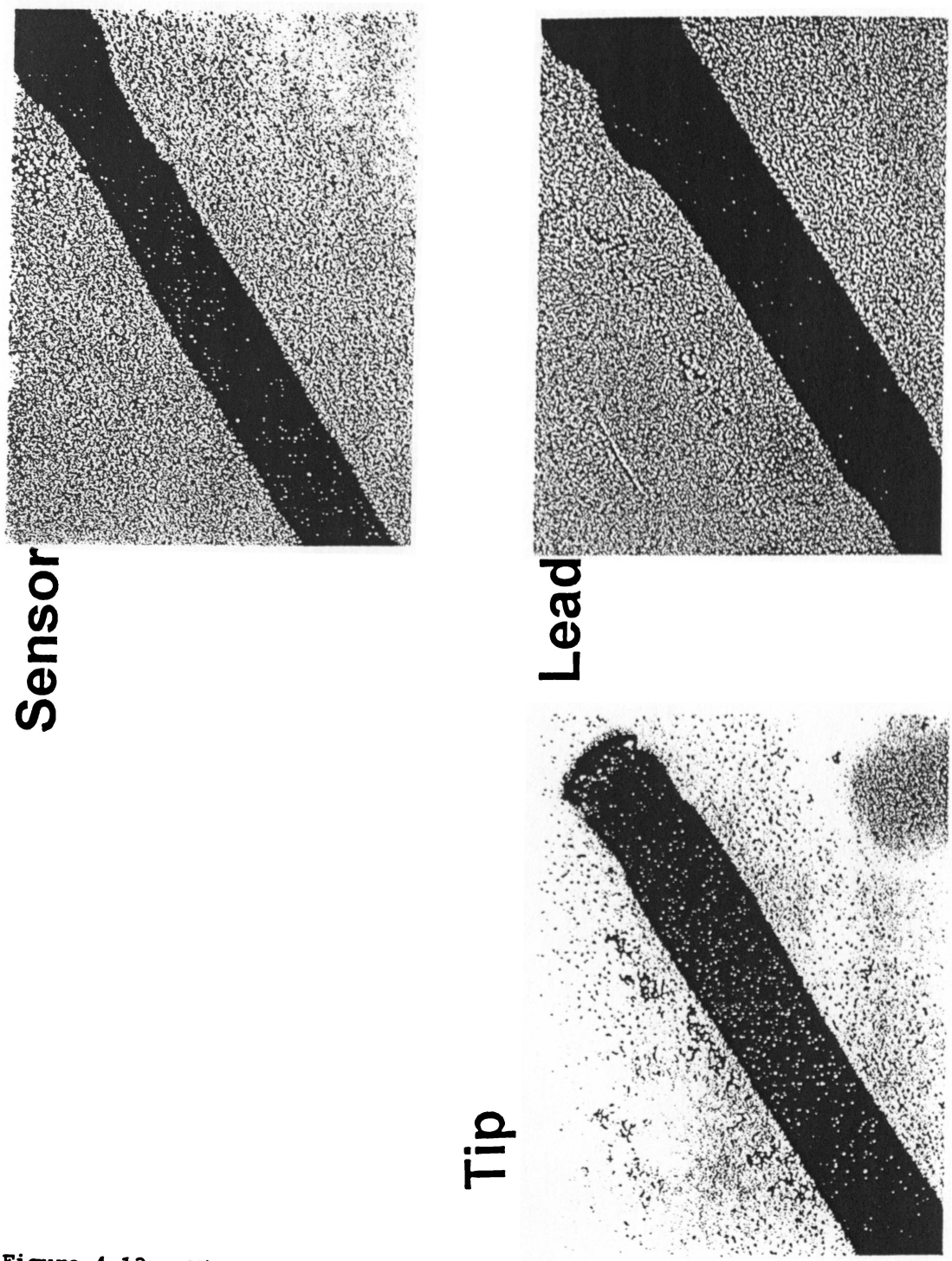

Figure 4.13. Microscopic Image of Sensor #261A.

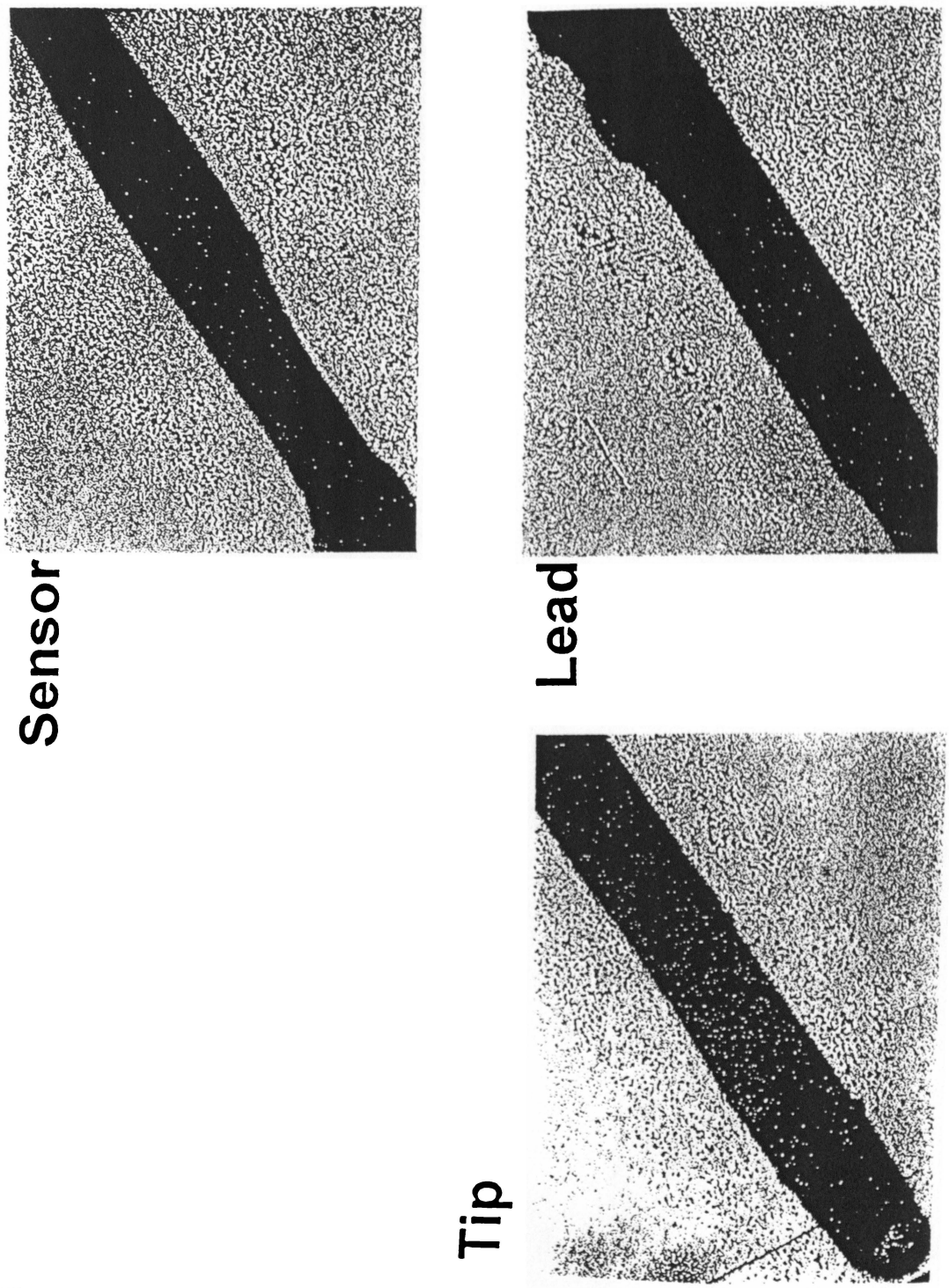

Figure 4.14. Microscopic Image of Sensor #262A.

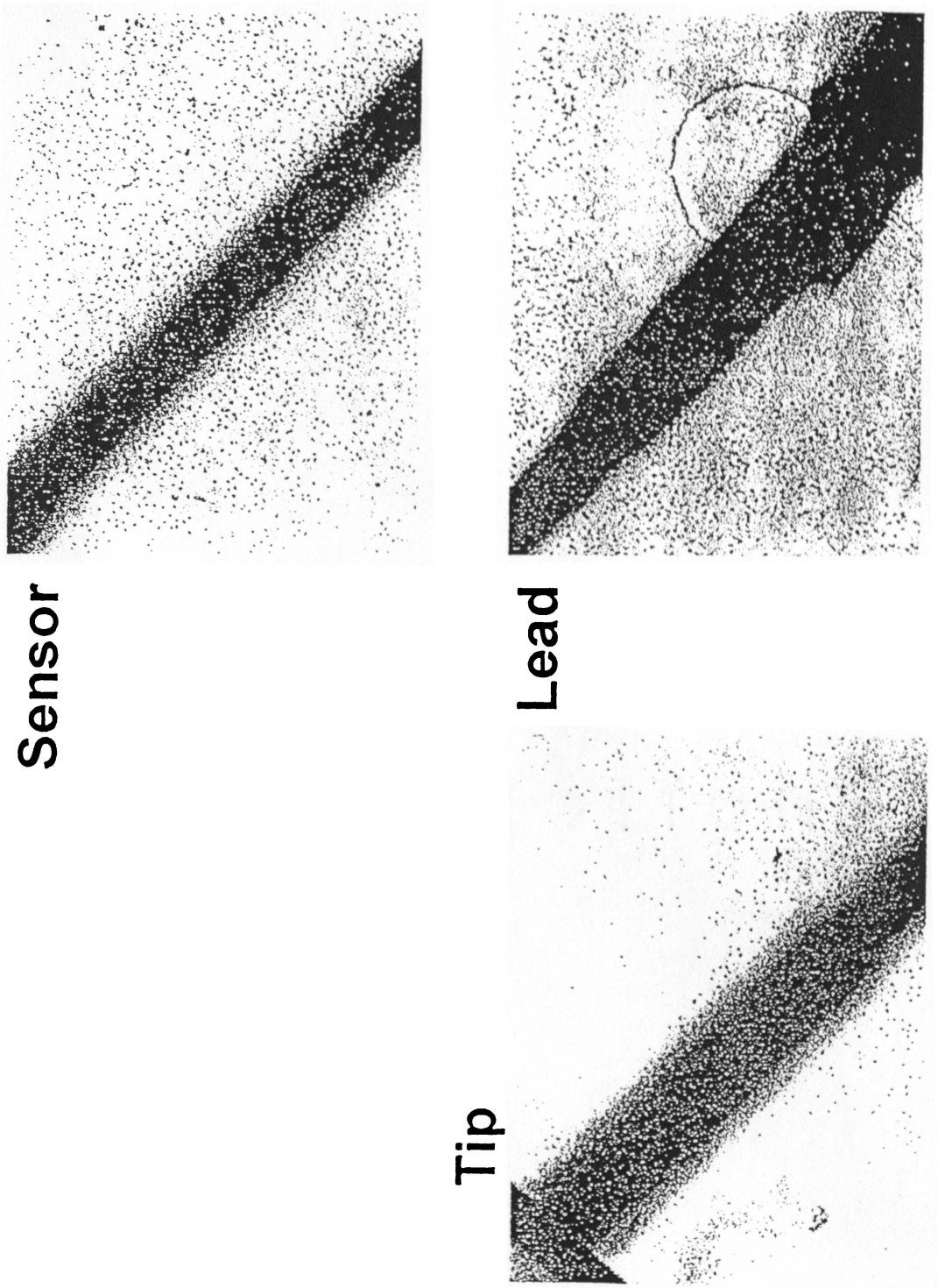

Figure 4.15. Microscopic Image of Sensor #251I.

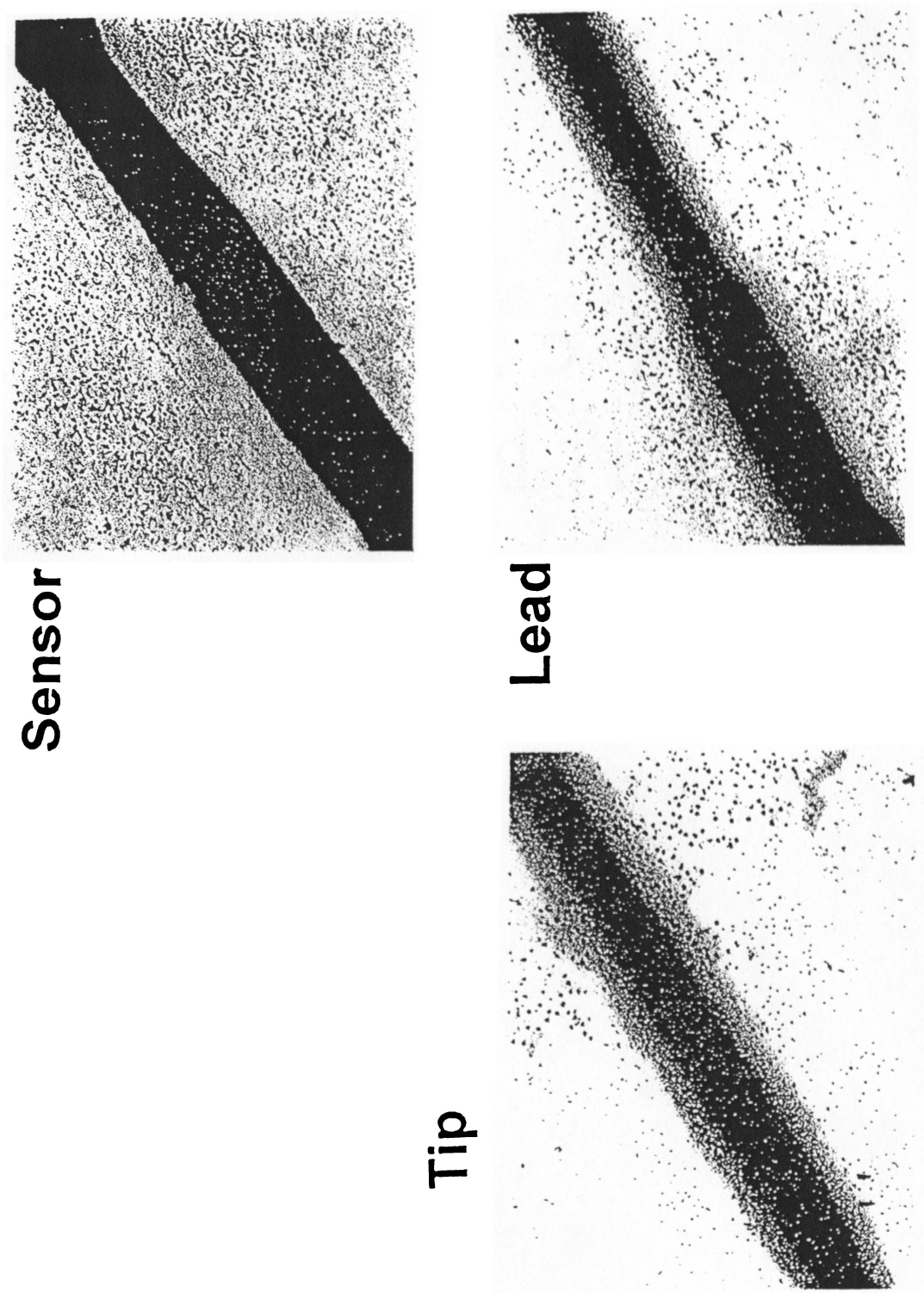

Figure 4.16. Microscopic Image of Sensor #253I.

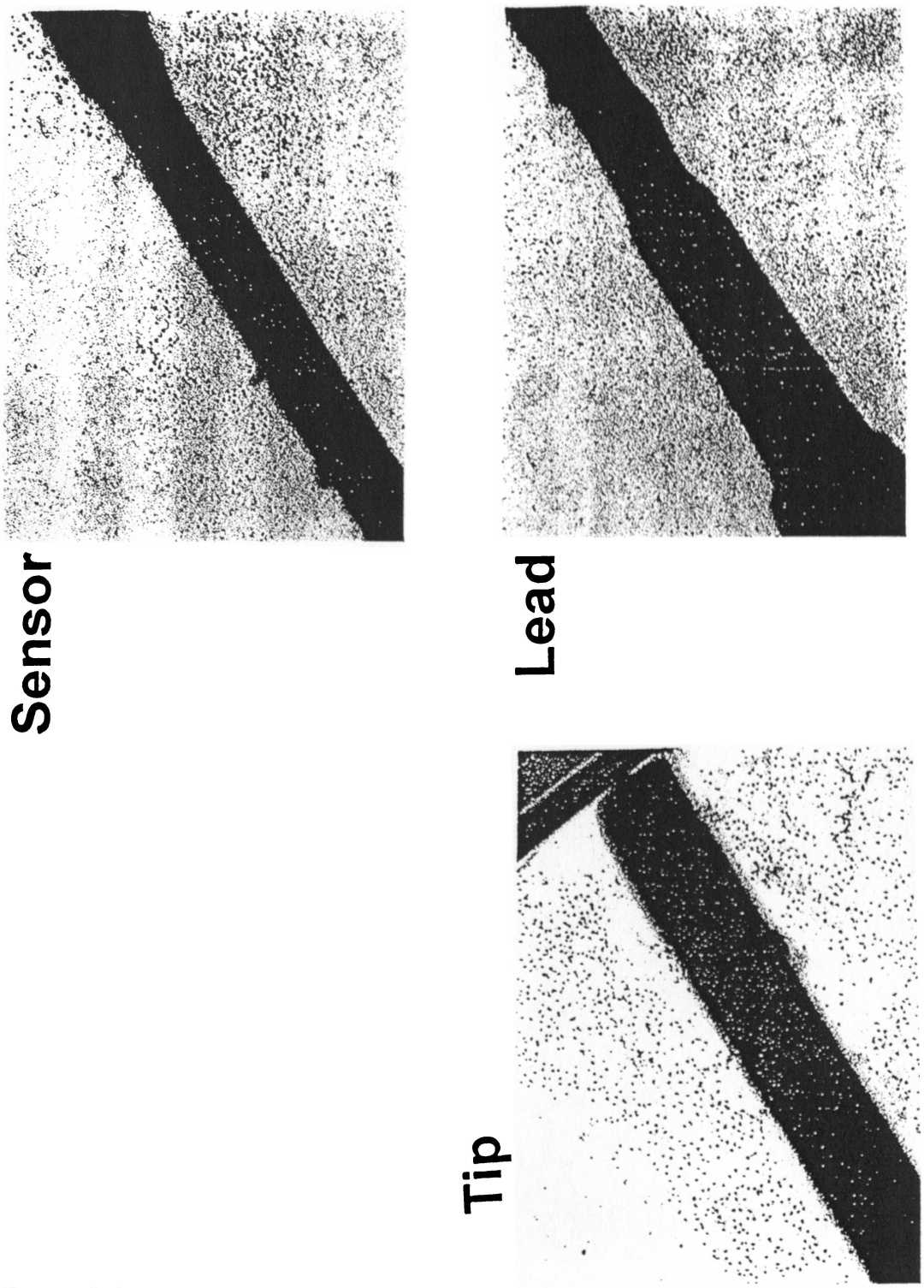

Figure 4.17. Microscopic Image of Sensor #258I.

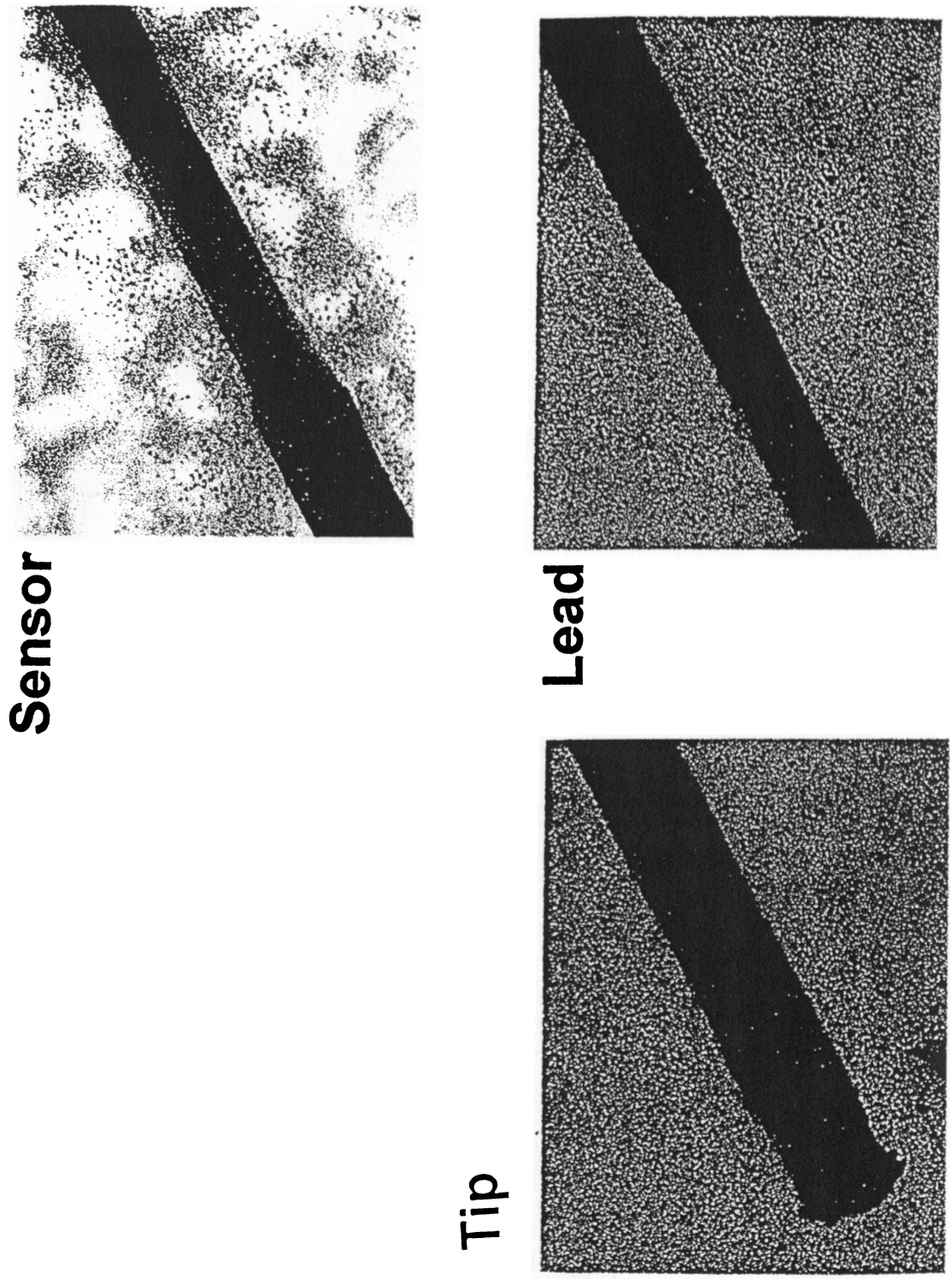

Figure 4.18. Microscopic Image of Sensor #261I.

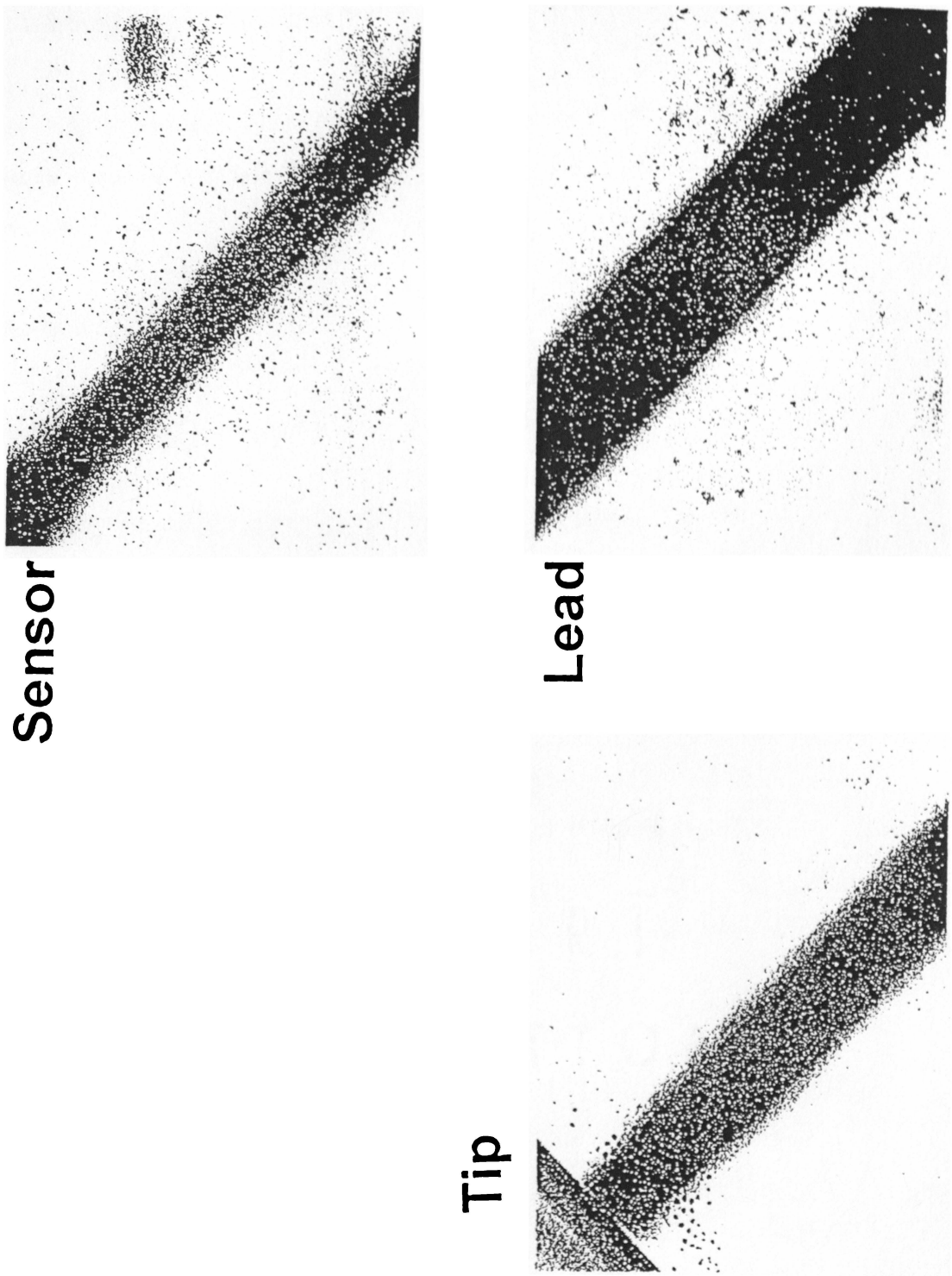

Figure 4.19. Microscopic Image of Sensor #262I.

5.3.3.Statistical Analysis

All ten sensors were ranked according to the average number of cells counted around the sensing area. Table 4.7. shows the results of the ranking.

Table 4.7.

Ranks for Active (A) and Inactive (I) Sensors.

SENSOR #	ACTIVE SENSORS (A)	INACTIVE SENSORS (I)
251	7	10
253	9	5
258	1	2
261	6	4
262	3	8
	$T_1 = 26$	$T_2 = 29$

T_1 = rank sum of active sensors

T_2 = rank sum of inactive sensors

The rankings were as follows: 1 = sensor #258A, 2 = sensor #258I, 3 = sensor #262A, 4 = sensor #261I, 5 = sensor #253I, 6 = sensor #261A, 7 = sensor #251A, 8 = sensor #262I, 9 = sensor #253A, and 10

= sensor #251I. The null hypothesis was H_0: A = I. For the null hypothesis to be rejected with 95% confidence, $T_1 \leq T_L$ and $T_2 \geq T_U$, where T_L is the lower-tailed critical rank sum value and T_U is the upper-tailed critical rank sum value. From tables of nonparametric statistics with one-tailed distributions, 10 total distributions, and $\alpha = 0.05$:

$$\mathbf{T_L = 19 \text{ and } T_U = 36}$$

Since $T_1 = 26$ is not ≤ 19, and $T_2 = 29$ is not ≥ 36, the null hypothesis cannot be rejected. There is no difference between cell growth in wells of active and inactive sensor with 95% confidence.

5.4.Discussion

Sensor characteristics before fixation in the wells were as expected: Sensitivity (stabilized) between 2nA/mM and 6nA/mM, linear range from 1mM to 20mM glucose, and stabilized response within 6%, with the exception of sensor #253, 2 weeks after sensor preparation.

After fixation in the wells, the characteristics of all sensors were altered. The sensitivity was reduced by as little as ~13% (sensor #251) to as high as ~64% (sensor #261). Although the cause of the sensitivity reduction isn't clear, it seems likely that the sealant is somehow involved, since the decrease was observed for all sensors after fixation in the well. Volatile organic solvents

from the sealant may have affected the enzyme activity leading to sensitivity reduction. Also, partial blockage of the sensing area, due to sensor fixation on the bottom of the well, could have led to reduced sensor response.

The linear range of the sensors was reduced from 1-20mM glucose to 1-10mM glucose. This result is probably due to limited oxygen availability to oxidize the reduced coenzyme and maintain a linear response. Oxygen availability can be affected by blockage/damage of the membrane(s) caused by sealant components or partial blockage of the sensing area. In these situations, oxygen can be the limiting substrate for the enzymatic reaction rather than glucose.

Approximately 1 week after fixation in the well, the response of sensors #253 and #258 appeared to be stable. However, the response of the other sensors increased on day 25. The cause of this increase is not known, but could have been due to alterations in the membrane(s) affecting glucose and/or hydrogen peroxide diffusion.

Another concern is the cause of the inconsistent cell growth throughout the well, which may have affected cell growth at the sensor's surface and subsequently the outcome of the statistical test. In this situation, meaningful results cannot be obtained from counting the cells around the sensing area and accounting differences in the numbers to competition for glucose and/or oxygen between the sensor and cells. It appears that some other factor(s) besides glucose and oxygen consumption by the sensor is contributing

to the inconsistent cell growth in the wells. Cell growth at the sensor tip and reference should have been consistent in all wells because from previous experiments there was no substantial effect of these areas on cell growth. Possible causes of inconsistent cell growth could be residual ethylene oxide poisoning the cells preventing cell growth in some areas of the well or a damaged/contaminated well surface.

5.5.Future Work

Future work on this project should include the following: 1. determination of the cause of the sensitivity loss upon fixation in the well, 2. Determination of the cause of inconsistent cell growth throughout the well, and 3. Determination of a more accurate method to count the cells.

To determine the cause of the reduction in sensitivity upon fixation of the sensor into the well, an alternative sealant should be used. If the response doesn't decrease after the substitution is made, it will be safe to assume that the sealant components had some affect on the enzyme activity. Epoxy or silicone may be good alternative sealants for sealing the hole on the inside.

It appears that inconsistent cell growth is due to some aspect of sensor preparation before the cell-culture. In this experiment, residual ethylene oxide was allowed to escape for 5 days. Wheaton Science Products has reported that 14 days must be allowed for outgassing of residual EtO from plastics (10). To determine whether

or not EtO effects cell growth, a series of 24-well plates can be sterilized and different lengths of time can be allowed for residual EtO to escape (i.e. 5 days, 10 days, and 14 days). Cells can be cultured in various wells of each of the plates and cell growth monitored and compared. If cells growth is greater in wells of plates in which longer period of time was allowed for residual ethylene oxide to escape, then it would be reasonable to conclude that EtO poisoning impaired cell growth.

The quality of the wells can be improved by more careful drilling of the holes and proper cleaning of the wells. Use of a light weight drill and smaller drill bit should improve the feasibility of drilling the holes, thus decreasing the chances that well damage will occur from the drilling process; since the surface of the wells are specially treated to promote cell adhesion, this could be a determining factor. The wells should also be cleaned scrupulously after drilling the holes. Contamination of the wells with debris from the plate or from the drill bit might effect cell adhesion and growth. Sonication of the plate with ethanol contained in the wells should suffice in cleaning the accumulated debris. Special attention must be given to removal of the debris afterwards.

Cell attachment to the surface of the sensor can be observed by bringing the light source from the top rather than from the bottom. Also, Scanning Electron Microscopy (SEM) may be used. Eventually, a study should be performed to measure the sensor's response. In this experiment, the sensor's response should be monitored during culture. Reduced sensor response in culture

compared to the *in-vitro* response might indicate that the sensor's function is effected by the presence of macrophages.

5.6.References

1. Carr, I. *Biological Defense Mechanisms*. Blackwell Scientific, Oxford, **1972**, p.23.
2. Carr, I. *The Macrophage a Review of Ultra structure and Function*, Academic, London, **1973**, p.49.
3. Van Furth, R., editor, *Mononuclear Phagocytes*. F.A. Davis Company, Philadelphia, PA, **1970**, p.104.
4. Auger, M.J.; Ross, J.A. "The Biology of the Macrophage" in *The Natural Immune System the Macrophage*, IRL, Oxford, **1991**, p.21.
5. Zhang, Y; Bindra, D.S.; Barrau, M.B.; Wilson, G.S. *Biosensors and Bioelectronics* **1991**; 6: 653-661.
6. DeFife, K.M.; Jenney, C.R.; McNally, A.K.; Colton, E.; Anderson, J.M. *J. Immunol.* **1997**, 158, 3385-3390.
7. Moore, G.E.; Gerner, R.E.; Franklin, H.A. Culture of Normal Human Leukocytes *J.A.M.A.* **1967**; 199 (8): 519-524.
8. McNally, A.K.; Anderson, J.M. *Proc. Natl. Acad. Sci.* USA. **1994**; 91: 10119-10123.
9. Sincich, T. *Business Statistics By Example*. Dellen, San Francisco, California, **1989**, p. 964-967.
10. *Wheaton Science Products*, Milliville, NJ, **1997/98** catalog, p.273.

6. Chapter 5: Possible Causes of the *In-Vivo* Sensitivity Loss

Because of the different parameters that need to be addressed, data obtained from the cell-culture experiment do not support or contradict the hypothesis that macrophages are responsible for the gradual *in-vivo* sensitivity loss of the implanted sensor. However, some conclusions can be made about the cause of the initial sensitivity loss.

The sensor sensitivity is recovered after explantation of the sensor from the tissue and placement in buffer solution; this observation suggests that the cause of the initial sensitivity loss is not due to local changes in the sensor's environment, but is due to alterations to the device itself. It also supports a reversible change. Therefore, the strategies taken in this research were to consider possible alterations to the device that could lead temporarily to reduced sensitivity.

The more likely causes of reduced sensitivity *in-vivo* seem to be accumulation of material on the sensor outer membrane and/or accumulation of material on the electrode surface. Accumulation of material on the sensor outer membrane could block glucose and/or oxygen transport to the enzyme layer leading to apparent reduced sensor sensitivity. Accumulation of material on the electrode surface could interfere with hydrogen peroxide electrochemistry.

Because adsorption of proteins onto the surface of a foreign object implanted *in-vivo* is the first step initiating the foreign body reaction, it seems plausible that proteins may contribute to

the sensitivity loss. A substantial amount of protein (several hundred μg/ml) was detected in the samples extracted from the explanted sensors. Components of wide molecular weight range were detected in the samples. Possible identities were given in Table 3.7. These include serum albumin; fibrinogen, IgG, coagulation factors, proteoglycans, and interleukins.

Recently, investigators have reported that small molecules may also contribute to the *in-vivo* sensitivity loss. The outer polyurethane membrane does not retain small molecules, neither does the inner cellulose acetate/nafion membrane. Therefore, small molecules could accumulate on the electrode surface and interfere with hydrogen peroxide detection. There was one SEC peak around 1025 Da detected and several small peaks around 900 Da and 1100 Da detected for sample 2. These low molecular weight molecules are in the range of peptides and could be due to the hormones given in Table 3.7.

There is also a possibility that some molecules were not detected in the sample because of their small size or because they were not present at a high enough concentration. One clue to support this claim is that the major plasma proteins albumin, fibrinogen, and IgG detected in the sample totaled only 1% of the total amount of protein detected using the BCA Assay. There are many potential interferences in the assay (i.e. reducing sugars, ascorbic acid, uric acid, amino acids) of low molecular weight. Contribution from these undetected species to the assay and hence to the *in-vivo* sensitivity loss is likely.

Coating the biocompatible polymer on the sensor outer membrane did not lead to improved *in-vivo* sensitivity. This observation could suggest that small molecules and not proteins may be the major contributor to the reduced sensor *in-vivo* sensitivity. However, it is also possible that the biocompatible polymer did not completely cover the sensor outer surface, in which case an improvement in sensor response may not have been observed.